

Analysis of Bird and Marine Mammal Data for Billia Croo Wave Test Site, Orkney





Scottish Natural Heritage
Dualchas Nàdair na h-Alba

All of nature for all of Scotland
Nàdar air fad airson Alba air fad

COMMISSIONED REPORT

Commissioned Report No. 592

Analysis of Bird and Marine Mammal Data for Billia Croo Wave Test Site, Orkney

For further information on this report please contact:

Alex Robbins
Scottish Natural Heritage
Battleby
Redgorton
PERTH
PH1 3EW
Telephone: 01738 458653
E-mail: alex.robbs@snh.gov.uk

This report should be quoted as:

Robbins, A. 2012. Analysis of Bird and Marine Mammal Data for Billia Croo Wave Test Site, Orkney. *Scottish Natural Heritage Commissioned Report No. 592.*

This report, or any part of it, should not be reproduced without the permission of Scottish Natural Heritage. This permission will not be withheld unreasonably. The views expressed by the author(s) of this report should not be taken as the views and policies of Scottish Natural Heritage.

© Scottish Natural Heritage 2013.



COMMISSIONED REPORT

Summary

Analysis of Bird and Marine Mammal Data for Billia Croo Wave Test Site, Orkney

Commissioned Report No.: 592
Contractor: Alex Robbins
Year of publication: 2013

Background

The purpose of this report is to provide a review of the bird and marine mammal observation data for the EMEC Billia Croo wave test site from 2009 to 2011. The primary aim was to explore any relationships between site usage and environmental variables.

This report can assist in understanding the spatial and temporal distribution of wildlife at the test site, and specifically enable identification of where and when particular species are more likely to encounter test devices or related deployment activity. It provides information on how the most frequently occurring bird and marine mammal species use Billia Croo wave test site. This included: common eider, red-throated diver, northern fulmar, northern gannet, European shag, great skua, gull species, black-legged kittiwake, tern species, common guillemot, razorbill, black guillemot and Atlantic puffin, as well as grey and common seals, and harbour porpoise.

Main findings

- Almost all species showed spatial variation in their use of the Billia Croo site. There are slight differences in the locations of hotspots and the extent to which different species used the wave test site. However, for a number of species (e.g. shag, auks and eider), sightings were concentrated between the Black Craig observation Tower and/or off Breck Ness.
- Many species also showed seasonal variation in their use of the site, which reflected the breeding and wintering habits that are typical for the species. Fulmar, gannet, Arctic tern, black guillemot and puffin, were found to vary in their usage of the site throughout the day.
- Encounter rates for some species were found to vary with tidal state and also under different environmental conditions, including wind strength, direction and glare extent.

For further information on this project contact:

Alex Robbins, Scottish Natural Heritage, Battleby, Redgorton, Perth, PH1 3EW.
Tel: 01738 458653

For further information on the SNH Research & Technical Support Programme contact:

Knowledge & Information Unit, Scottish Natural Heritage, Great Glen House, Inverness, IV3 8NW.
Tel: 01463 725000 or research@snh.gov.uk

| Table of Contents | Page |
|---|-------------|
| 1. INTRODUCTION | 1 |
| 1.1 Hypotheses | 1 |
| 2. METHODS | 2 |
| 2.1 Data Collection | 2 |
| 2.2 Data Preprocessing | 2 |
| 2.3 Data Analysis | 2 |
| 2.3.1 Environmental Variables | 2 |
| 2.3.2 Co-linearity | 3 |
| 2.3.3 Modelling | 3 |
| 3. RESULTS AND DISCUSSION | 5 |
| 3.1 Birds | 5 |
| Common Eider <i>Somateria mollissima</i> | 5 |
| Red-throated Diver <i>Gavia stellata</i> | 5 |
| Northern Fulmar <i>Fulmarus glacialis</i> | 6 |
| Northern Gannet <i>Morus bassanus</i> | 7 |
| European Shag <i>Phalacrocorax aristotelis</i> | 7 |
| Great Skua <i>Stercorarius skua</i> | 8 |
| Arctic Skua <i>S. parasiticus</i> | 8 |
| <i>Larus spp.</i> | 8 |
| Black-legged Kittiwake <i>Rissa tridactyla</i> | 9 |
| Arctic Tern <i>Sterna paradisaea</i> | 10 |
| Common Guillemot <i>Uria aalga</i> | 10 |
| Razorbill <i>Alca torda</i> | 11 |
| Black Guillemot <i>Cephus grylle</i> | 12 |
| Atlantic Puffin <i>Fratercula arctica</i> | 12 |
| 3.2 Marine Mammals | 13 |
| Seals | 13 |
| Harbour Porpoise <i>Phocoena phocoena</i> | 14 |
| 4. CONCLUSIONS AND RECOMMENDATIONS | 15 |
| 4.1 Conclusions | 15 |
| 4.2 Recommendations | 15 |
| 5. REFERENCES | 17 |
| ANNEX 1: TABLES AND FIGURES | 18 |
| ANNEX 2: DISTRIBUTION MAPS WITHIN 5KM OF BLACK CRAIG | 91 |
| ANNEX 3: AN EXAMPLE OF THE R SCRIPT USED | 105 |

1. INTRODUCTION

The purpose of this report is to provide a review of the bird and marine mammal observational data for the EMEC Billia Croo wave test site. In addition, recommendations are made for improving data collection. The principal aims are:

1. To explore the relationships (if any) between bird and marine mammal distributions and site usage with the collected environmental variables.
2. To provide any further recommendations for improving the wildlife monitoring protocols and data management.

1.1 Hypotheses

In order to achieve the aims, the following hypotheses will be tested for birds and marine mammals at Billia Croo test site:

1. There will be a seasonal difference in the use of Billia Croo site by marine birds and mammals.
2. The number of marine birds and mammals observed at Billia Croo site will vary between different periods of the day.
3. The spatial distribution of marine birds and mammals will vary across the site.
4. The number of marine birds and mammals observed at Billia Croo site will vary under different tidal conditions.
5. The number of marine birds and mammals observed at Billia Croo site will vary with changing wind conditions.
6. The number of marine birds and mammals observed at Billia Croo site will vary between dry and precipitation conditions.
7. The number of marine birds and mammals observed at Billia Croo site will vary with changing glare conditions.

2. METHODS

2.1 Data Collection

Land-based observations take place from a look-out shelter on Black Craig, Billia Croo (58°58.746'N 03°21.499'W), approximately 110m above sea level. The observations for birds and marine mammals commenced at Billia Croo on 11th March 2009, with a four-hour watch format, five days per week (i.e. approximately 80 hours of observation per month), which are timetabled to cover different tidal states and times of day. This analysis will use data collected over a period of two years.

2.2 Data Preprocessing

These data required significant preparation prior to analysis, which included:

- Alteration of misspelled species names and categorical variables.
- Sorting of environmental and observation data including matching the correct environmental observations with sightings.
- Separating bird records where mixed species had been seen in a group and the numbers of individual species were recorded in a comment/text string.
- Inference of missing values, where possible.
- Removal of erroneous records.
- Re-calculation of latitude and longitude for observations, using the recorded declination and horizontal angles.
- Calculation of additional variables such as “time from low tide” and “time lapse”.
- Inference of missing values, where possible, removal of records if this was not possible.

2.3 Data Analysis

All data analyses were completed using the statistical data package R, with relevant packages (R Development Core Team, 2011). The total survey effort (in hours) is summarised for the entire data set. For all bird and marine mammal species with sufficient data, modelling of the effects of environmental variables was then undertaken. In addition, seasonal and behavioural distribution maps were plotted in ArcGIS for bird species (and groups of species) with sufficient data.

2.3.1 Environmental Variables

In addition to the wildlife count data, a range of environmental variables were monitored during observations. These variables included:

| | |
|-----------------|---|
| Wind direction | This was subdivided into the following five categories “North”, “South”, “East”, “West” and “None”. |
| Wind strength | This was defined using the Beaufort scale. |
| Sea state | This was defined also using the Beaufort scale. |
| Cloud cover | This was recorded as a percentage. |
| Weather weather | This was recorded as “Fair”, “Rain” or “Snow”. |
| Glare extent | This was subdivided into ordinal categories “None”, “Slight”, “Moderate” and “Severe”. |

| | |
|--------------------|--|
| Tidal state | This was subdivided into “High Slack”, “Ebb”, ‘Low Slack” “Flood”. |
| Time from low tide | This was the time calculated (in decimal hours) from low tide. |
| Julian day | Is the ordinal date for the day the observation occurred (with the year omitted). |
| Season | The months were grouped in to “Winter” (December, January and February); “Spring” (March, April and May); “Summer” (June, July and August) and “Autumn” (September, October and November). |
| Time of day | This was recorded as the hour in which the observation occurred, i.e. 10:30 was “10” and 14:15 was “14”. This covariate was fitted as a smooth. |
| Daylapse | The number of days from the start of the data collection, where the first day is 1 and 380 th is 380. |
| Observer ID | This was defined by the initials of the two observers or “NA” if unknown. |

2.3.2 Co-linearity

Similar variables were tested for co-linearity using Variance Inflation Factors (VIF). Sea state, swell height and wind strength were all found to have co-linearity. Wind strength was found to be the most representative variable and was subsequently used in the analysis.

2.3.3 Modelling

Modelling of marine bird and mammal abundance with the EMEC Billia Croo wave test site was achieved using an extension of generalized additive model (GAM) techniques. These additive models can be used when data are non-linear, and a transformation of the data is inappropriate. They allow for non-linear relationships between response and explanatory variables through the use of smoothing models (Zuur *et al.* 2009).

The counts of each species were used as the response variable to investigate the influence of the different habitat and environmental conditions. Only observations within 5km of the vantage point were used. Generalized additive mixed models (GAMM) were used with Negative Binomial errors (and adjusted theta) and log link functions. To account for temporal auto-correlation, i.e. for counts that occurred on the same day and may be correlated, generalized estimation equations (GEE) were used, which enabled estimation of robust standard errors. The AR1 correlation structure was applied to the daylapse variable. Continuous variables were modelled as splines (i.e. Lat/Long, Julian day, time of day and time from low tide) or linear terms (i.e. wind strength and cloud cover) and categorical variables were added as factors. Variable significance was calculated using GEE-based *p*-values (refer to Appendix III for an example of the R script).

The results reported include the GAMM model coefficient estimates, GEE-based *p*-values and standard errors. The plots presented within this report incorporate GAMM model coefficient estimates, the encounter rate of mean number of birds or mammals observed (per hour) or percentage of overall observations. The higher model coefficient values represent a greater number of predicted birds or marine mammals.

Model Validation

GAMM model validation was undertaken by plotting and reviewing the distribution of the selected model's residuals and fitted values. However, residuals of the estimated models still showed patterns, which were more pronounced in those species with fewer observations. Consequently, the results within this report should be considered as preliminary until further investigation of these patterns is completed. Due to this issue a higher significance level has been applied to the terms in the model, i.e. where p is <0.01 .

3. RESULTS AND DISCUSSION

The results are presented in two sections, first the results for each of the key foraging bird groups and species are outlined; this is then followed by an outline of the modelling results for the most frequently observed marine mammals. The observations were carried out between March 2009 and March 2011. The total hours of survey that birds and mammals were observed in (by month) are summarised in Table 1.

3.1 Birds

Common Eider *Somateria mollissima*

A total of 2,635 eider were observed between March 2009 and March 2011 at Billia Croo wave test site. The selected model suggests that the number of eider at the site varied throughout the year, under different tidal conditions and with varying glare conditions. There was a small amount of auto-correlation as $\rho = 0.06$.

The distribution maps highlight a clear spatial pattern, with the all sightings occurring in the southern part of Billia Croo test site, close to the shoreline around Breck Ness (refer to figures 75 and 76). This pattern is consistent with literature on eiders, which notes that, as benthic feeders, they forage close to shore and in water up to 4m deep (Owen *et al.* 1986).

The numbers observed within the site showed seasonal variation, which was found to be highly significant within the chosen models ($p = 0.000427$, refer to table 2 and figure 1). Figure 1 indicates that eider were most frequently observed around February (Julian Date 32), after which the numbers rapidly decreased until June (Julian Date 152). The numbers of eider observed increased after July. This decreasing temporal pattern in the spring is consistent with the eider breeding season: the onset of incubation starts around April, when females incubate eggs on land and males leave the area to congregate offshore while they moult (Owen *et al.* 1986).

Eider sightings varied under different tidal states, although this was not highly significant ($p = 0.0346$). Eider were more frequently observed during ebbing tides and significantly less frequently in flooding tides ($p=0.00531$) (refer to table 2 and 3, and figure 2). The proportion of eider observed resting and feeding was found to differ between tidal states (refer to figure 3). Overall 2,346 eider were observed resting and only 254 eider were recorded feeding: 4% of eider were observed feeding during ebbing tides, while only 1% were observed feeding during slack tide. Conversely, 34% of eider were observed resting during low slack tide and 17% of eider were observed resting during high slack tide and also flood tides (refer to figure 5).

Glare extent was not found to be significant ($p=0.0889$), however, figure 3 highlights that significantly more eider were observed under moderate glare conditions ($p=0.01302$) (refer to table 2 and 3).

Time of day was not selected for, however the mean number of birds encountered per hour suggests that feeding increased during the morning, with a peak mean of 5 birds at 10:00, the mean remained above 2 birds per hour for the duration of the day. Greater numbers of birds were observed resting, compared with feeding, and the mean number of resting birds encountered peaked at 15 birds in the evening (18:00).

Red-throated Diver *Gavia stellate*

A total of 50 red-throated divers were observed at Billia Croo during the observation period. *Modeling* was not undertaken on these data.

The distribution map shows red-throated diver sightings were in the southern and western parts of the site, with the majority of birds observed within 1,000m of the coastline (refer to figure 77). The map indicates a temporal change in distribution across this site, with summer sightings being further from the coastline. This does contradict literature, as red-throated divers are known to forage on inshore waters during the breeding season (Gibbons *et al.* 1997; Jackson, 2002). Outside of the breeding season they are considered to use the marine environment extensively, spending a large proportion of their time on the sea, including sleeping (Stone *et al.* 1995).

The sightings of red-throated diver at Billia Croo indicate temporal variation in usage of the site. Figure 6 highlights a seasonal difference in the number of birds encountered; the greatest numbers of birds were observed during the spring and winter, 42% and 34% of sightings, respectively. Only 4% of the red-throated divers were observed in the autumn. Figure 7 shows fluctuations in the mean number of birds encountered throughout the day, with the peaks means at 6 hourly intervals: 5:00, 11:00 and 17:00. Figure 8 indicates that mean numbers of red-throated divers varies with time from low tide. The highest mean number of birds occurred 1h after high tide (5h before low tide), while no birds were observed 1h before high tide (5h after low tide). The figure also highlights secondary peak of encounters 2h after low tide.

Northern Fulmar *Fulmarus glacialis*

54,576 fulmar were recorded within 5km of the vantage point during the observation period. The selected model suggests that fulmar sightings at the Billia Croo test site showed spatial and temporal variation, both seasonally and diurnally, and observer ID was also selected for. There was some auto-correlation within these data, as $\rho = 0.09$.

The distribution maps (figures 78 and 79) show sightings across the test site, but with a concentration of records immediately to the west of the Black Craig observation point. Figure 9 also highlights this same concentration, with standard error lines for higher abundances at the southern end of the site; the spatial smooth term was highly significant ($p = 2.54E-13$). The figures indicate that higher numbers of fulmar were observed per sighting in the southern part of the site, with great number of sightings in the western part of the site, adjacent to the coastline.

Fulmar sightings were found to show both seasonal and diurnal patterns. Figure 10 shows the peak numbers of fulmar sightings were in December, during the wintering period. After this winter peak numbers decrease until September (approx. Julian day 250), however there are two small increases in numbers around May and August, which coincides with the onset of laying and then the fledging period. Figure 11 shows a steady increase in fulmar observations in the morning, peaking around mid-day, and a steady decline until the evening.

Fulmar use the site predominantly for resting/stationary behaviours: 97.76% of the fulmar that behaviour was recorded for were observed resting, with only 0.38% feeding and 1.86% travelling. The fulmar activity distribution map also shows a greater number of resting birds. Figure 12 explores the diurnal fluctuation in sightings further, by separating fulmar that are feeding and resting. The mean number of birds/hour observed resting follows the same diurnal pattern, with a 2-3 hourly cycle of peaks and troughs. However, the mean encounter rate for feeding fulmar shows two periods of increased encounters, the first at 08:00 (16 birds/hour) and the second at 16:00 (13.5 birds/hour).

Northern Gannet *Morus bassanus*

A total of 8,944 gannets were counted during the observation period, within 5km of the vantage point. The selected model indicates that number of gannets at Billia Croo varied across the site, throughout the year and day and under different glare conditions. There was a small amount of auto-correlation as $\rho = 0.05$.

The distribution maps show gannet sightings across the Billia Croo test site, with a greater concentration of sightings off Breck Ness. The significant smooths of latitude and longitude ($p = 3.73E-14$) in figure 13 also predict higher number of birds in the southern part of the site. The distribution map showing gannet behaviour indicates that many of the observations of feeding birds were in the area off of Breck Ness.

Figure 14 and table 6 highlights a significant pattern in gannet numbers throughout the year ($p = 2.00E-12$), with numbers increasing from the start of the year to a peak in sightings around May/June, which coincides with the gannet incubation period. The numbers decrease after this period until a smaller peak in August, this coincides with the fledging period. Gannets were also found to show a significant temporal pattern throughout the day ($p = 6.58E-05$). Figure 15 indicates the numbers encountered increased steadily throughout the day until 13:00-14:00, after which the numbers declined. 89% of the observations were behaviour was recorded gannets were recorded as stationary; only 10% of the observations were gannets seen to be feeding. Figure 17 also shows that the mean encounter rate of gannets resting was higher than gannets feeding throughout the day, except at 13:00 and 19:00.

Glare extent was included within the model as it was found to contribute towards explaining variation in gannet numbers observed ($p = 0.0414$) (refer to table 6 and 7, and figure 16). Interestingly, the model predicted fewer birds observed under slight glare conditions, with higher numbers of birds observed under moderate and severe glare conditions, although the differences between these is not significant.

European Shag *Phalacrocorax aristotelis*

36,781 European shag were observed at Billia Croo during the period analysed. The selected GAMM contained the variables for latitude and longitude, Julian day, time from low tide, glare extent and observer ID (refer to tables 6 and 7). There was auto-correlation; $\rho = 0.12$.

The distribution maps show a clear spatial concentration of observations at the southern part of the site: most records were within 2,000m of the coastline between the Black Craig observation tower and Breck Ness. Figure 18 shows the highly significant smooth for latitude and longitude ($p = <2e-16$). This predicts that shag relative abundance increases south of the 0 smooth line and within a circled hotspot (58.97°N, 3.38°W).

Shags, although a year-round resident, were found to show seasonal variation and the model also predicts a temporal pattern around low tide. Figure 19 indicates the numbers of shag sightings steeply declined at the beginning of the year, until early spring (i.e. March) when numbers increase, which coincides with main onset of egg-laying. A peak occurs around Julian day 150 (the beginning of June), which is followed by another decline until the end of July/beginning of August (~ Julian day 200). After this, numbers steadily increase until the end of the year, which may reflect the numbers in the area increasing due to fledglings. Figure 20 shows the models predication of a gradual peak in relative abundance between 1 h before low tide and 3h after. However, figure 23 shows that the peak mean number of feeding shags was encountered around low tide, but there was an additional peak around

two hours after high tide. The mean number of resting shags encountered shows a slight increase on the flooding tide. These patterns could be for a number of reasons, such as optimal flow speeds at particular points in the tidal cycle, and depth of the water around preferred feeding areas. Figure 22 also highlights diurnal peaks in feeding activity at mid-morning (i.e. 08:00-09:00) and mid-day (i.e. 12:00-13:00). While the mean number of resting shag encountered increases in the early morning, with a peak at 06:00, and decreases in the evening, the numbers encountered remained consistent through most of the day.

The number of shag encountered was related to the extent of glare, with significantly fewer birds detected in severe glare conditions ($p=0.0321$) than other glare conditions (refer to tables 8 and 9 and figure 21). The observer ID was also selected for by the model with significantly more shags observed by SW ($p=2.32E-05$) (refer to tables 8 and 9).

Great Skua *Stercorarius skua*

1,076 great skua were observed at Billia Croo during the study period. Great skua observations suggest both a temporal and seasonal pattern of use at Billia Croo. The GAMM model only selected for latitude and longitude by mixed and single species flocks and for glare extent and observer ID. There was a minimal amount of auto-correlation as $\rho = 0.00053179$.

The model highlighted that great skua showed significant spatial variation in their use of the Billia Croo site, but also that this spatial pattern differed when they were in a single-species flock ($p=0.0968$) v. a mixed species flock ($p=1.66E-09$). Figure 24 highlights hotspots of increased relative abundance, particularly around the centre and southern parts of the site. This corresponds to the pattern seen in the distribution maps (figures 84 and 85) notably where the feeding great skua are observed, off of Breck Ness and the southern area of the site. Interestingly, this feeding pattern mirrors that of locations of feeding gannets (refer to figure 81), which is a species commonly kleptoparasitised by great skua. Such observations, according to the Billia Croo protocol would be recorded with both species, i.e. a mixed flock. Figure 25 highlights that great skua in single-species flocks were more frequently observed further from observation point, in a southwesterly direction, although this was not significant.

Great skua did show strong seasonal variation in abundance at Billia Croo (refer to figure 27), however due to an absence of any sightings during winter months, this was not selected for by the model. As the figure highlights, 68.59% of all sightings occurred during the summer, with 23.98% during the spring and only 7% during the autumn.

Glare extent did not significantly affect the numbers of great skua observed, however a slight pattern occurred, which enabled a better fit of the preferred model. Figure 26 demonstrates that the number of great skua observed decreased within increasing glare extent. Observer ID was selected for ($p=0.0144$).

Arctic Skua *S. parasiticus*

Only 76 Arctic skua were observed at Billia Croo during the period analysed. These observations only occurred during spring (59%) and summer (41%). Figure 86 plots these sightings, which suggests a slightly different spatial usage to that of the great skua, with a greater proportion of the Arctic skua sightings to the west and northwest of the observation point.

Larus spp.

3,729 *Larus spp.* were observed at Billia Croo. These included 833 common gulls (*L. canus*), 1,871 great black-backed gulls (*L. marinus*), 660 herring gulls (*L. argentatus*) and 365

unidentified to species (refer to figure 32). The *Larus* gulls showed spatial and temporal variation in their use of the site, with the model selecting for latitude and longitude, Julian day (by species), wind strength and glare extent. There was a small amount of auto-correlation as $\rho = 0.0571814$.

Larus spp. observations showed a significant spatial pattern across the Billia Croo site. ($p=0.015113$) The distribution maps (refer to figures 87 and 88) show most of the sightings around Breck Ness and near to the coastline along the southern part of the site, which also reflects the latitudinal and longitudinal abundance smooth (refer to figure 28).

The gull species observed showed different seasonal temporal patterns, all of which were significant (common gull, $p=0.000532$; great black-backed gull, $p=1.31E-06$; herring gull, $p=0.002446$, *Larus spp.*, $p=6.26E-05$). Figure 29 highlights the different smooths for each species, all of which show peaks and troughs at different point. Common gulls show an increase in relative abundance towards the end of the year (after Julian day 300), while great black-backed gulls and herring gulls both show a spring time peak (after Julian day 100). The unidentified to species *Larus spp.* smooth highlights a trough in sightings, with the lowest number of observations around July (~Julian day 175). This may reflect better observation conditions during the summer, which would enable better identification of individuals to a species level.

Gull numbers were found to vary under certain environmental conditions. Wind strength was found to significantly affect the numbers of gulls observed ($p=0.00157$), and while glare extent was not found to be significant ($p=0.27271$) there was a clear pattern and the inclusion of the variable provided a better fit of the model. Figure 30 shows the decrease in relative abundance of gulls with increasing severity of glare. Likewise, figure 31 shows the mean number of birds encountered decreased with wind strength between forces 0 and 6, however numbers of gulls observed peaked during high winds of force 7.

Gulls at Billia Croo were predominantly observed resting at the site (shown by figures 33 and 88), with 47.06% of all observations (for which behaviours were recorded) being of resting great black-backed gulls, while 4.66% of these observations were of feeding gulls, unidentified to species. This is likely to reflect the inherent difficulty of identifying individuals within a gull feeding flock. Figure 34 highlights a diurnal pattern in the behaviour of gulls at Billia Croo, with a peak in the mean number of birds encountered feeding at 09:00 (17). The mean number of resting birds showed an evening peak of 9 birds/hour at 17:00.

Black-legged Kittiwake *Rissa tridactyla*

Over the period analysed 5,610 kittiwakes were observed at the Billia Croo test site. The selected model indicates that kittiwake activity at the site shows both spatial and temporal patterns, including variation over the season and with the diurnal tidal cycle. The model also selected for environmental variables, including wind direction, glare extent and observer ID. There was autocorrelation within these data, as $\rho = 0.1579383$.

Kittiwakes were recorded across the Billia Croo site (as shown in figures 35 and 89), however the model predicts that greater numbers of kittiwakes were observed further away from the observation point, suggesting a more pelagic use of the test site. The longitudinal and latitudinal smooth was highly significant ($p=1.74E-11$). This is consistent with literature on kittiwakes, as they are considered to be offshore feeders (Camphuysen *et al.* 2006).

Kittiwakes showed significant temporal variation, both seasonally and with the diurnal tidal cycle. Figure 36 highlights the peak in relative abundance during the spring months (when 60% of observations occurred), numbers decreased over the summer, with only 31% of the observations occurring during this time. Kittiwakes are known to abandon breeding colonies

after failed breeding attempts, which may reflect this decrease in observations. The remaining 9% of observations occurred during the autumn and winter months. The model also selected time from low tide as important, although with a higher threshold this isn't significant ($p=0.0219$). Figure 37 shows an increase in sightings an hour before low tide, peaking an hour after low tide and decreasing until 3 hours after high tide. Kittiwakes are known to adjust their daily foraging patterns to coincide with the appropriate phase of the tide (Irons, 1998) and their behaviour is also known to vary with spring and neap tides. Figure 40 demonstrates the behaviours observed at over the same diurnal cycle, whilst the mean number of birds observed resting and feeding both follow the same pattern, of greater number around low tide, there are also peaks in foraging activity 4 hours before and (more notably) after low tide.

The model also selected the environmental variables for wind direction and glare (and also observer ID). With the higher p value threshold these were not significant but did allow for a better fitting model (wind direction, $p=0.02811$; glare extent, $p=0.02847$; and observer ID, $p=0.00606$). The model estimated fewer birds would be observed during westerly winds, which at Billia Croo is the offshore wind direction. The model also predicted that fewer birds would be observed during moderate glare conditions, however it did predict a greater number of birds in severe glare conditions, which typically decrease visibility over water.

Arctic Tern *Sterna paradisaea*

A total of 2,315 Arctic tern were observed at Billia Croo. The model selected indicates that arctic tern sightings at Billia Croo varied seasonally and diurnally, and also with different wind directions, glare conditions and observer ID.

Figure 90 shows the sightings of Arctic tern are scattered across the centre of the study site, within 2km of the coastline. However, with such few and scattered sightings no pattern has emerged.

Arctic tern are migratory, heading to the Antarctic for the winter months, therefore no sightings of this species occurred during the autumn or winter. This is similar to findings by Stone *et al.* (1995), who highlighted that from August onwards terns were observed less in waters around the Northern Isles, as a result of the southern movement. 75% of the Billia Croo sightings occurred during the spring and the remaining 25% during the summer. As such, figure 41 only shows the within seasonal pattern during the spring and summer months, but the smooth clearly shows a decline in the number estimated, with a greater number of terns observed during the spring. This was found to be highly significant ($p=5.88E-10$). Terns also showed a highly significant diurnal pattern ($p=2.25E-05$). Figure 42 shows a smaller peak in predicted numbers around 08:00, but the numbers increase throughout the day until 15:00-16:00, after which they decrease.

Arctic tern numbers were found to vary significantly with the direction of the wind ($p=0.000172$). Greater numbers of birds were observed when the wind was in a southerly direction, with fewer birds observed when the winds were offshore, i.e. a westerly direction (refer to figure 43). Glare extent was also found to contribute significantly ($p=0.005709$) (refer to figure 44). However, as with the kittiwakes, the model predicted fewer birds would be observed during slight glare conditions compared with moderate or severe conditions.

Common Guillemot *Uria aalga*

A total of 10,433 guillemot were counted during the observation period at Billia Croo. The preferred model for guillemot counts included the variables for season (Julian day) and glare extent. The correlation between observations was estimated as $\rho = 0.04554506$.

The selected model did not include any spatial variables, however figures 91 and 92 shows a clear concentration of guillemot sighting in the central part of the site, directly west and within 2km of the observation point.

Guillemots showed a significant seasonal pattern ($p=1.10E-06$) (refer to figure 45), with numbers steeply increasing through the spring to a peak in June, after which numbers rapidly decline. This is likely to reflect the species' breeding phenology; by late June/early July many of the chicks have left the colonies and gone to sea with their fathers (Harris and Wanless 2004).

Glare extent was the only environmental variable selected for by the model. While the variable itself was not significant ($p=0.0543$), figure 46 clearly highlights that the number of guillemot observed decreased with increasing levels of glare. Table 15 also shows that there was significantly fewer guillemot observed under severe glare conditions.

Figure 47 and 48 highlight some patterns in guillemot foraging behaviour at Billia Croo. In particular, figure 47 shows a peak in the mean number of birds encountered foraging between 07:00 and 09:00. Figure 48 also shows two clear peaks in the mean number of guillemot encountered foraging approximately one hour either side of low tide, although there is a drop in numbers observed at low tide. There also are two smaller peaks in activity approximately one hour either side of high tide. The mean numbers of resting birds encountered is fairly consistent across the tidal cycle and throughout the day.

Razorbill *Alca torda*

A total of 380 razorbills were counted during the observation period. The preferred model indicates that razorbills numbers are a function of latitude and longitude, and Julian day. The correlation between observations was estimated as $\rho = 0.2024892$.

Razorbills showed highly significant spatial variation in their use of the Billia Croo site ($p=0.00094$). Figures 93 and 94 show a very similar distribution to that of the guillemot, at the test site (with fewer data points). Figure 49 indicates the model predicts higher numbers of razorbills to be encountered nearer the shore. Razorbills, like guillemots spend time in waters close to the colony, carrying out essential maintenance and social behaviours, including displaying, bathing and preening (McSorley *et al.* 2003). However with both species, the greater numbers of birds observed nearer to shore may be a consequence of their detectability, i.e. fewer birds are detected with increased distance from the observer.

Figure 50 shows the estimated seasonal pattern of razorbill numbers at Billia Croo ($p=0.01235$). Similar to guillemots, numbers steeply increase through the spring to a peak in late May/early June, after which number rapidly decline. This is likely to reflect razorbills' similar breeding phenology, as the successful males by late June/early July also leave the colony with their chicks, heading to sea (Harris and Wanless, 2004).

Figures 51 and 52 show the mean numbers of feeding and resting razorbills encountered. Figure 51 shows fluctuations in the numbers of feeding razorbills throughout the day, but with a mean peak of 5 birds at 18:00. The numbers of resting razorbills is more consistent throughout the day with a peak of 7.2 birds at 15:00. Figure 52 shows two clear patterns. First, the numbers of feeding birds encountered are highest on an ebbing tide, while the numbers of resting birds encountered are highest on a flooding tide, second, there is a peak in both feeding and resting behaviours (3 birds and 4.6 birds, respectively) one hour before low tide. There is also a mean peak of 5 feeding birds 4 hours prior to high tide.

No environmental variables were selected for by the GAMM.

Black Guillemot *Cephus grille*

A total of 2,786 black guillemot were observed at Billia Croo site. The best-fitting model indicates that the observed black guillemot numbers are a function of latitude and longitude, time of year (Julian Date), time of day and wind strength (refer to table 22 and 23). The correlation between observations was estimated as $\rho = 0.07063577$.

Black guillemot showed significant spatial variation in their usage of the Billia Croo test site ($p=2.82E-05$). Figures 53, 94 and 95 show most records were within 2,000m of the coastline between the Black Craig observation tower and Breck Ness. The smooth within figure 53 also highlights this hotspot, although there are some scattered sightings to the south of the site, <1% of the feeding and resting birds were observed in the northern part of the site.

Black guillemot also showed highly significant temporal variation in site usage, despite being one of the few resident seabird species. Figure 54 highlights the seasonal variation, with black guillemot more frequently recorded during the spring and summer months, with a peak in May ($p=2.59E-13$). Figure 55 highlights the significant crepuscular trend in the number of black guillemots observed throughout the day ($p=1.99E-14$), with peak encounters occurring at approximately 04:00-05:00 and numbers decreasing until 15:00, after which the encounter rate increased.

From figure 56 it can be seen that the mean number of black guillemot encountered decreased with increasing wind strength. Although this was not significant, wind strength did provide the model with a better fit (refer to table 22 and 23).

Figure 57 shows the mean number of feeding and resting birds encountered per hour, which reflects the crepuscular peaks observed in figure 55. The encounter rate for resting birds decreased from the 04:00 peak (2.69 birds/hour) until 17:00 after which it increases, peaking at 19:00 (2.56 birds/hour). The encounter rate for feeding birds indicates four peaks of feeding activity: early morning at 05:00 (2.5 birds/hour), mid-morning at 09:00 (1.8 birds/hour), approximately 16:00, and then evening at 19:00 (2.5 birds/hour). Figure 58 suggests a fluctuating encounter rate across the tidal states, with slightly more birds encountered during the flooding and slack tides. The mean number of feeding birds encountered shows a low and high tide peak, similarly the mean number of resting birds encountered shows a peak one hour after low tide and again at high tide.

Atlantic Puffin *Fratercula arctica*

A total of 690 puffin were observed at Billia Croo site. The best fitting model indicates that puffin numbers are a function of latitude and longitude, season, time of day, tidal state and glare extent, although not all these variables were significant (refer to table 24 and 25). The correlation between observations was estimated as $\rho = -0.06453384$.

Puffin observations indicate a spatial pattern across the Billia Croo test site. As with the other auk species, figures 59, 96 and 97 show that puffin observations were in the central part of the site, directly west and within 2km of the observation point. However, this was not significant ($p=0.0673$).

Puffins were observed more frequently during the spring and summer months (refer to figure 60). This smooth, albeit with larger confidence patterns, shows a similar seasonal pattern to the other dispersive breeding auk species, with late spring/early summer peak in abundance. However, with the higher p -value thresholds, this was not significant ($p=0.0235$). Similarly, puffin were found to show a diurnal pattern, but this was not significant ($p=0.0156$). Figure 61 shows the model predicts number of puffins encountered to increase throughout the day, peaking at approximately 15:00. Figure 51 also suggests a pattern in puffin numbers relative

to the tidal cycle. The smooth highlights a peak in numbers around low tide, although this is not significant ($p=0.1673$).

Puffin numbers were found to vary under different glare conditions, with significantly more puffin observed during moderate conditions ($p=0.00789$) (refer to table 25 and figure 62).

Figure 63 shows the mean number of feeding and resting puffin encountered per hour. This identifies a clear late morning peak in feeding activity, with a mean of 11 birds at 10:00. The number of resting birds shows little fluctuations throughout the day, and a minor increase in the mean number of birds encountered. Figure 64 suggests a fairly consistent encounter rate of resting puffin across the tidal states. However, the encounter rate for feeding puffin fluctuates greatly: it clearly shows peaks in foraging activity at low tide and also an hour after high tide.

3.2 Marine Mammals

Seals

A total of 470 seals were recorded during the observation period, 9% of these were harbour seals, *Phoca vitulina*, 66% of these were grey seals, *Halichoerus grypus*, and 25% were unidentified to species. Due to the smaller numbers of seals observed, the modelling was undertaken on all sightings. The best-fitting model indicates that seal numbers are a function of latitude and longitude, season and wind direction and strength (refer to table 26 and 27). The correlation between observations was estimated as $\rho = 0.1281074$.

Figure 66 highlights the spatial distribution of sightings across the Billia Croo test site, which was highly significant ($p < 2e-16$). From this, most sightings can be seen to be in a similar location to the bird species, around the coastline between Black Craig observation tower and Breck Ness, however the model predicts increasing abundance towards the Southeastern part of the site.

Collectively, both seal species were found to show a seasonal pattern (although not significant with the higher threshold: $p=0.0262$). Figure 67 shows the numbers of sightings increasing until around August and then decreasing again. Harbour and grey seals have different breeding phenology, therefore there are typically higher concentrations of each species at different times in the year. Harbour seals breed during the summer months, giving birth on land, but spend most of the lactation in the sea with their pups, (Thompson *et al.* 1994); while grey seals pup during the autumn, with the peak around October to November (Bonner 1981). It is likely that with more data this seasonal smooth may change to reflect the two different species peaks. However, the seasonal proportions of sightings, broken down by species, does already reflect this (refer to figure 70). From this it can be seen that there is an increase in harbour seal sightings during the summer (3.62% of all seal observations) and the proportion of grey seals peaks in the autumn and winter (19.79% in both seasons).

Seal sightings were found to vary significantly with wind direction ($p=1.68E-07$) (refer to figure 69). In particular, greater numbers of seals were encountered with onshore winds (i.e. Easterly), which may be a consequence of reduced swell in the test site, enabling better detection of the seals. However, the mean number of seals encountered with increasing wind strength appears to increase (refer to figure 69).

Figure 71 shows the breakdown of behaviours observed by species, for all seal observations. From this 45.3% of observations were of stationary grey seals, with 5.5% of stationary harbour seals. 15.7% of observations were of bottling grey seals and 1.5% of harbour seals. 3% of observations were of grey seals swimming; 0.9% were of grey seals feeding and also 0.9% surfacing.

Harbour Porpoise *Phocoena phocoena*

A total of 397 harbour porpoise were observed at Billia Croo site. The selected model indicates that harbour porpoise numbers are a function of latitude and longitude, season and glare extent (refer to table 28 and 29). The correlation between observations was estimated to be $\rho = -0.1259167$.

Figure 72 shows the spatial smooth of harbour porpoise sightings across the site. The figure highlights the smooth going in a diagonal axis across the site (from NE to SW) and predicts a greater abundance in the Southeastern part of the site. This pattern is not significant, using the higher thresholds ($p=0.02037$).

Harbour porpoise were found to show a significant seasonal pattern, ($p=0.00485$). Figure 73 predicts a peak in encounters between May and August. Harbour porpoise sightings were also found vary under different glare conditions, with significantly fewer porpoise observed during severe conditions ($p=0.00772$) (refer to figure 74).

From the observations at Billia Croo 88.59% were of surfacing porpoise and 10.08% were of feeding porpoise. Only 1.06% were observed performing aerial behaviours (refer to figure 75).

4. CONCLUSIONS AND RECOMMENDATIONS

4.1 Conclusions

This study provides information on how the most frequently occurring bird and marine mammal species use Billia Croo wave test site. This information can be used in understanding the spatial and temporal distribution of wildlife at the test site, and specifically enable identification of where and when particular species are more likely to encounter test devices or related deployment activity.

Almost all species showed spatial variations in their use of the Billia Croo site. While many species showed slight differences in the locations of 'hotspots' and the extent to which they used the wave test site, for a number of species (e.g. shags, auks and eider), sightings were concentrated between the Black Craig observation Tower and/or off Breck Ness.

Almost all species analysed also showed seasonal variation in their use of the site, which reflected the breeding and wintering habits that are typical for the species. Fulmar, gannet, Arctic tern, black guillemot and puffin were found to vary in their usage of the site throughout the day.

Several species' encounter rates were found to vary with tidal state, i.e. eider, shag, kittiwake, guillemot and puffin. Greater numbers of eider, shag and foraging guillemot were observed during slack tides. Puffin numbers were found to peak an hour before low tide and kittiwake an hour after.

Encounter rates were found to differ under particular environmental conditions, including wind strength, direction and glare extent. Wind strength was found to affect numbers of gulls, black guillemots and seals observed. While wind strength was found to affect kittiwakes, terns and seals observed, with either more birds encountered during onshore winds (easterly) or fewer birds encountered during offshore winds (westerly). This is likely to be a result of the wind direction affecting sea state (i.e. causing "choppiness") and subsequently reducing the observers' ability to observe and/or identify the species. Glare extent was included in the preferred models for a number of species, including gannet, shag, great skua, *Larus spp.*, kittiwake and Arctic tern, guillemot, puffin and harbour porpoise. Increased glare reflects off the water and can affect the observers' ability to see and identify individuals. Precipitation was not found to be significant with any species. Observer ID was found to be significant for a couple of species, including gannet, fulmar, shag, kittiwake and Arctic tern.

4.2 Recommendations

There are several recommendations for methodology improvements that would benefit future analyses:

1. The dataset currently requires considerable cleaning prior to analysis, and it may be useful for future reviewers to have access to the cleaned data, and for the dataset to undergo regular maintenance, to enable summaries etc. to be pulled out.
2. It was not possible to consider habitat types and depth within Billia Croo test site. Therefore it was not possible to consider, for example, the seabed substrate or slope, which may influence which species forage where within the site. This information and other habitat variables may be useful in future analyses.
3. An inherent concern with land-based observations is that there is a decreased probability of detecting wildlife with an increase in distance from the observation point (Bibby *et al.* 2000; Buckland *et al.* 2001). It is therefore recommended that boat-

based surveys undertake line-transects randomly across the test site to calibrate these land-based vantage point observations. These surveys should be carried out according to standardized methodologies (e.g. Buckland *et al.* 2001 and Camphuysen *et al.* 2004).

5. REFERENCES

- Bibby, C.J., Burgess, N.D., Hill, D.A., and Mustoe, S.H., 2000. *Bird Census Techniques*. 2nd Ed. London: Academic Press.
- Bonner, W.N. 1981. Grey seal. In: Ridgway, S.H., and Harrison, R.J., eds., 1981. *Handbook of Marine Mammals*: 2. London: Academic Press, pp. 111–144.
- Buckland, S.T., Anderson, D.R., Burnham, K.P., Laake, J.L., Borchers, D.L., and Thomas, L. 2001. *Introduction to Distance Sampling*. Oxford: Oxford University Press.
- Camphuysen, C.J., Fox, A.D., Leopold, M.F., Peterson, I.K., 2004. *Towards standardized seabirds at sea census techniques in connection with environmental impact assessments for offshore wind farms in the UK*. Report to COWRIE: Koninklijk Nederlands Instituut Voor Onderzoek Der Zee, The Netherlands.
- Camphuysen, C.J., Scott, B.E., and Wanless, S., 2006 Chapter 6: Distribution and foraging interactions of seabirds and marine mammals in the North Sea: multispecies foraging assemblages and habitat-specific feeding strategies. In: Boyd, I., Wanless, S., Camphuysen, C.J., eds., 2006. *Top Predators in Marine Ecosystems: Their Role in Monitoring and Management*. Cambridge, UK: Cambridge University Press. pp. 82-97.
- Gibbons D.W. Bainbridge I.P. Mudge G.P. Tharme A.P. and Ellis P.M., 1997. The status and distribution of the red-throated diver *Gavia stellata* in Britain in 1994. *Bird Study*, 44(2), p.12.
- Jackson, D.B., 2002. Between-lake differences in the diet and provisioning behaviour of black-throated divers *Gavia arctica* breeding in Scotland. *Ibis*, 145(1), pp.30-44.
- Harris, M.P., and Wanless, S., 2004. Common Guillemot *Uria aalge*. In: Mitchell, P. I. et al., eds. 2004. *Seabird populations of Britain and Ireland*. London, UK: T & A D Poyser, pp. 351-363.
- Irons, D.B., 1998. Foraging area fidelity of individual seabirds in relation to tidal cycles and flock feeding. *Ecology*, 79(2), pp.647–655.
- McSorley, C.A., Dean, B.J., Webb, A., and Reid, J.B. 2003. Seabird use of waters adjacent to colonies: Implications for seaward extensions to existing breeding seabird colony Special Protection Areas. *JNCC Report No. 329*.
- Owen, M., Atkinson-Willes, G.L., and Salmon, D.G., 1986. *Wildfowl in Great Britain*. 2nd Ed. Cambridge University Press: Cambridge, UK.
- R Development Core Team. 2011. *R: A Language and Environment for Statistical Computing*. R Foundation for Statistical Computing, Vienna, Austria. <http://www.R-project.org>
- Stone, C.J., Webb, A., Barton, C., Ratcliffe, N., Reed, T.C., Tasker, M.L., Camphuysen, C.J. & Pienkowski, M.W., 1995. *An atlas of seabird distribution in north-west European waters*. Peterborough, Joint Nature Conservation Committee.
- Thompson, P.M., Miller, D., Cooper, R., and Hammond, P.S., 1994. Changes in the Distribution and Activity of Female Harbour Seals During the Breeding Season: Implications for their Lactation Strategy and Mating Patterns. *Journal of Animal Ecology*: 63(1), pp.24-30.
- Zuur, A.F., Ieno, E.N., Walker, N.J., Saveliev, A.A., Smith, G.M. 2009. *Mixed Effects Models and Extensions in Ecology with R*. Springer Science+Business Media: New York, USA.

ANNEX 1: TABLES AND FIGURES

SUMMARY OF OBSERVATIONS

Table 1: The total number of hours of survey that marine birds and mammals were observed in between 15th March 2005 and 15th March 2011.

| | 2009 | 2010 | 2011 |
|--------------|-------------|-------------|-------------|
| January | | 55 | 79 |
| February | | 72 | 57 |
| March | 55 | 90 | 44 |
| April | 107 | 85 | |
| May | 90 | 86 | |
| June | 93 | 79 | |
| July | 101 | 80 | |
| August | 81 | 86 | |
| September | 76 | 77 | |
| October | 55 | 83 | |
| November | 64 | 81 | |
| December | 48 | 67 | |
| Total | 770 | 941 | 180 |

Common Eider

Table 2: The significance of the parametric and smooth terms in the chosen model for eider use of Billia Croo.

Model: gamm(NUMBER ~ s(JULIANDAY,bs="cc") + oTIDE + oGLAREEXTENT, correlation=corAR1 (form=~1|DAYLAPSE), family=negative.binomial (theta=1.7), gamma=1.4, data=eider1)

Significance of parametric terms:

| | df | F | p-value | Signif. 1 |
|--------------|----|-------|---------|-----------|
| Tidal State | 3 | 2.897 | 0.0346 | * |
| Glare Extent | 3 | 2.184 | 0.0889 | |

Approximate significance of smooth terms:

| | edf | Ref.df | F | p-value | Signif. |
|---------------|-------|--------|-------|----------|---------|
| s(Julian Day) | 3.651 | 3.651 | 5.445 | 0.000427 | *** |

Table 3: Parameter estimates, standard errors, probability values for the GAMM investigating eider counts as a function of julian day, tidal state and glare extent.

| | Estimate | Std. error | Wald | Pr (> W) | Signif. |
|-----------------|----------|------------|--------|-----------|---------|
| (Intercept) | 1.33284 | 0.09766 | 13.648 | < 2e-16 | *** |
| Tide: Ebb | 0.04019 | 0.10415 | 0.386 | 0.69975 | |
| Tide: Low Slack | -0.07691 | 0.09805 | -0.784 | 0.43313 | |
| Tide: Flood | -0.25417 | 0.09083 | -2.798 | 0.00531 | ** |
| Glare: Slight | 0.12659 | 0.13043 | 0.971 | 0.33217 | |
| Glare: Moderate | 0.48238 | 0.19364 | 2.491 | 0.01302 | * |
| Glare: Severe | 0.04297 | 0.23743 | 0.181 | 0.85644 | |

R-sq.(adj) = 0.0486 Scale est. = 1.4575 n = 577

¹ Significance codes: 0 '***' 0.001 '**' 0.01 '*' 0.05 '.' 0.1 ' ' 1

Figure 1: The estimated seasonal pattern of relative number of eider observed. The solid line is the smoothing curve for Julian date and dotted lines are 95% confidence bands.

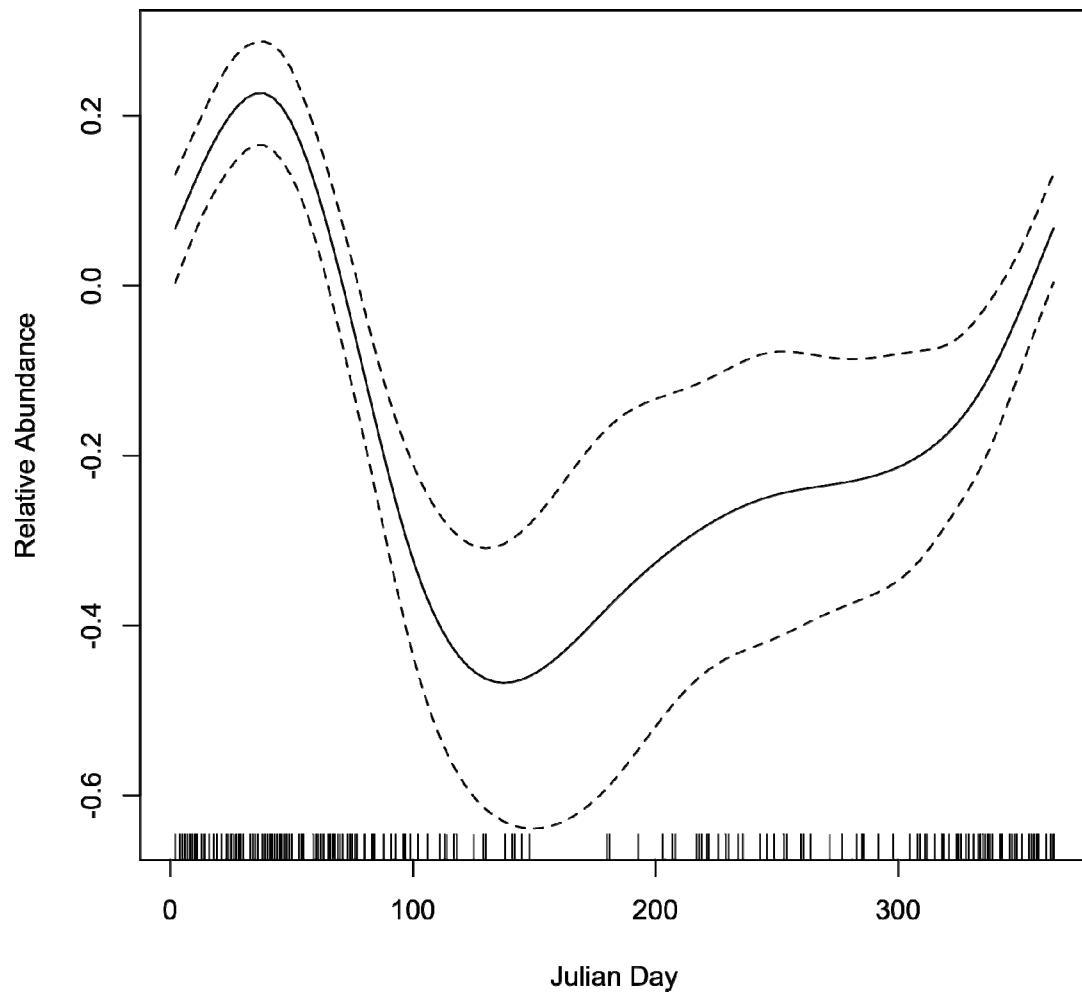


Figure 2: GAMM coefficient estimates (and standard errors) for eiders observed by tidal state at Billia Croo.

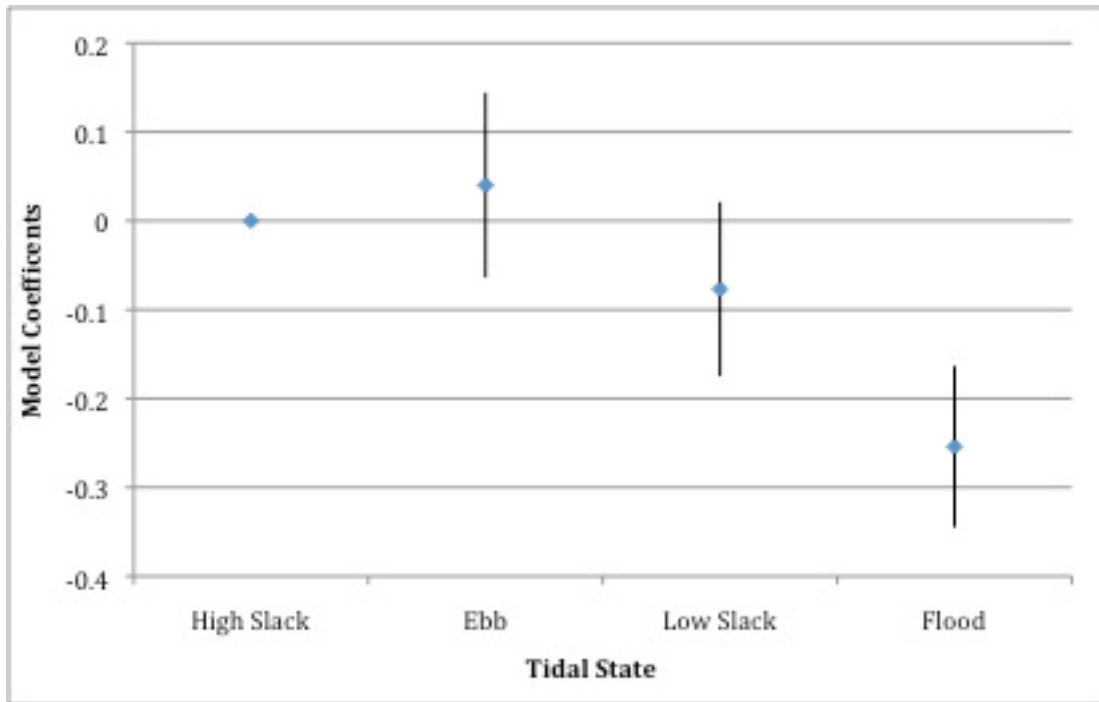


Figure 3: GAMM coefficient estimates (and standard errors) for eiders observed by glare extent at Billia Croo.

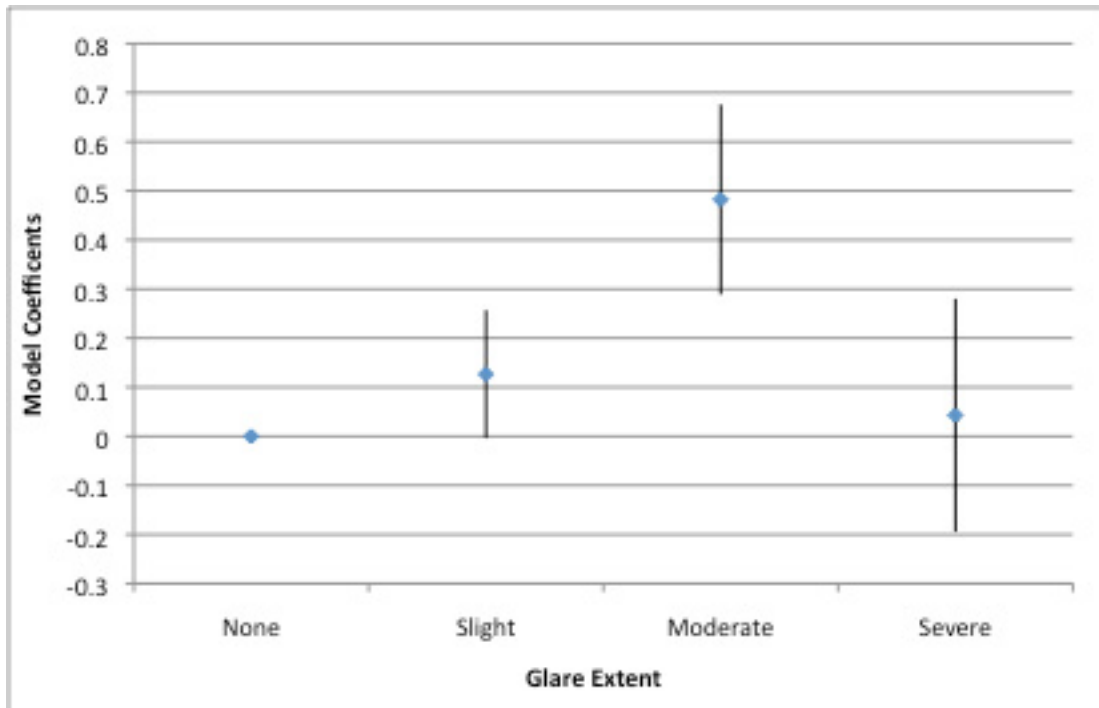


Figure 4: Mean number of feeding and resting eider observed per hour, throughout the day at Billia Croo.

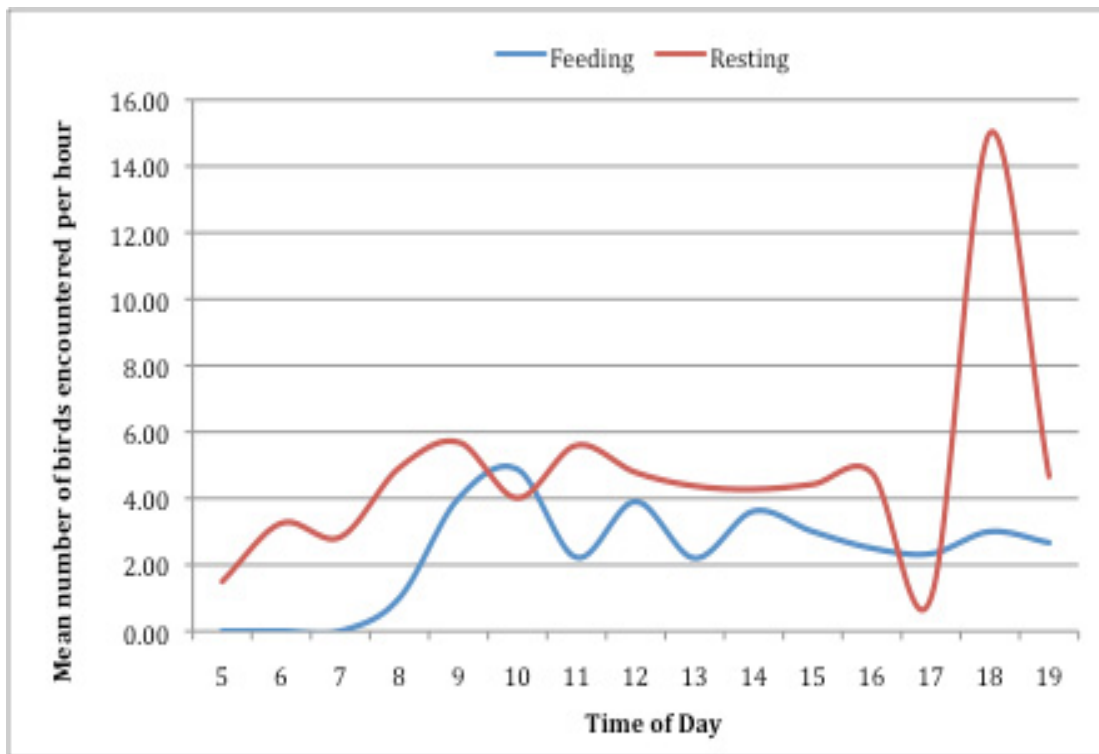
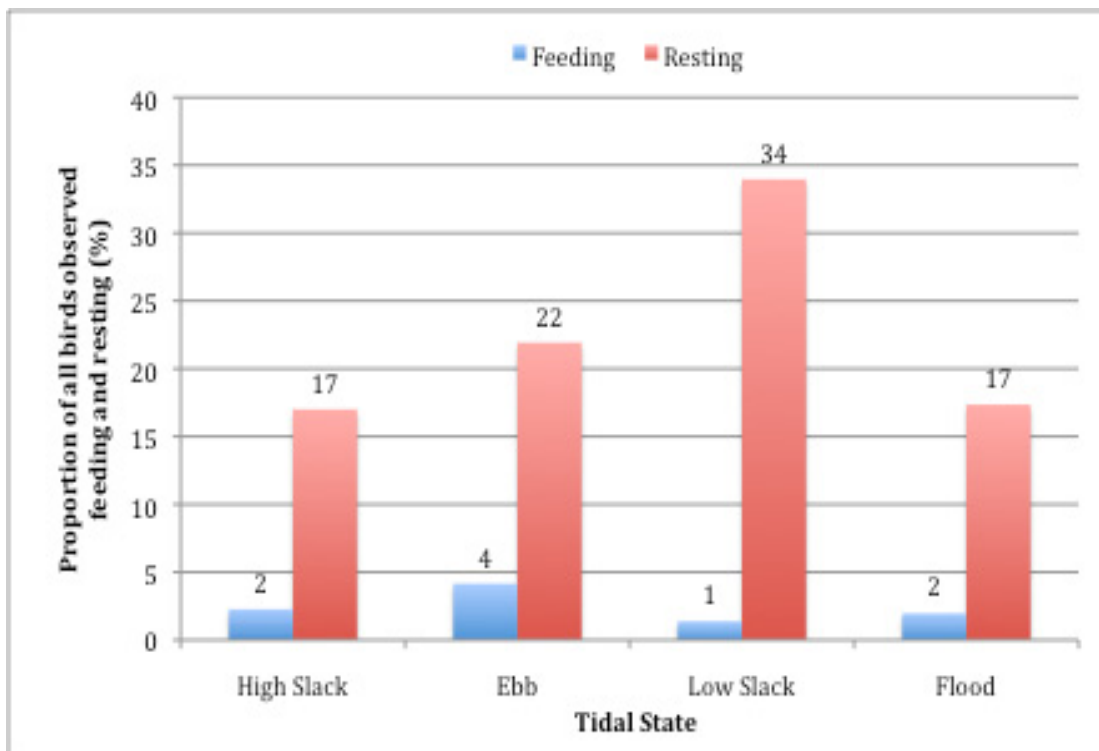


Figure 5: The proportion of observations of feeding and resting eider observed at different tidal states, at Billia Croo.



Red-throated Diver

Figure 6: The proportion of red-throated diver sightings by season at Billia Croo.

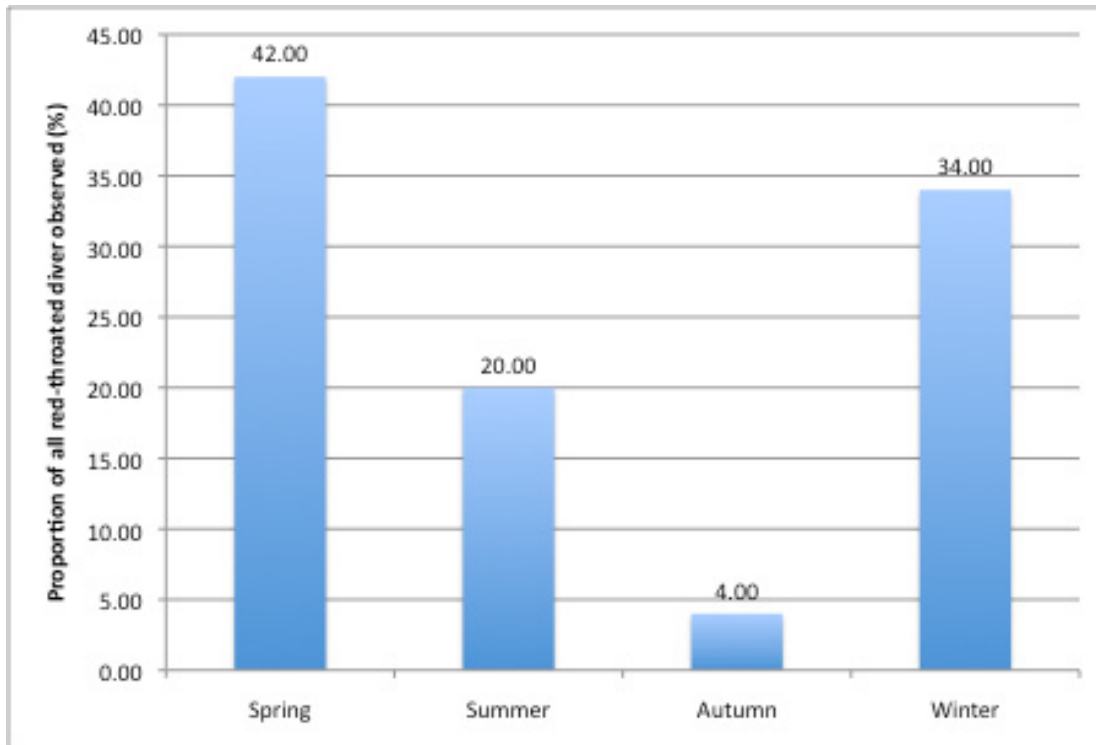


Figure 7: Mean number of red-throated divers observed per hour, throughout the day at Billia Croo.

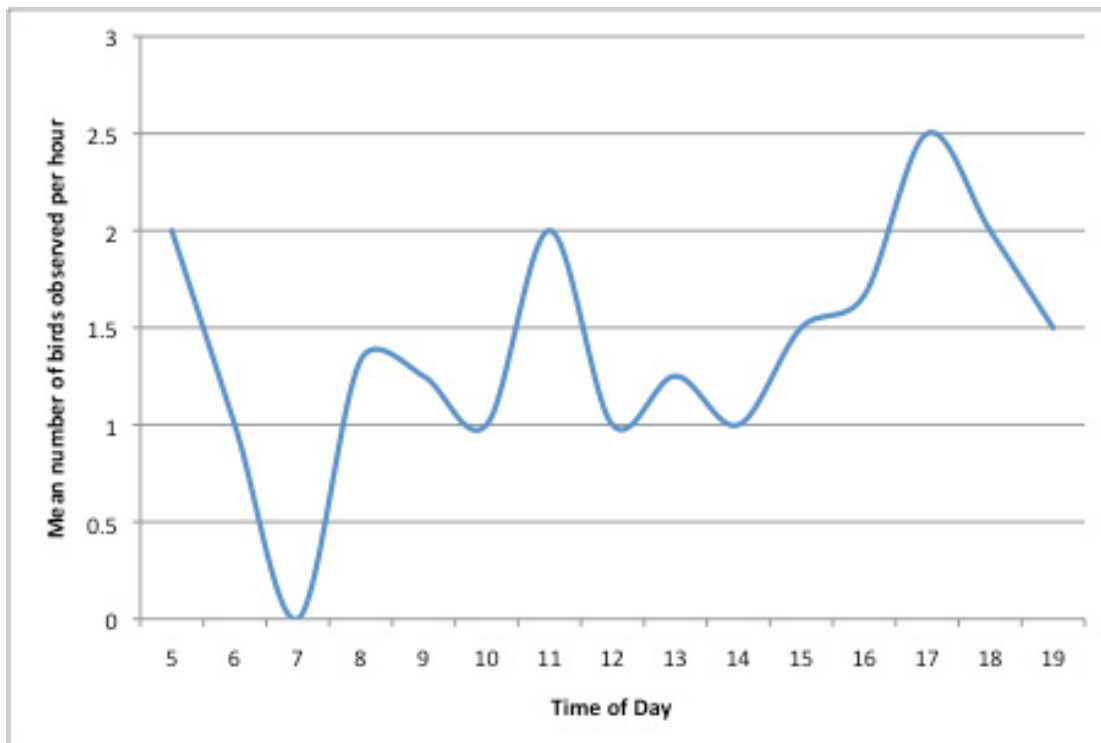
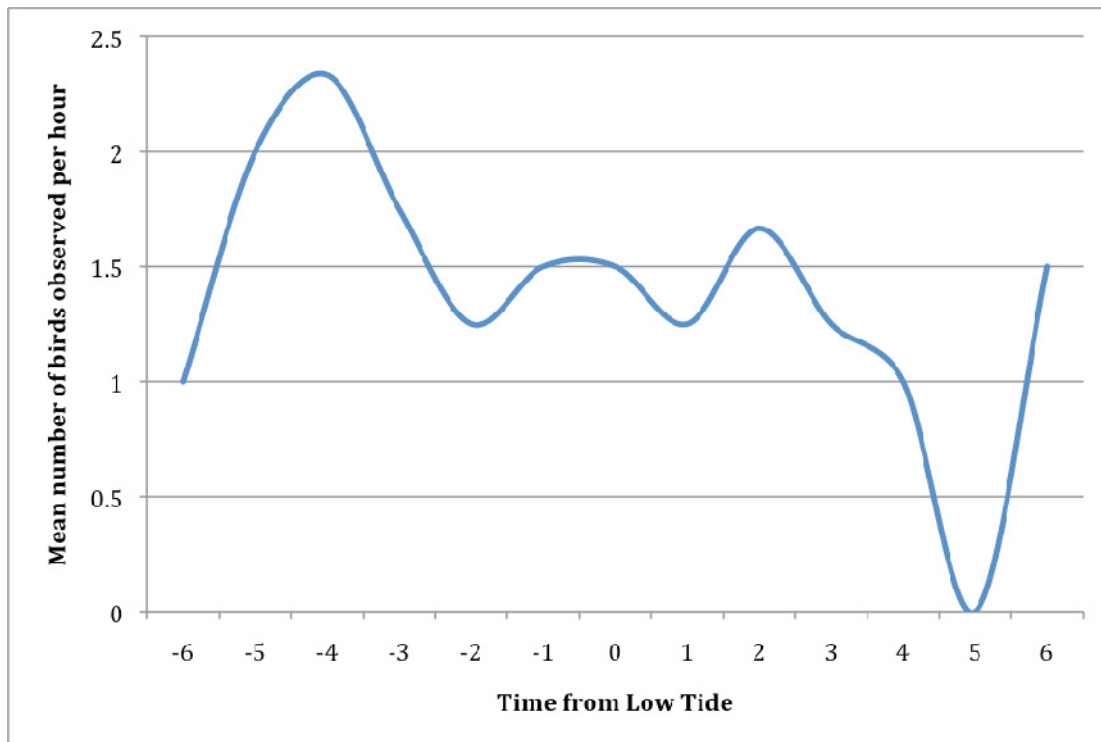


Figure 8: Mean number of red-throated divers observed per hour, by time from low tide at Billia Croo.



Northern Fulmar

Table 4: The significance of the parametric and smooth terms in the chosen model for fulmar use of Billia Croo.

Model: `gamm(NUMBER~s(Long,Lat)+s(JULIANDAY,bs="cc")+s(TIMEHOUR,bs="cs") +Observer, correlation=corAR1(form=~1|DAYLAPSE), family=negative.binomial (theta=1.00078), gamma=1.4,data=fulmar1)`

Significance of parametric terms:

| | df | F | p-value | Signif. |
|----------|----|------|---------|---------|
| Observer | 1 | 8.07 | 0.00451 | ** |

Approximate significance of smooth terms:

| | edf | Ref.df | F | p-value | Signif. |
|---------------|--------|--------|-------|----------|---------|
| s(Long,Lat) | 11.295 | 11.295 | 7.538 | 2.54E-13 | *** |
| s(Julian Day) | 6.655 | 6.655 | 9.44 | 3.09E-11 | *** |
| s(Timehour) | 2.394 | 2.394 | 4.405 | 0.00803 | ** |

Table 5: Parameter estimates, standard errors, probability values for the GAMM investigating fulmar counts as a function of latitude and longitude, Julian day, time of day and observer.

| | Estimate | Std. error | Wald | Pr (> W) | Signif. |
|--------------|----------|------------|--------|-----------|---------|
| (Intercept) | 1.506 | 0.107 | 14.074 | < 2e-16 | *** |
| Observer: SW | 0.3615 | 0.1273 | 2.841 | 0.00451 | ** |

R-sq.(adj) = 0.0532 Scale est. = 12.819 n = 6407

Figure 9: The estimated spatial pattern of relative number of fulmar observed. The solid line is the smoothing curve for 0, red dotted lines are -1 standard error from the smoothing curve and the green dotted lines are +1 standard error from the smoothing curve.

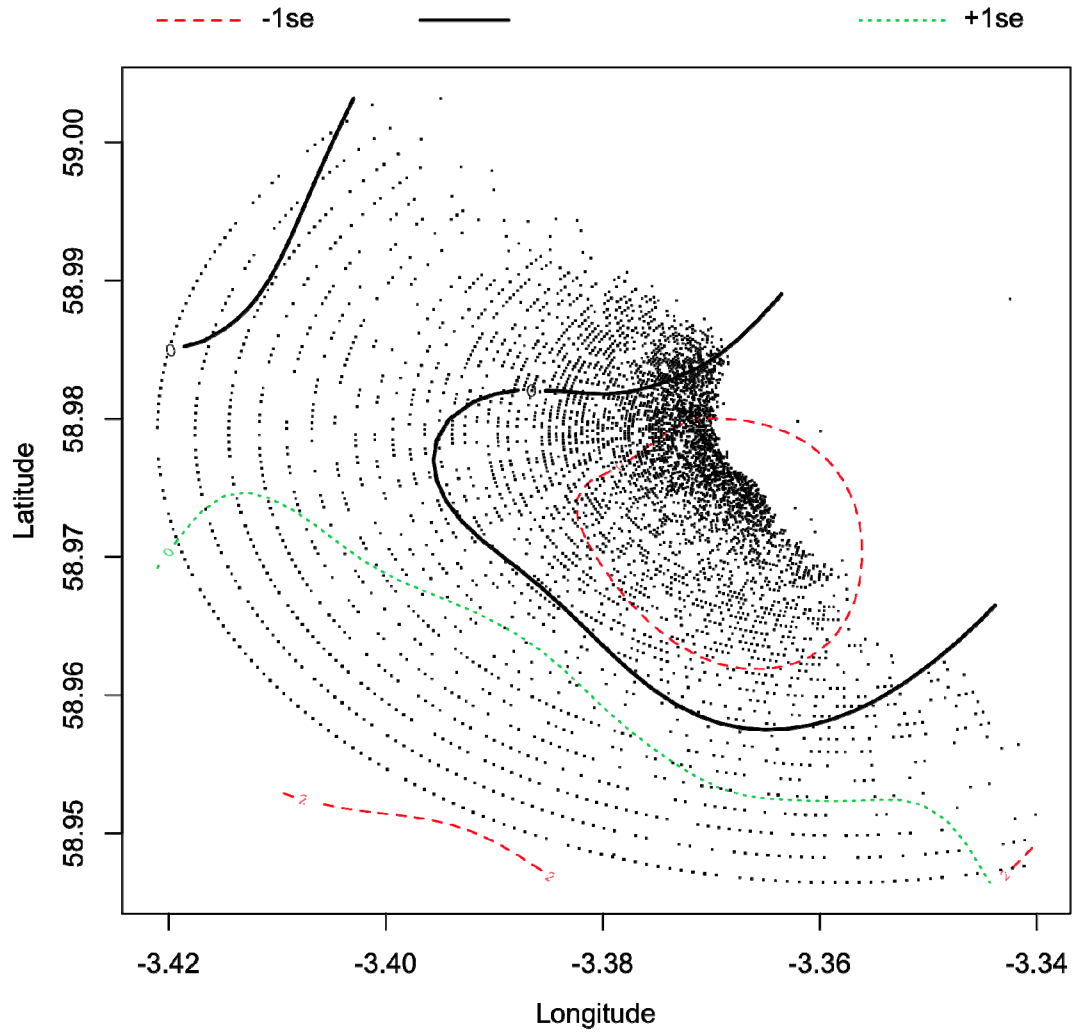


Figure 10: The estimated seasonal pattern of relative number of fulmar observed. The solid line is the smoothing curve for Julian day and dotted lines are 95% confidence bands.

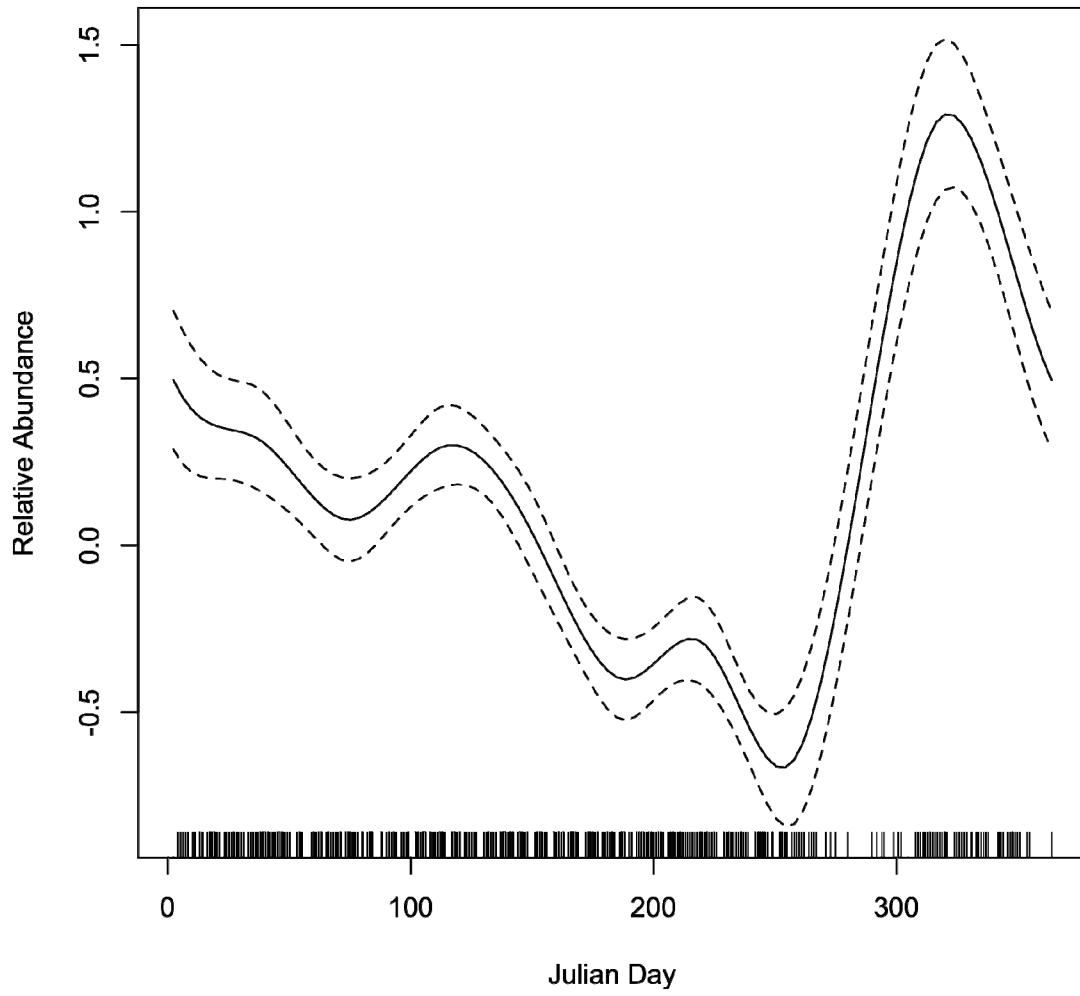


Figure 11: The estimated diurnal pattern of relative number of fulmar observed. The solid line is the smoothing curve for time of day and dotted lines are 95% confidence bands.

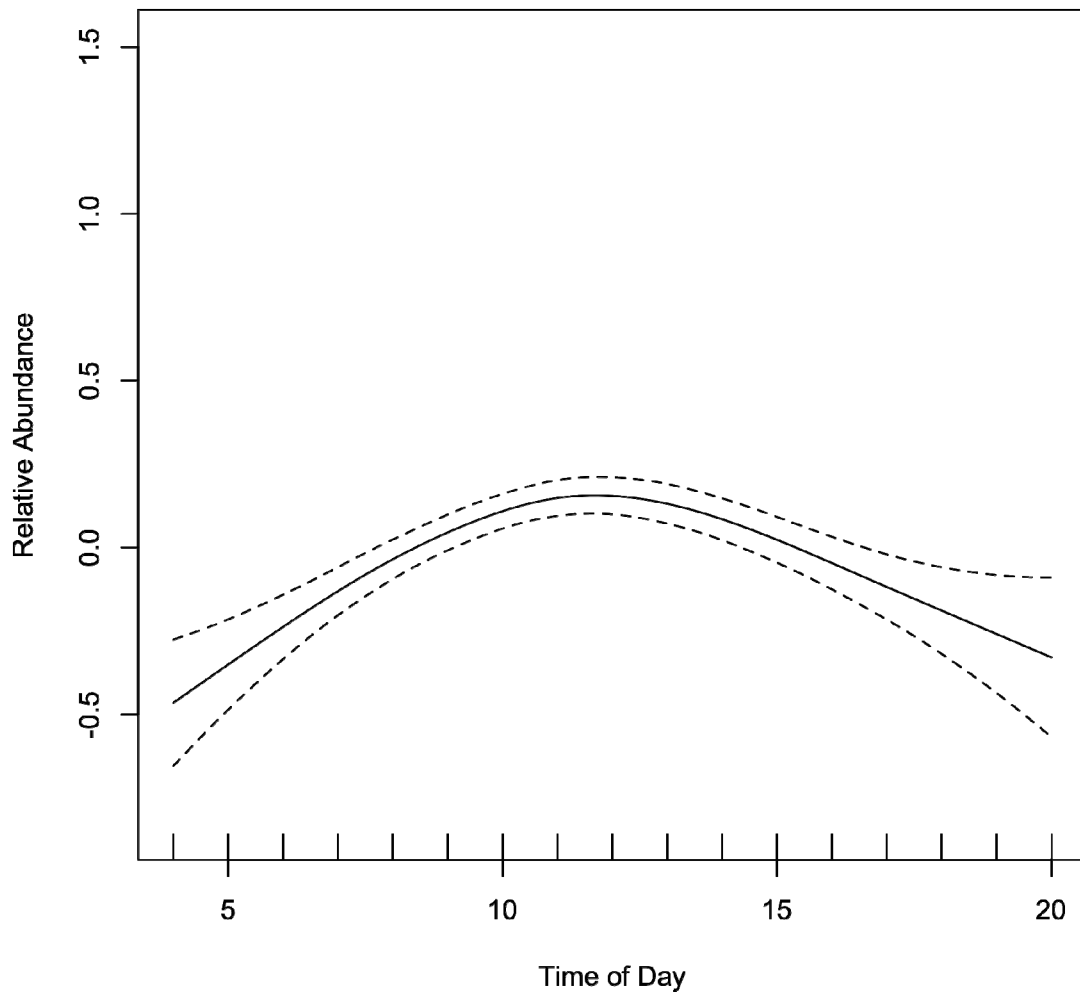
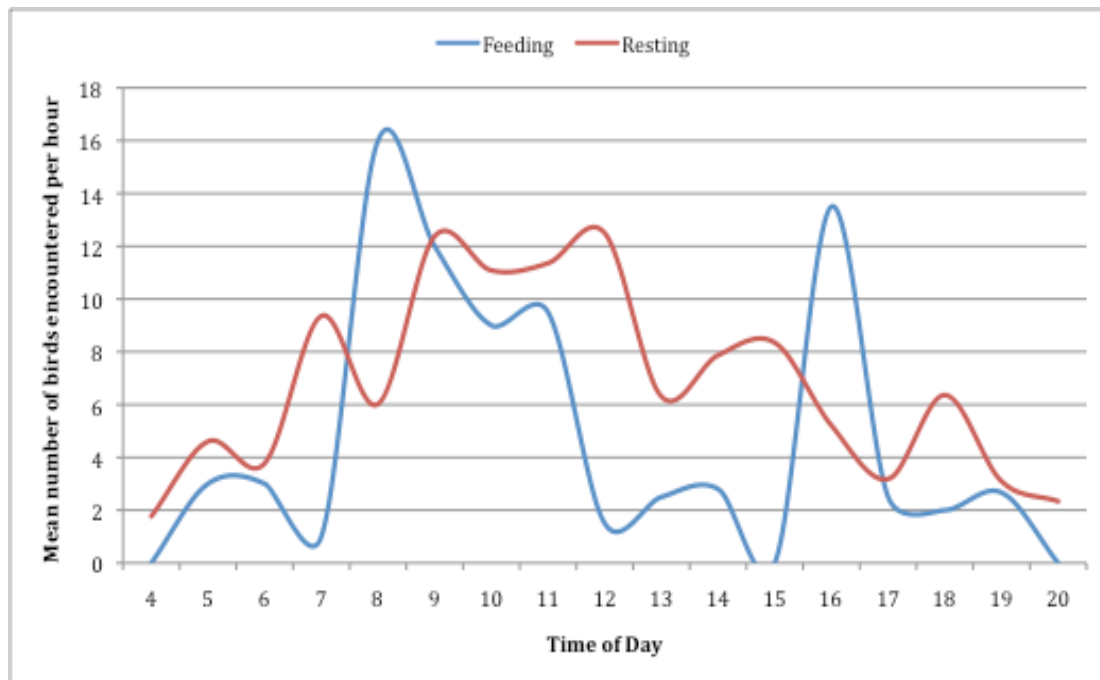


Figure 12: Mean number of feeding and resting fulmar observed per hour, throughout the day at Billia Croo.



Northern Gannet

Table 6: The significance of the parametric and smooth terms in the chosen model for gannet use of Billia Croo.

Model: gamm(NUMBER~s(Long,Lat)+s(JULIANDAY,bs="cc")+s(TIMEHOUR,bs="cs") +oGLAREEXTENT, correlation=corAR1(form=~1|DAYLAPSE), family=negative.binomial (theta=1.371285), gamma=1.4, data=gannet5k1)

Significance of parametric terms:

| | df | F | p-value | Signif. |
|--------------|----|-------|---------|---------|
| Glare Extent | 3 | 2.748 | 0.0414 | * |

Approximate significance of smooth terms:

| | edf | Ref.df | F | p-value | Signif. |
|---------------|-------|--------|--------|----------|---------|
| s(Long,Lat) | 6.767 | 6.767 | 11.547 | 3.73E-14 | *** |
| s(Julian Day) | 5.475 | 5.475 | 12.018 | 2.00E-12 | *** |
| s(Timehour) | 2.815 | 2.815 | 7.665 | 6.58E-05 | *** |

Table 7: Parameter estimates, standard errors, probability values for the GAMM investigating gannet counts as a function of latitude and longitude, Julian day, time of day and glare extent.

| | Estimate | Std. error | Wald | Pr (> W) | Signif. |
|-----------------|----------|------------|--------|-----------|---------|
| (Intercept) | 0.84133 | 0.06367 | 13.215 | <2e-16 | *** |
| Glare: Slight | -0.1514 | 0.09454 | -1.602 | 0.109 | |
| Glare: Moderate | 0.17815 | 0.12084 | 1.474 | 0.141 | |
| Glare: Severe | 0.14506 | 0.14386 | 1.008 | 0.313 | |

R-sq.(adj) = 0.0436 Scale est. = 3.0006 n = 3140

Figure 13: The estimated spatial pattern of relative number of gannets observed. The solid line is the smoothing curve for 0, red dotted lines are -1 standard error from the smoothing curve and the green dotted lines are +1 standard error from the smoothing curve.

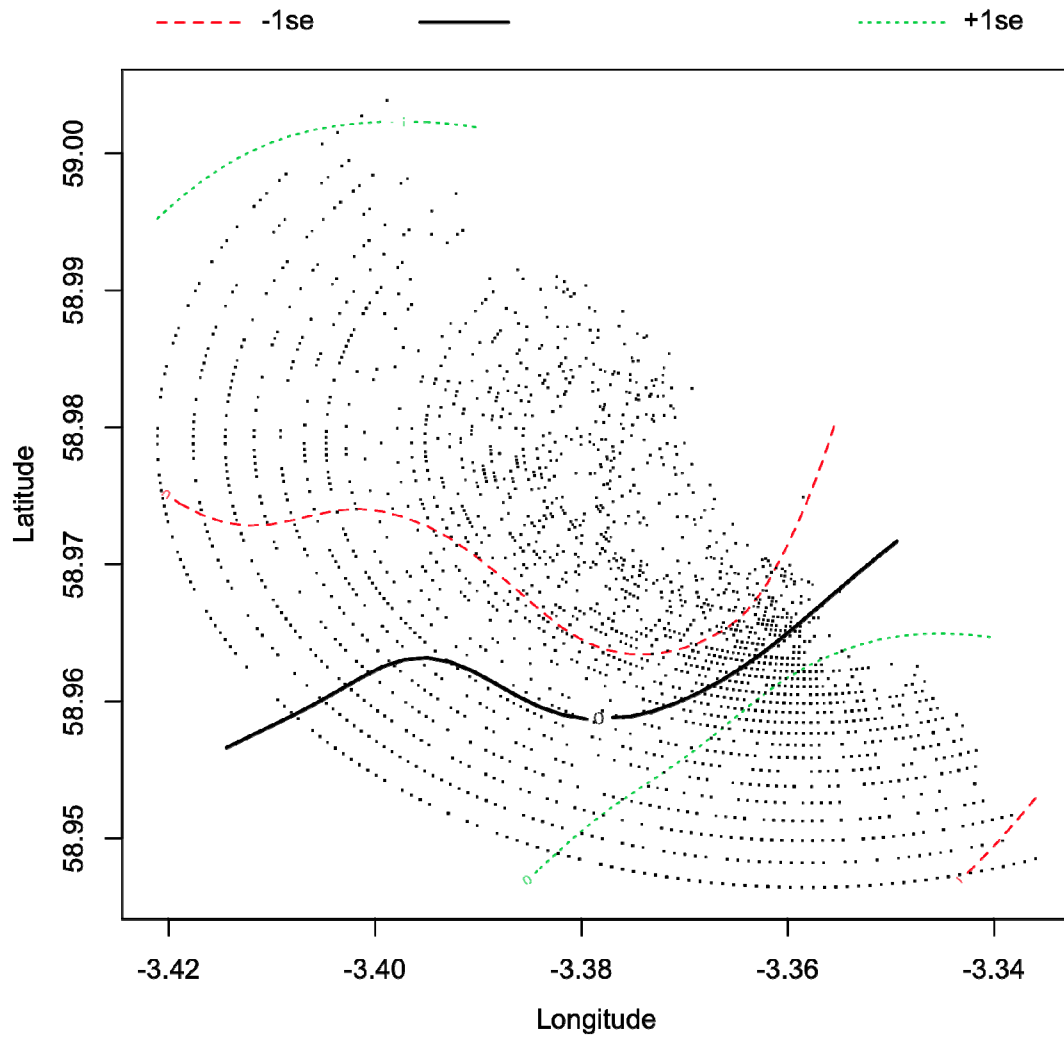


Figure 14: The estimated seasonal pattern of relative number of gannets observed. The solid line is the smoothing curve for Julian day and dotted lines are 95% confidence bands.

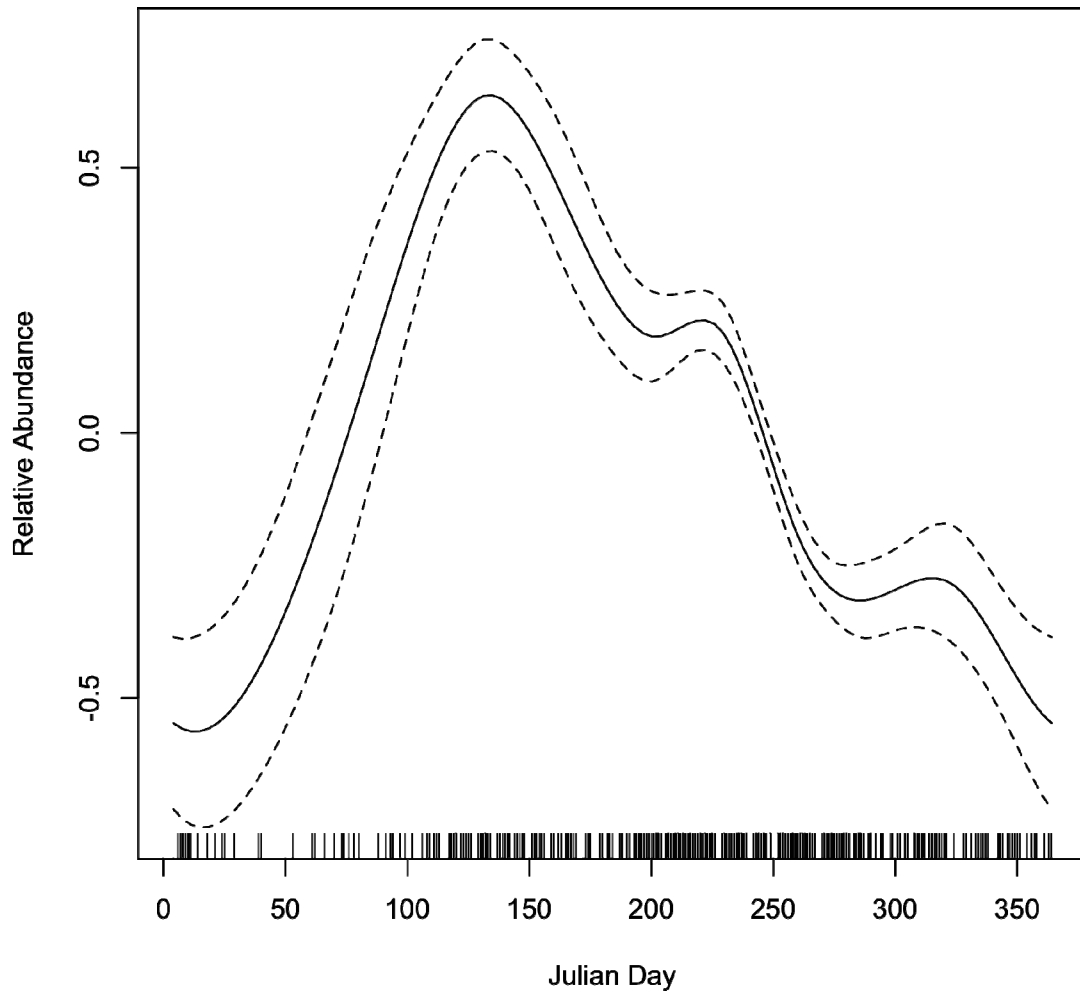


Figure 15: The estimated diurnal pattern of relative number of gannets observed. The solid line is the smoothing curve for time of day (hours) and dotted lines are 95% confidence bands.

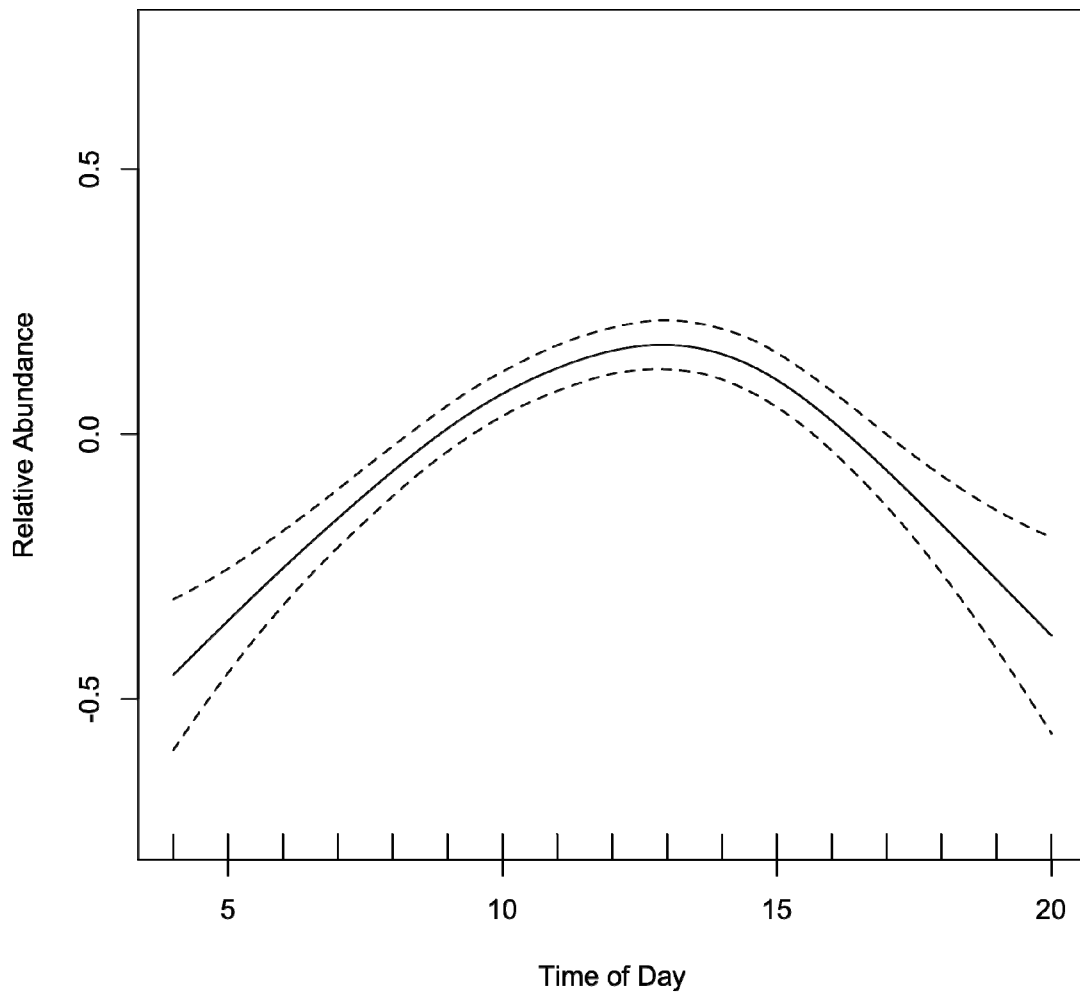


Figure 16: GAMM coefficient estimates (and standard errors) for gannets observed by glare extent at Billia Croo.

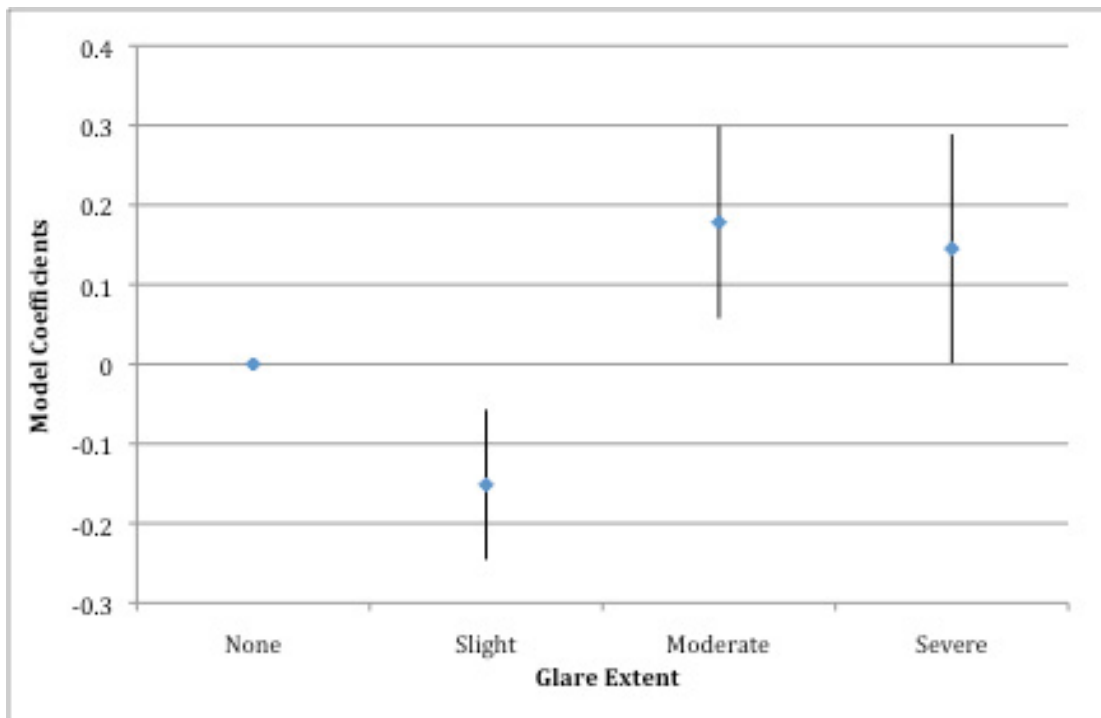
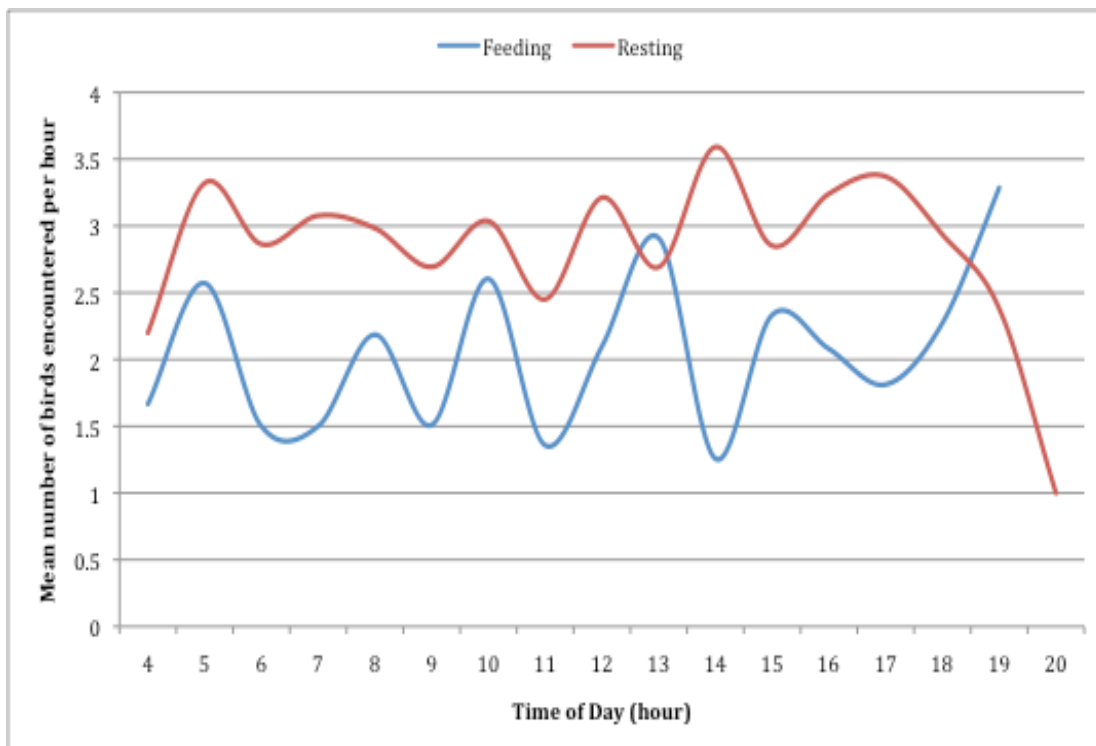


Figure 17: Mean number of feeding and resting gannets observed per hour, throughout the day at Billia Croo.



European Shag

Table 8: The significance of the parametric and smooth terms in the chosen model for shag use of Billia Croo.

Model: gamm(NUMBER~s(Long,Lat)+s(JULIANDAY,bs="cc")+s(TimetolowHR2,bs="cc")+oGLAREEXTENT+Observer, correlation=corAR1 (form=~1|DAYLAPSE), family=negative.binomial (theta=1), gamma=1.4,data=shag5K1)

Significance of parametric terms:

| | df | F | p-value | Signif. |
|--------------|----|--------|----------|---------|
| Glare Extent | 3 | 1.592 | 0.189 | |
| Observer | 1 | 17.928 | 2.32E-05 | *** |

Approximate significance of smooth terms:

| | edf | Ref.df | F | p-value | Signif. |
|---------------------|--------|--------|--------|---------|---------|
| s(Long,Lat) | 18.875 | 18.875 | 16.828 | <2e-16 | *** |
| s(Julian Day) | 6.484 | 6.484 | 25.769 | <2e-16 | *** |
| s(Time to low tide) | 1.652 | 1.652 | 3.617 | 0.0351 | *** |

Table 9: Parameter estimates, standard errors, probability values for the GAMM investigating shag counts as a function of latitude and longitude, Julian day, time to low tide and glare extent.

| | Estimate | Std. error | Wald | Pr (> W) | Signif. |
|-----------------|----------|------------|--------|-----------|---------|
| (Intercept) | 0.86682 | 0.08829 | 9.818 | < 2e-16 | *** |
| Glare: Slight | 0.04418 | 0.09228 | 0.479 | 0.6321 | |
| Glare: Moderate | 0.03131 | 0.12476 | 0.251 | 0.8018 | |
| Glare: Severe | -0.29794 | 0.13902 | -2.143 | 0.0321 | * |
| Observer: SW | 0.42843 | 0.10118 | 4.234 | 2.32E-05 | *** |

R-sq.(adj) = 0.0481 Scale est. = 5.1604 n = 7498

Figure 18: The estimated spatial pattern of relative number of shag observed. The solid line is the smoothing curve for 0, red dotted lines are -1 standard error from the smoothing curve and the green dotted lines are +1 standard error from the smoothing curve.

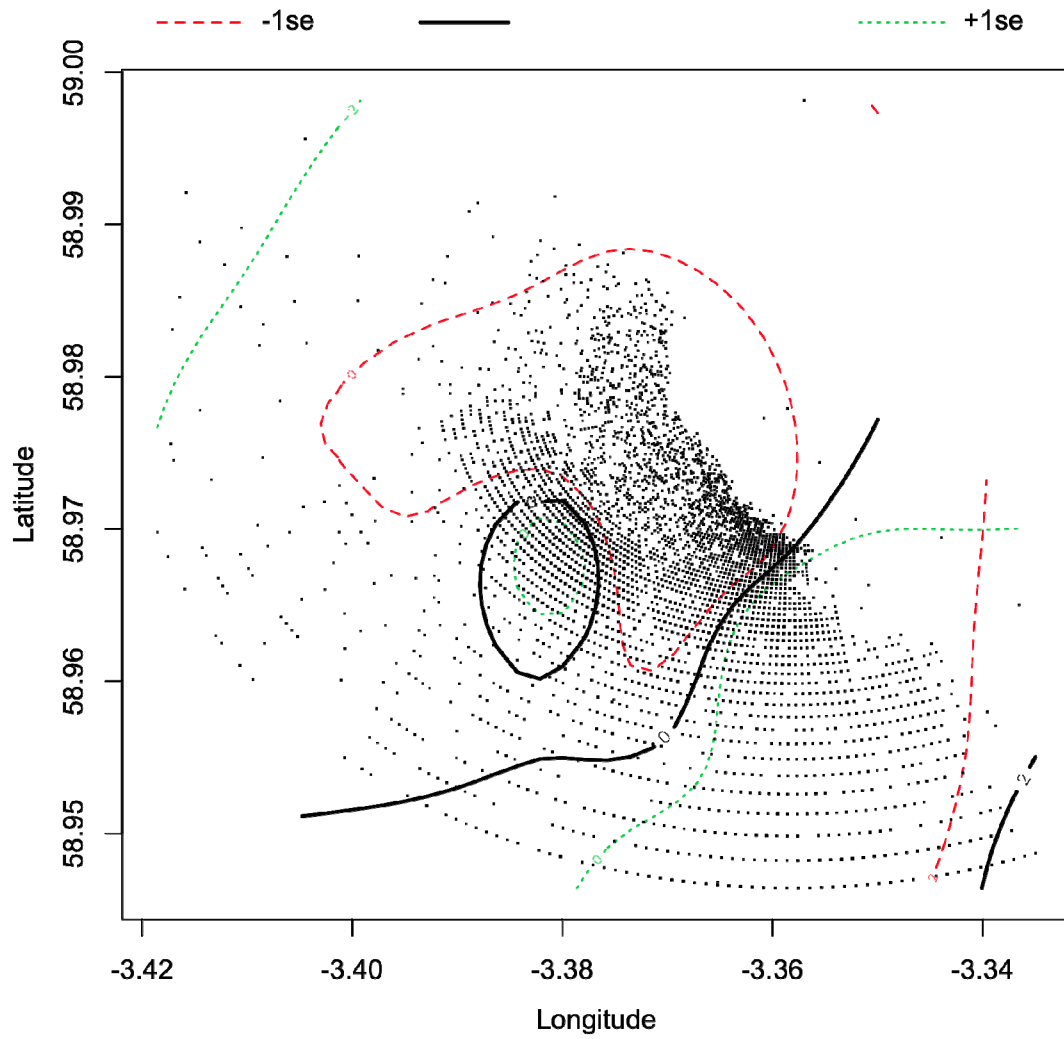


Figure 19: The estimated seasonal pattern of relative number of shag observed. The solid line is the smoothing curve for Julian day and dotted lines are 95% confidence bands.

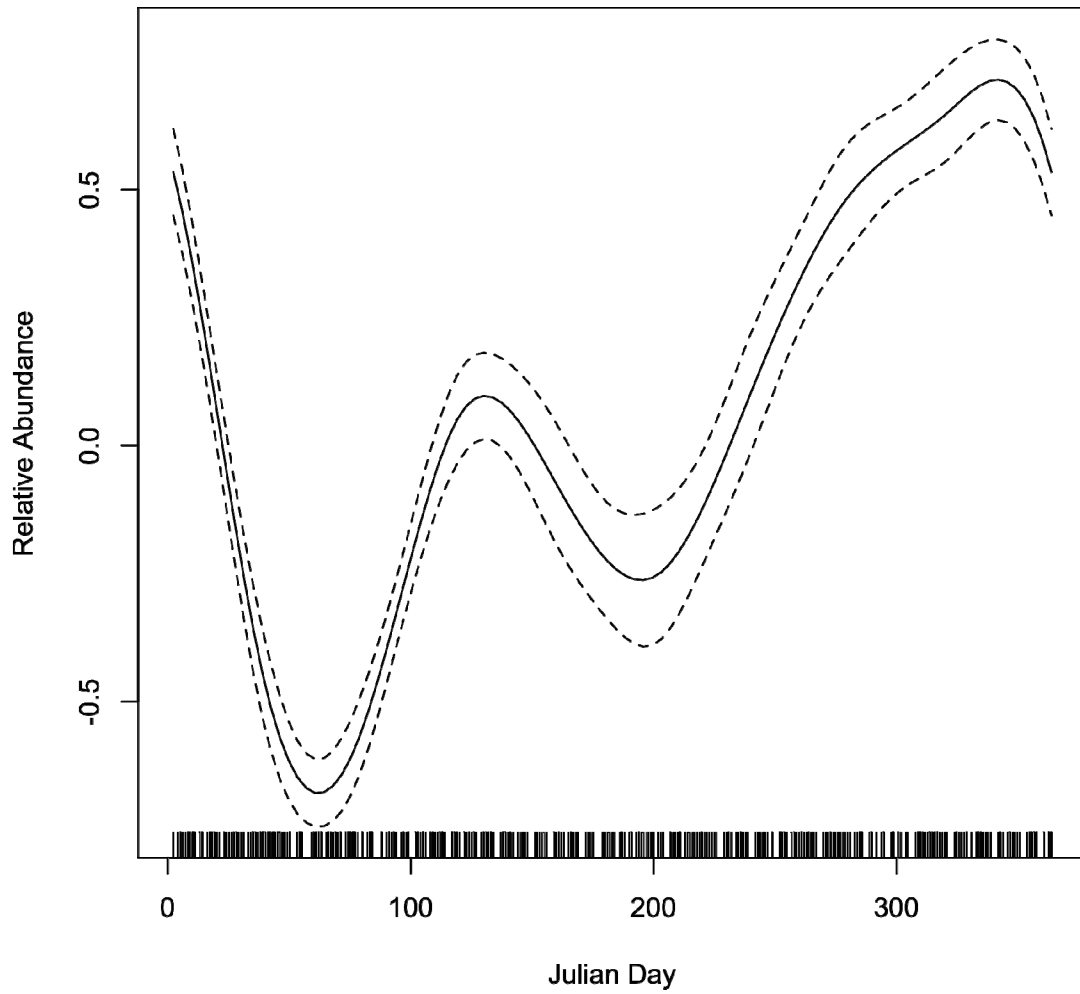


Figure 20: The estimated pattern of change in relative number of shag observed across the semi-diurnal tidal cycle. The solid line is the smoothing curve for time from low tide (hours) and dotted lines are 95% confidence bands.

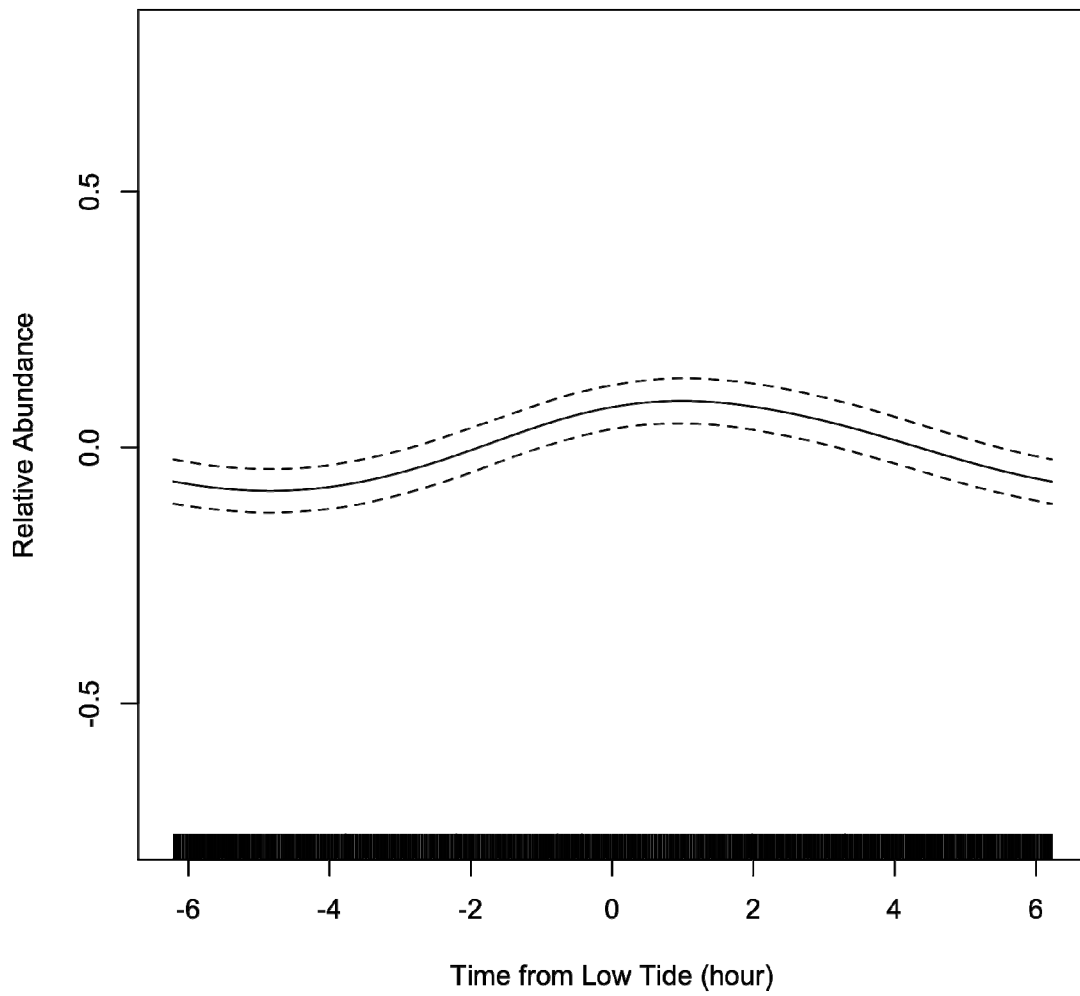


Figure 21: GAMM coefficient estimates (and standard errors) for shags observed by glare extent at Billia Croo.

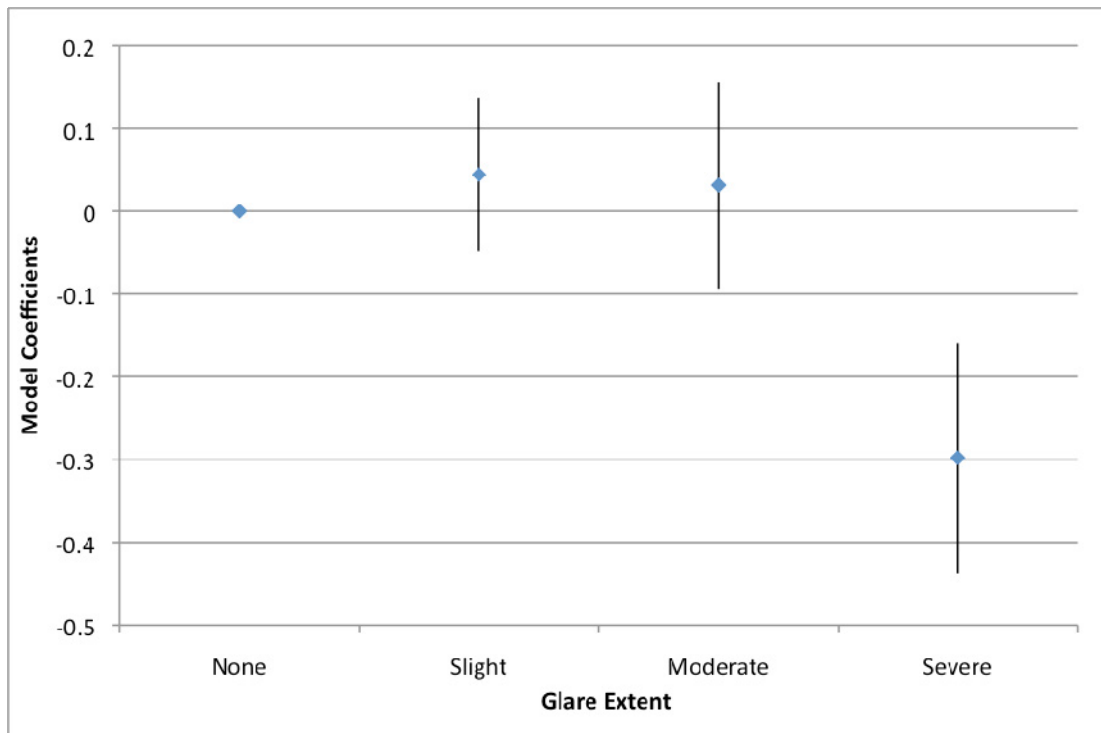


Figure 22: Mean number of feeding and resting shag observed per hour, throughout the day at Billia Croo.

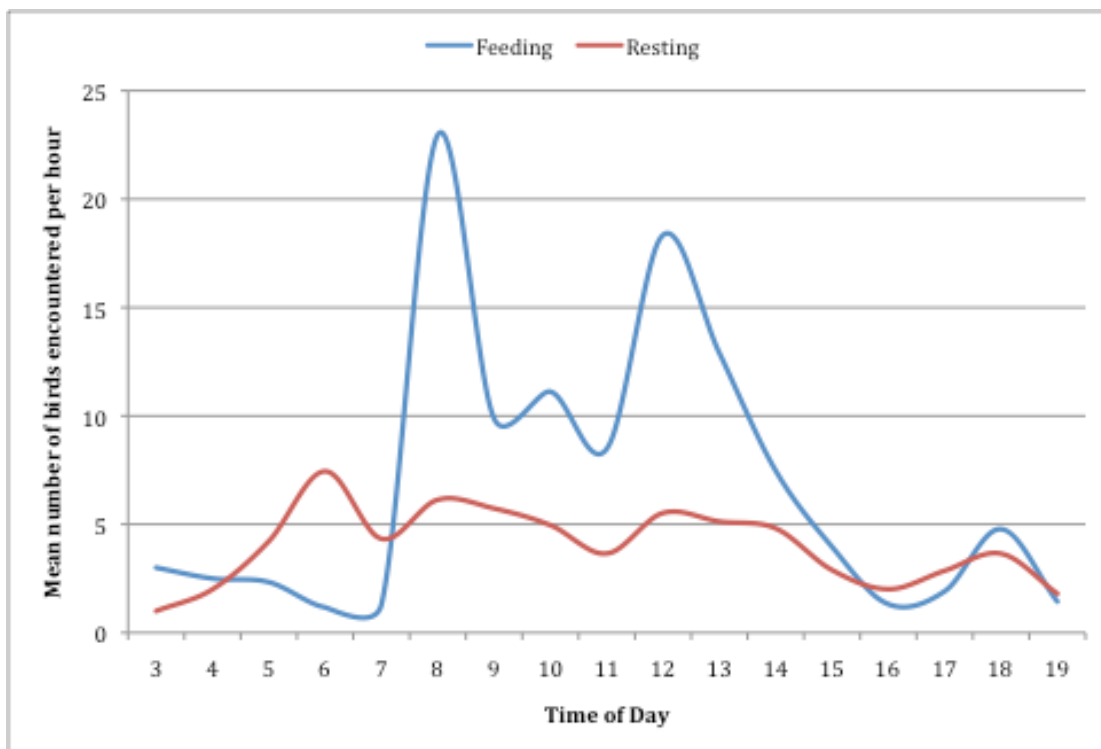
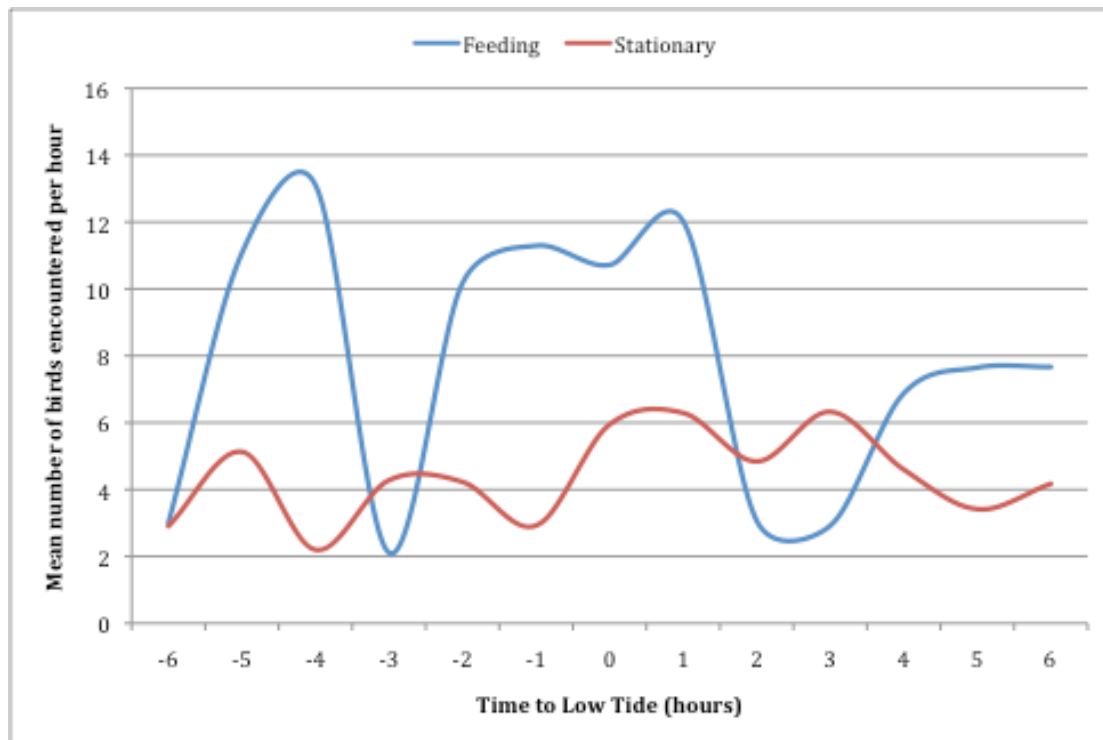


Figure 23: Mean number of feeding and resting shag observed per hour, by time from low tide at Billia Croo.



Great Skua

Table 10: The significance of the parametric and smooth terms in the chosen model for great skua use of Billia Croo.

Model: `gamm(NUMBER~s(Long,Lat,by=FLOCK)+oGLAREEXTENT+Observer, correlation=corAR1(form=~1|DAYLAPSE), family=negative.binomial(theta=2.557), gamma=1.4,data=bonxie1)`

Significance of parametric terms:

| | df | F | p-value | Signif. |
|--------------|----|-------|---------|---------|
| Glare Extent | 3 | 0.95 | 0.4157 | |
| Observer | 1 | 6.013 | 0.0144 | * |

Approximate significance of smooth terms:

| | edf | Ref.df | F | p-value | Signif. |
|------------------------|-------|--------|-------|----------|---------|
| s(Long,Lat): Mixed sp. | 21.85 | 21.85 | 4.064 | 1.66E-09 | *** |
| s(Long,Lat): Single Sp | 2 | 2 | 2.341 | 0.0968 | . |

Table 11: Parameter estimates, standard errors, probability values for the GAMM investigating great skua counts as a function of latitude and longitude by flock (mixed or single species), glare extent and observer.

| | Estimate | Std. error | Wald | Pr (> W) | Signif. |
|-----------------|----------|------------|--------|-----------|---------|
| (Intercept) | 0.49132 | 0.08589 | 5.721 | 1.44E-08 | *** |
| Glare: Slight | -0.08218 | 0.10691 | -0.769 | 0.4423 | |
| Glare: Moderate | -0.04199 | 0.13433 | -0.313 | 0.7546 | |
| Glare: Severe | -0.18297 | 0.15718 | -1.164 | 0.2447 | |
| Observer: SW | -0.20868 | 0.0851 | -2.452 | 0.0144 | * |

R-sq.(adj) = 0.211 Scale est. = 1.1054 n = 948

Figure 24: The estimated spatial pattern of relative number of great skua observed with other species. The solid line is the smoothing curve for 0, red dotted lines are -1 standard error from the smoothing curve and the green dotted lines are +1 standard error from the smoothing curve.

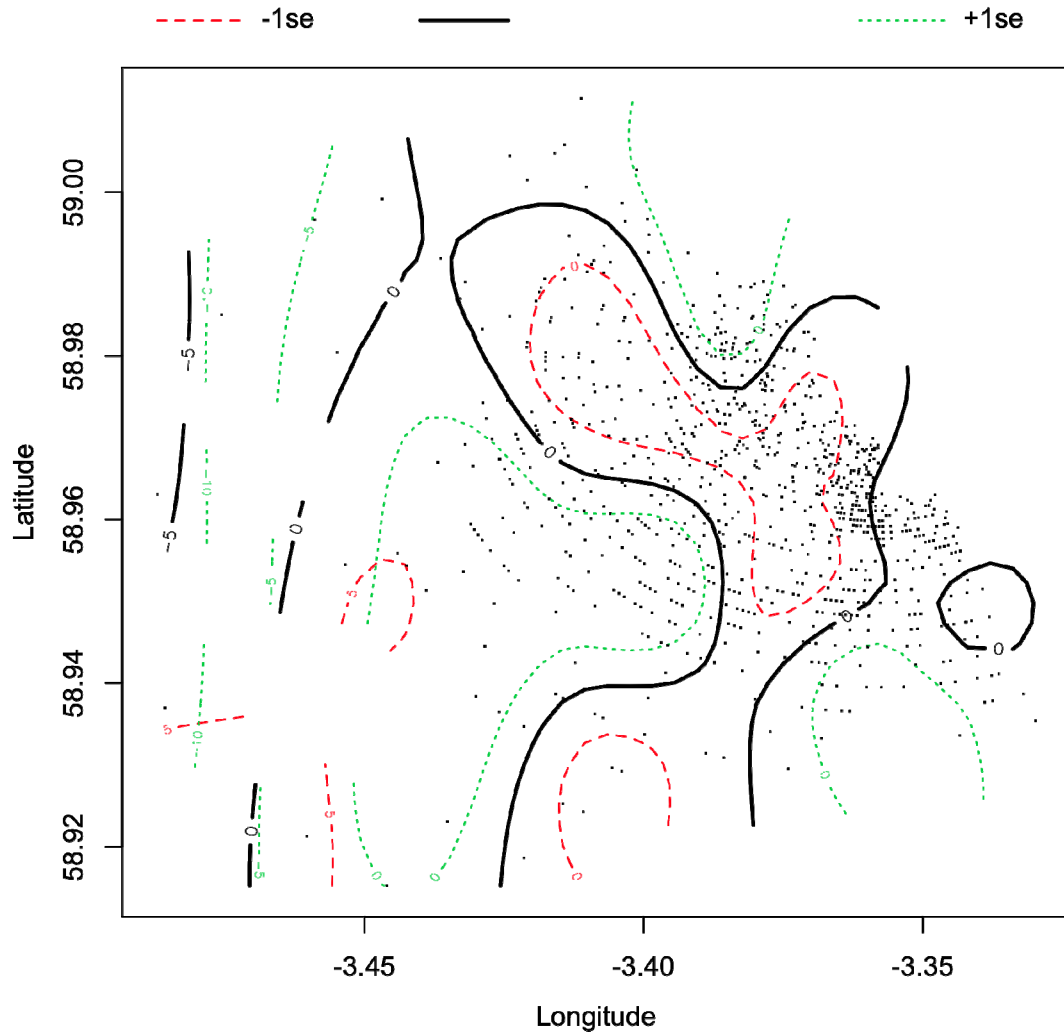


Figure 25: The estimated spatial pattern of relative number of great skua observed in single species groups. The solid line is the smoothing curve for 0, red dotted lines are -1 standard error from the smoothing curve and the green dotted lines are +1 standard error from the smoothing curve.

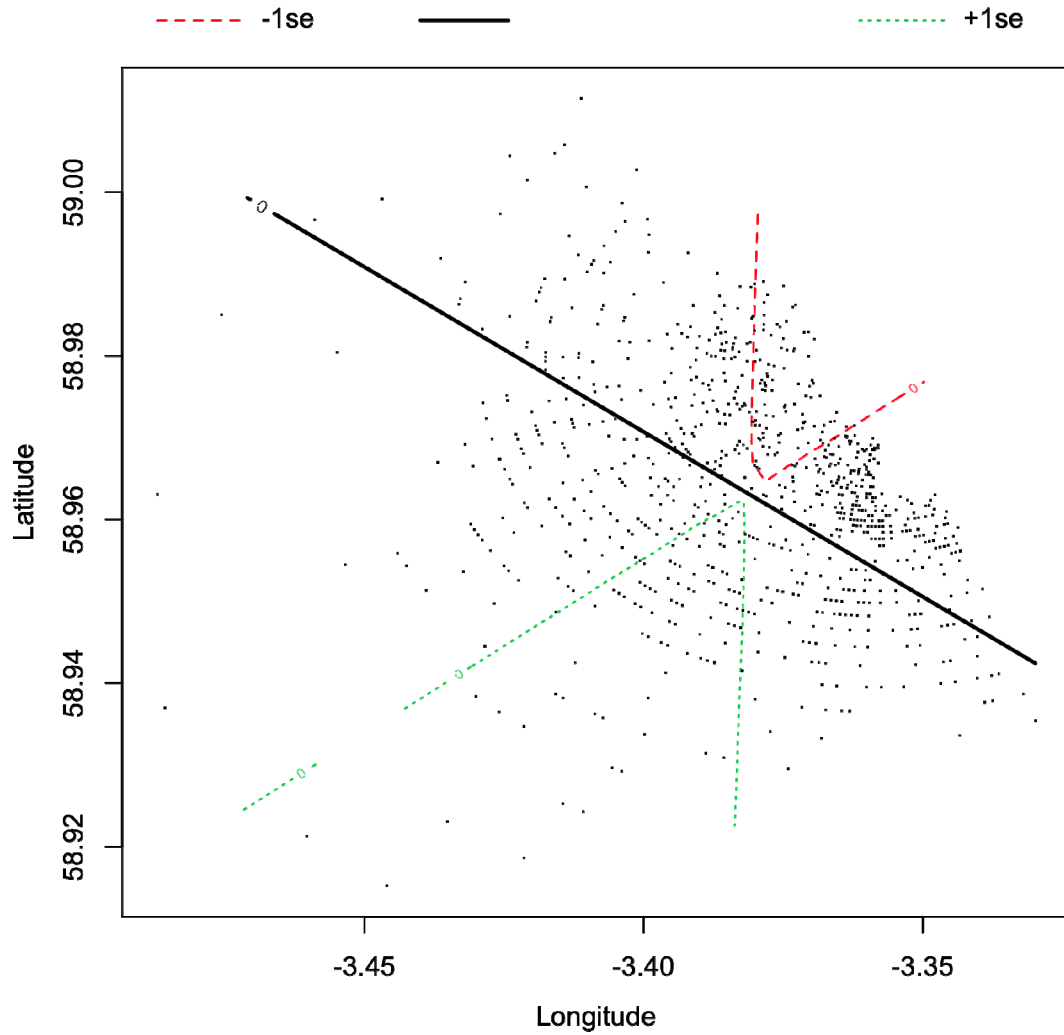


Figure 26: GAMM coefficient estimates (and standard errors) for great skua observed by glare extent at Billia Croo.

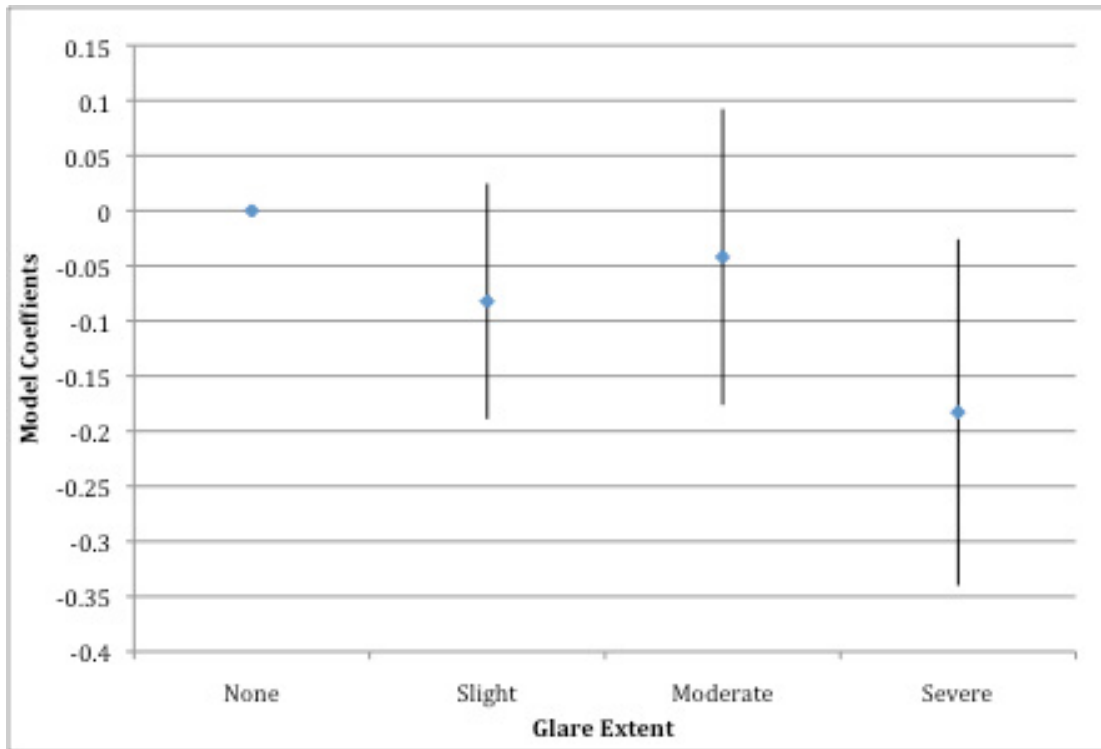
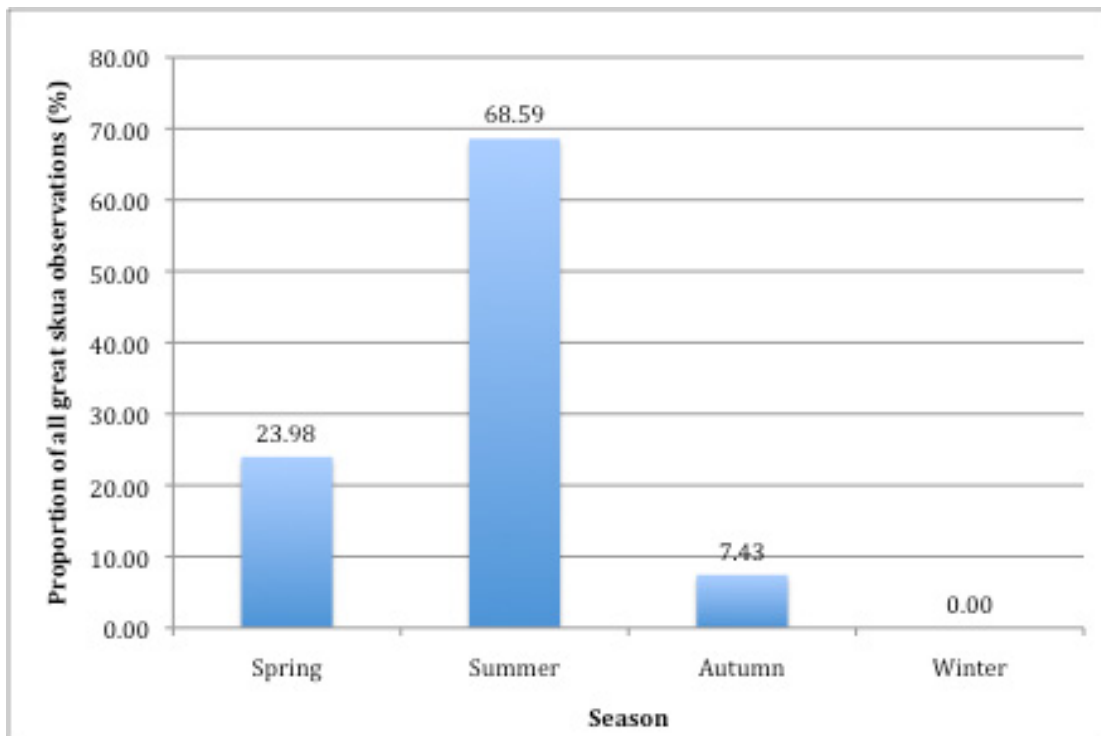


Figure 27: The proportion of great skua sightings by season, at Billia Croo.



Larus spp.

Table 12: The significance of the parametric and smooth terms in the chosen model for *Larus spp.* use of Billia Croo.

Model: gamm(NUMBER~s(Long,Lat)+s(JULIANDAY, bs="cc", by=SPECIES)
+WIND.STRENGTH+oGLAREEXTENT, correlation=corAR1
(form=~1|DAYLAPSE),
family=negative.binomial(theta=1.449),gamma=1.4,data=larus1)

Significance of parametric terms:

| | df | F | p-value | Signif. |
|---------------|----|--------|---------|---------|
| Wind Strength | 1 | 10.057 | 0.00157 | ** |
| Glare Extent | 3 | 1.301 | 0.27271 | |

Approximate significance of smooth terms:

| | edf | Ref.df | F | p-value | Signif. |
|--------------------------------------|-------|--------|-------|----------|---------|
| s(Long,Lat) | 7.627 | 7.627 | 2.425 | 0.015113 | * |
| s(Julian Day): Common | 2.556 | 2.556 | 6.517 | 0.000532 | *** |
| s(Julian Day): Great black-backed | 4.768 | 4.768 | 7.406 | 1.31E-06 | *** |
| s(Julian Day): Herring | 3.814 | 3.814 | 4.251 | 0.002446 | ** |
| s(Julian Day): <i>Larus spp.</i> | 2.08 | 2.08 | 9.514 | 6.26E-05 | *** |

Table 13: Parameter estimates, standard errors, probability values for the GAMM investigating *Larus spp.* counts as a function of latitude and longitude, Julian day by species, wind strength and glare extent.

| | Estimate | Std. error | Wald | Pr (> W) | Signif. |
|-----------------|-----------|------------|--------|-----------|---------|
| (Intercept) | 1.290865 | 0.137555 | 9.384 | < 2e-16 | *** |
| Wind Strength | -0.131901 | 0.041593 | -3.171 | 0.00157 | ** |
| Glare: Slight | 0.001433 | 0.14669 | 0.01 | 0.99221 | |
| Glare: Moderate | -0.308883 | 0.196107 | -1.575 | 0.11557 | |
| Glare: Severe | -0.240856 | 0.23575 | -1.022 | 0.3072 | |

R-sq.(adj) = 0.167 Scale est. = 2.6817 n = 992

Figure 28: The estimated spatial pattern of relative number of gulls observed. The solid line is the smoothing curve for 0, red dotted lines are -1 standard error from the smoothing curve and the green dotted lines are +1 standard error from the smoothing curve.

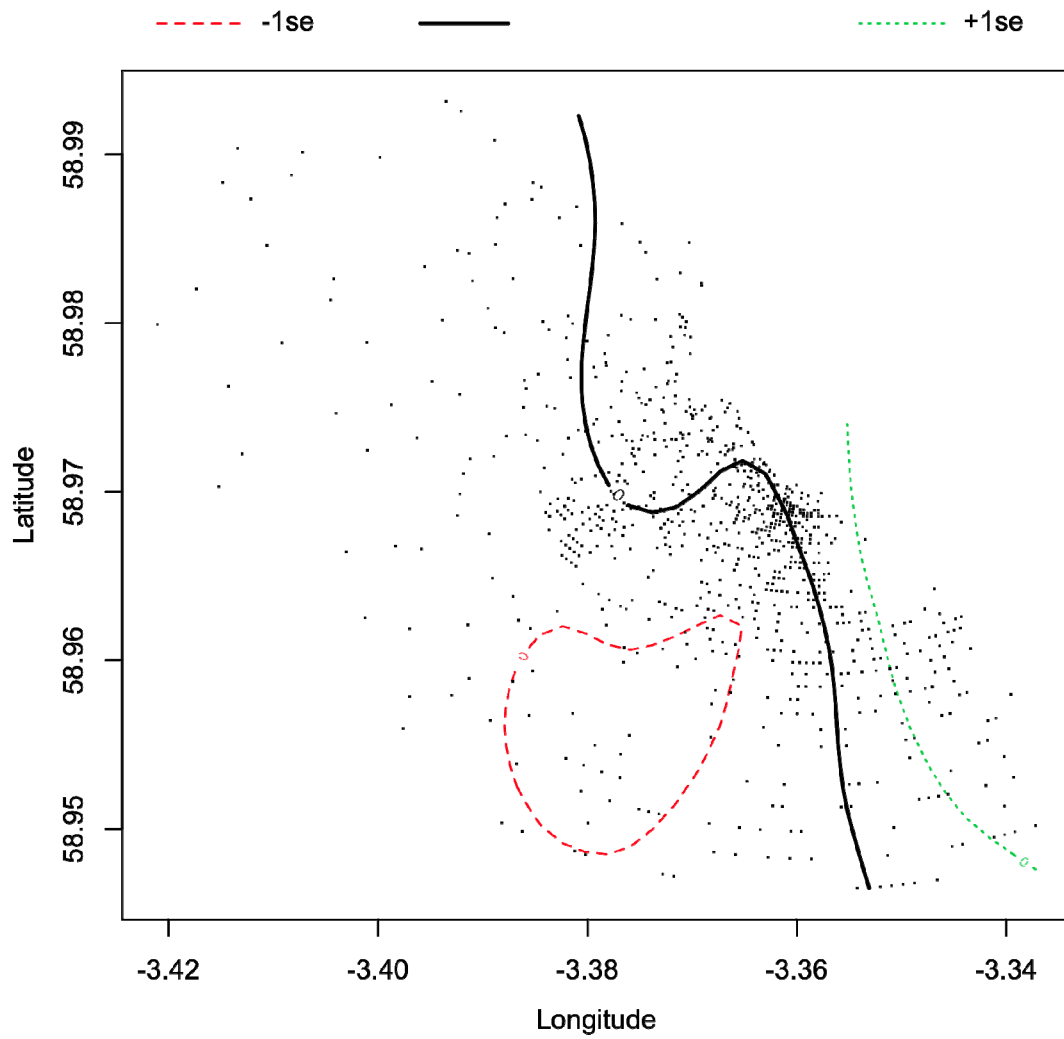


Figure 29: The estimated seasonal pattern of relative number of *Larus spp.* observed. The solid line is the smoothing curve for Julian day and dotted lines are 95% confidence bands.

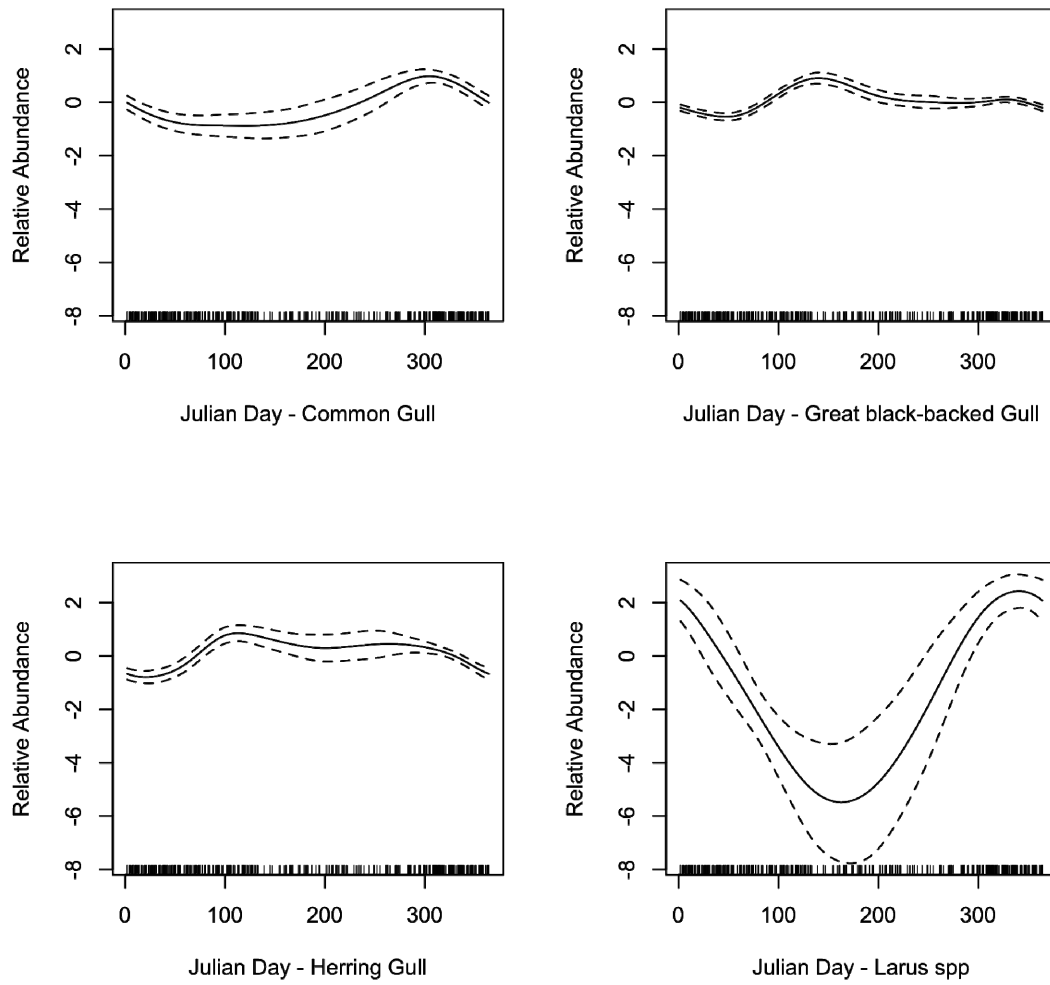


Figure 30: GAMM coefficient estimates (and standard errors) for *Larus spp.* observed by glare extent at Billia Croo.

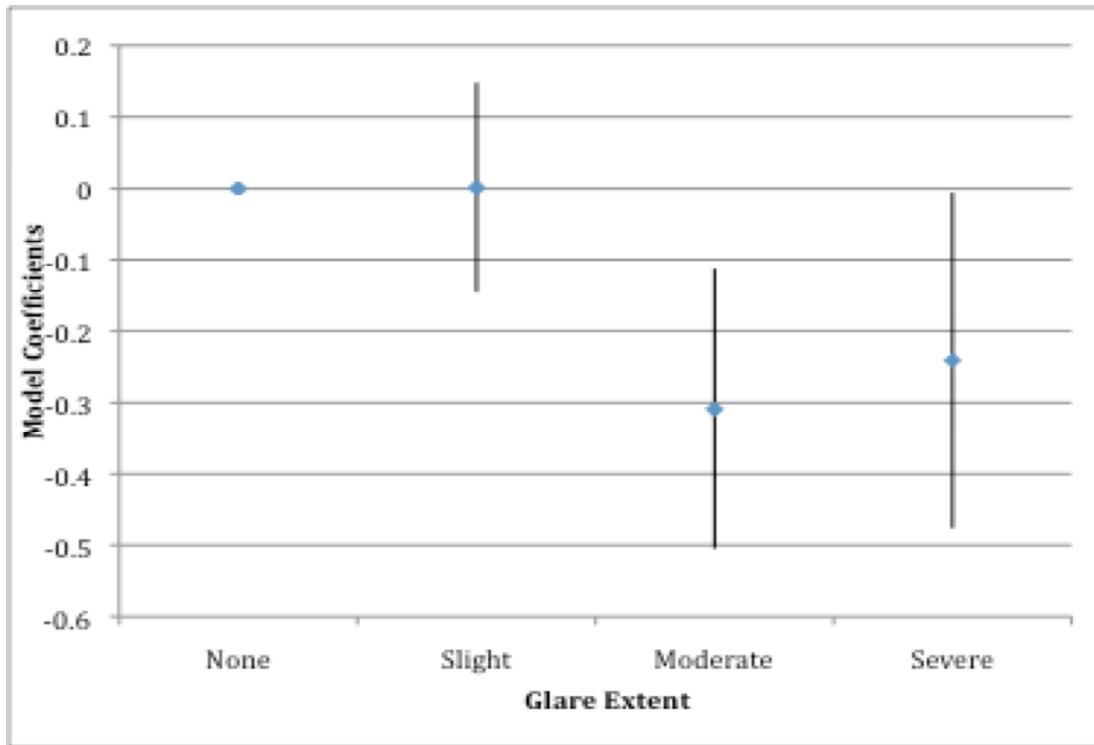


Figure 31: Mean number of gulls encountered, by wind strength at Billia Croo.

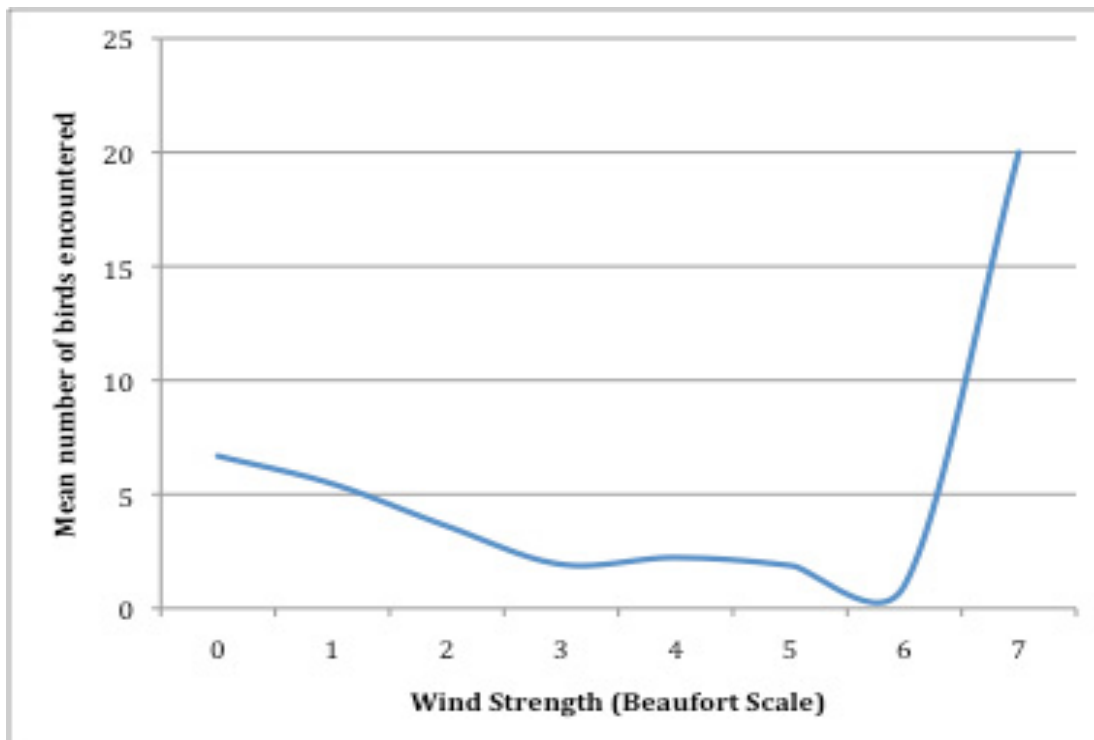


Figure 32: Proportion of *Larus spp.* sightings, by species at Billia Croo.

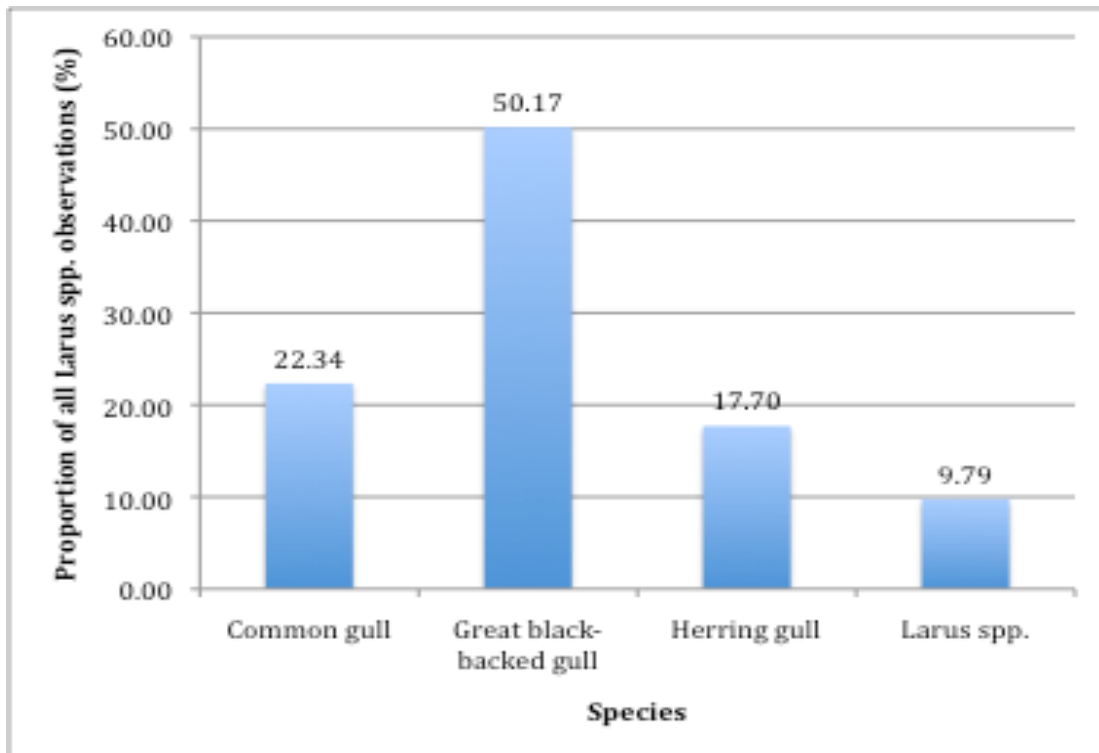


Figure 33: Proportions of all feeding and resting gull species, at Billia Croo.

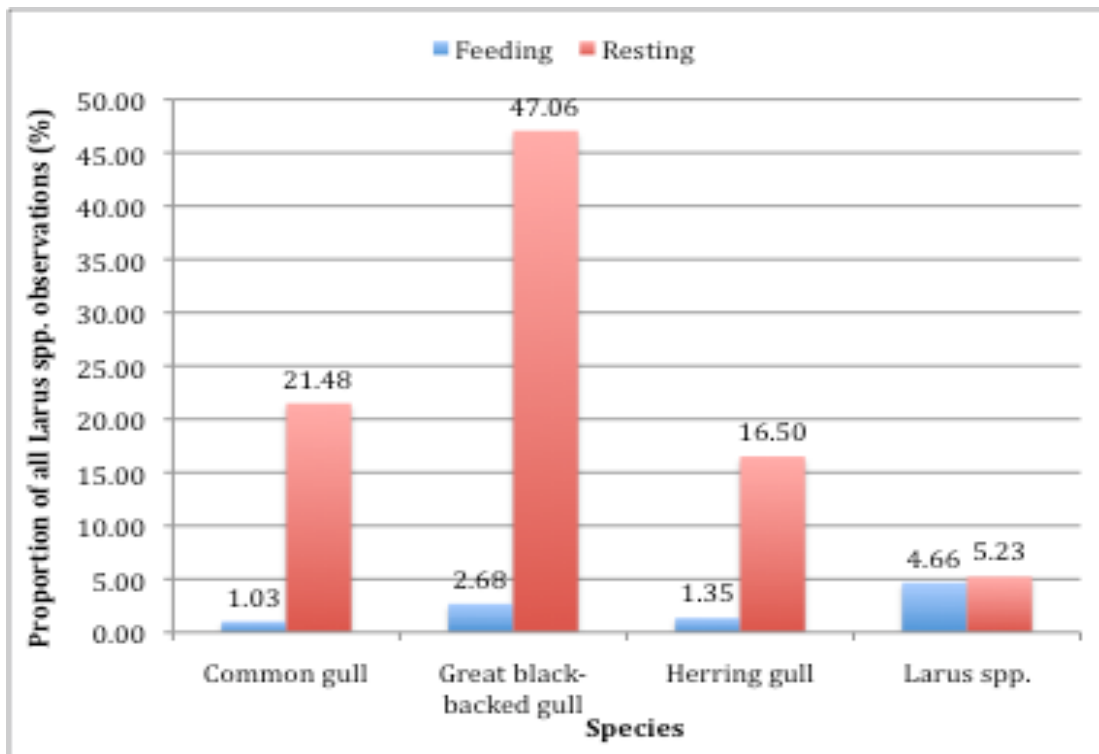
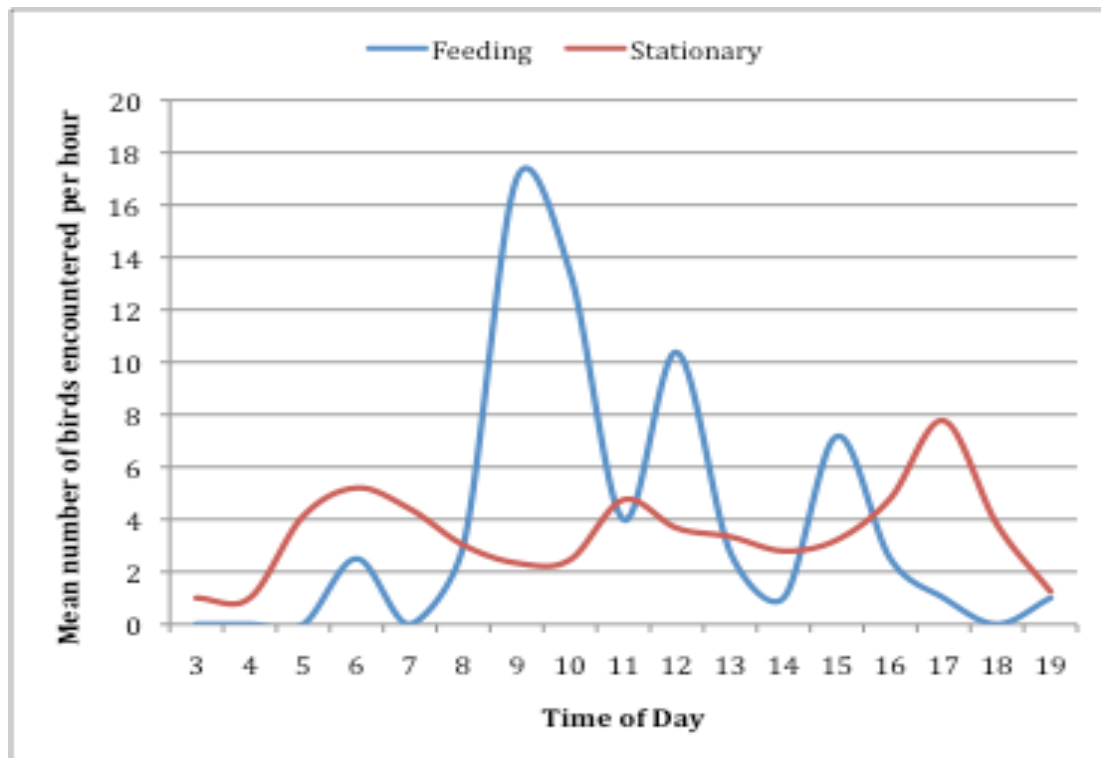


Figure 34: Mean number of feeding and resting gulls observed per hour, throughout the day at Billia Croo.



Black-legged Kittiwake

Table 14: The significance of the parametric and smooth terms in the chosen model for kittiwakes use of Billia Croo.

Model: `gamm(NUMBER~s(Long,Lat)+s(JULIANDAY,bs="cc")+s(TimetolowHR2,bs="cc")+WINDIR2+oGLAREEXTENT+Observer, correlation=corAR1(form=~1|DAYLAPSE), family=negative.binomial (theta=1), gamma=1.4, data=blki1)`

Significance of parametric terms:

| | df | F | p-value | Signif. |
|----------------|----|-------|---------|---------|
| Wind Direction | 4 | 2.753 | 0.02811 | * |
| Glare Extent | 3 | 3.058 | 0.02847 | * |
| Observer | 1 | 7.63 | 0.00606 | ** |

Approximate significance of smooth terms:

| | edf | Ref.df | F | p-value | Signif. |
|---------------------|-------|--------|--------|----------|---------|
| s(Long,Lat) | 2 | 2 | 26.732 | 1.74E-11 | *** |
| s(Julian Day) | 6.026 | 6.026 | 51.517 | < 2e-16 | *** |
| s(Time to Low Tide) | 3.639 | 3.639 | 3.015 | 0.0219 | * |

Table 15: Parameter estimates, standard errors, probability values for the GAMM investigating kittiwake counts as a function of latitude and longitude, Julian day, time from low tide, wind direction, glare extent and observer.

| | Estimate | Std. error | Wald | Pr (> W) | Signif. |
|-----------------------|----------|------------|--------|-----------|---------|
| (Intercept) | 1.61899 | 0.31459 | 5.146 | 4.58E-07 | *** |
| Wind Direction: North | 0.09936 | 0.3108 | 0.32 | 0.7494 | |
| Wind Direction: None | -0.02742 | 1.43873 | -0.019 | 0.98481 | |
| Wind Direction: South | -0.19124 | 0.30736 | -0.622 | 0.53423 | |
| Wind Direction: West | -0.71637 | 0.36811 | -1.946 | 0.05249 | . |
| Glare: Slight | -0.40584 | 0.20683 | -1.962 | 0.05058 | . |
| Glare: Moderate | -0.66525 | 0.23233 | -2.863 | 0.00446 | ** |
| Glare: Severe | -0.13907 | 0.25877 | -0.537 | 0.59135 | |
| Observer: SW | 0.49507 | 0.17923 | 2.762 | 0.00606 | ** |

R-sq.(adj) = 0.0268 Scale est. = 1.2993 n = 350

Figure 35: The estimated spatial pattern of relative number of kittiwakes observed. The solid line is the smoothing curve for 0, red dotted lines are -1 standard error from the smoothing curve and the green dotted lines are +1 standard error from the smoothing curve.

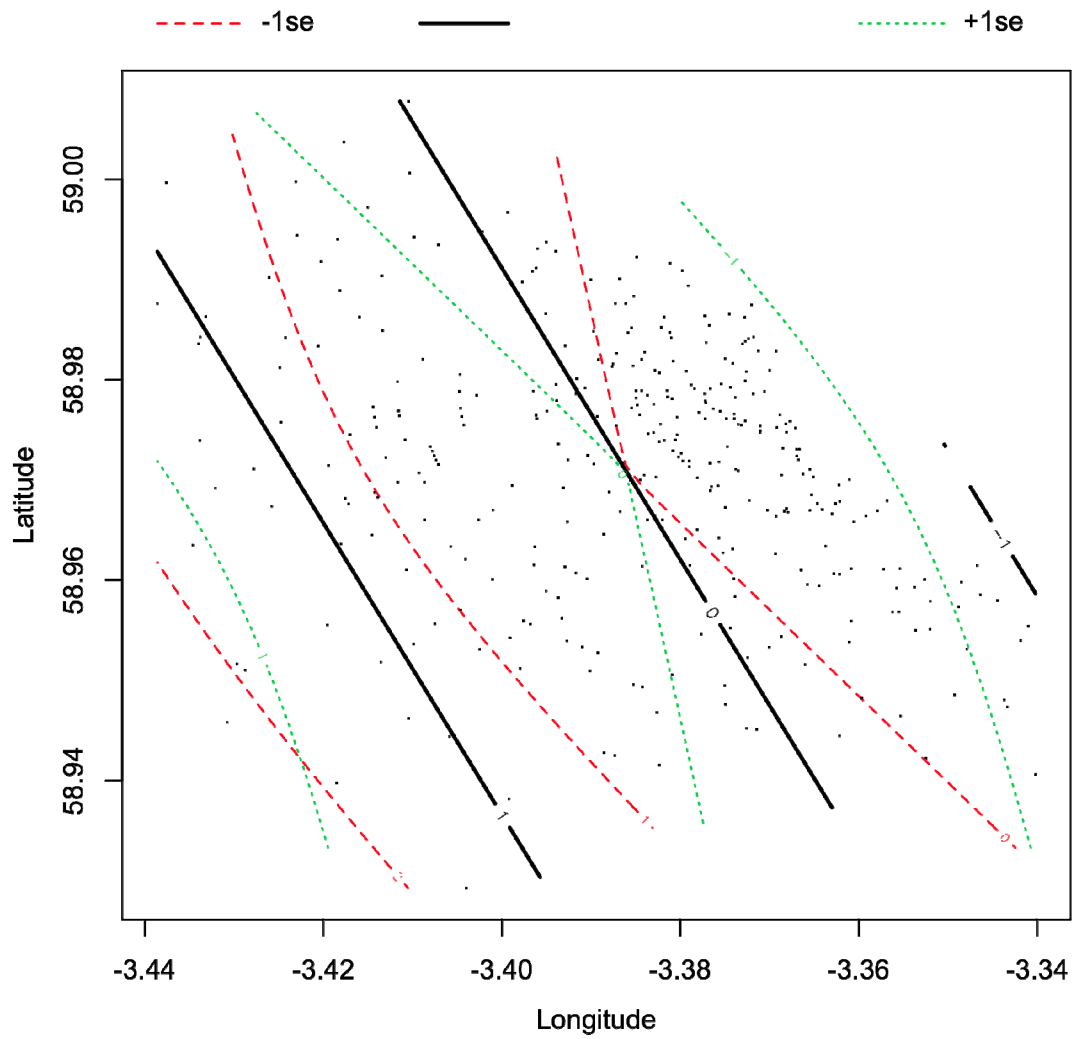


Figure 36: The estimated seasonal pattern of relative number of kittiwakes observed. The solid line is the smoothing curve for Julian day and dotted lines are 95% confidence bands.

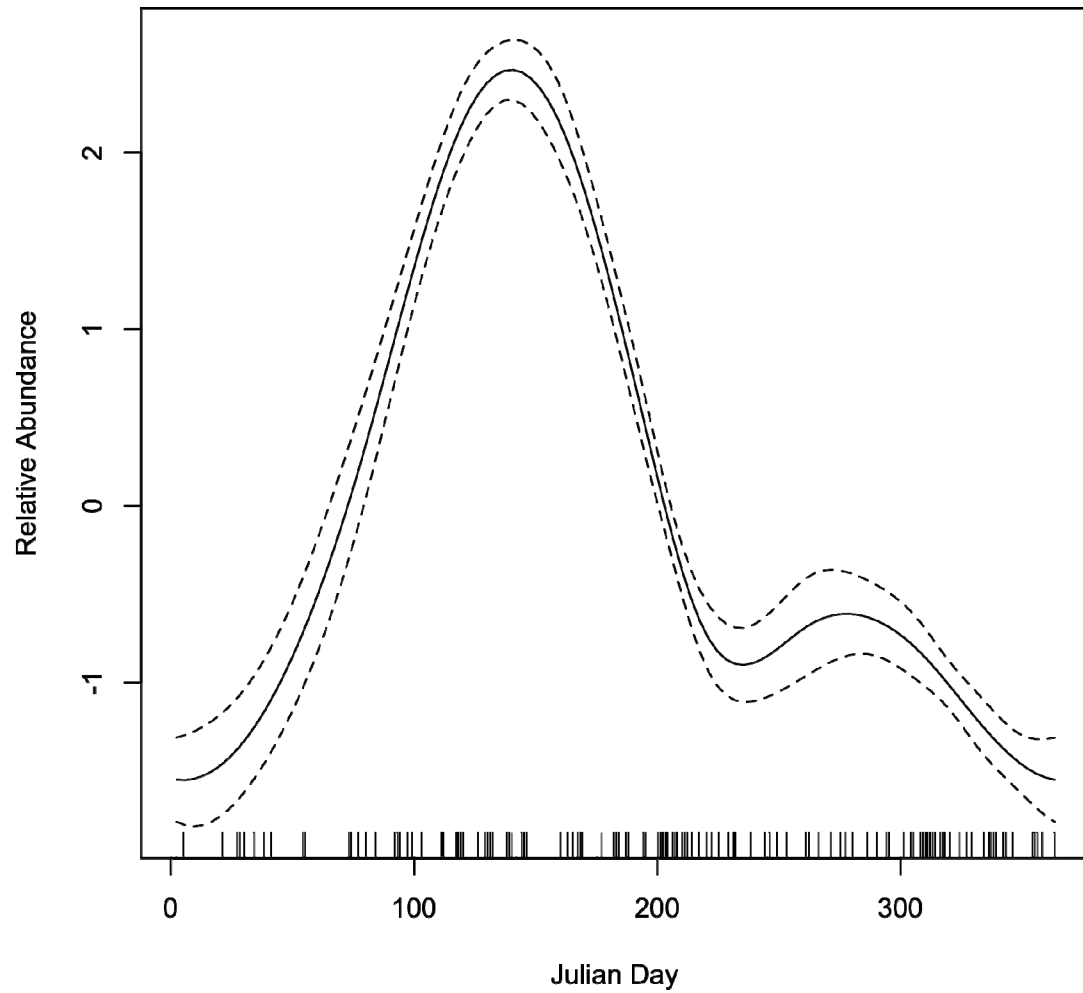


Figure 37: The estimated pattern of change in relative number of kittiwakes observed across the semi-diurnal tidal cycle. The solid line is the smoothing curve for time from low tide (hours) and dotted lines are 95% confidence bands.

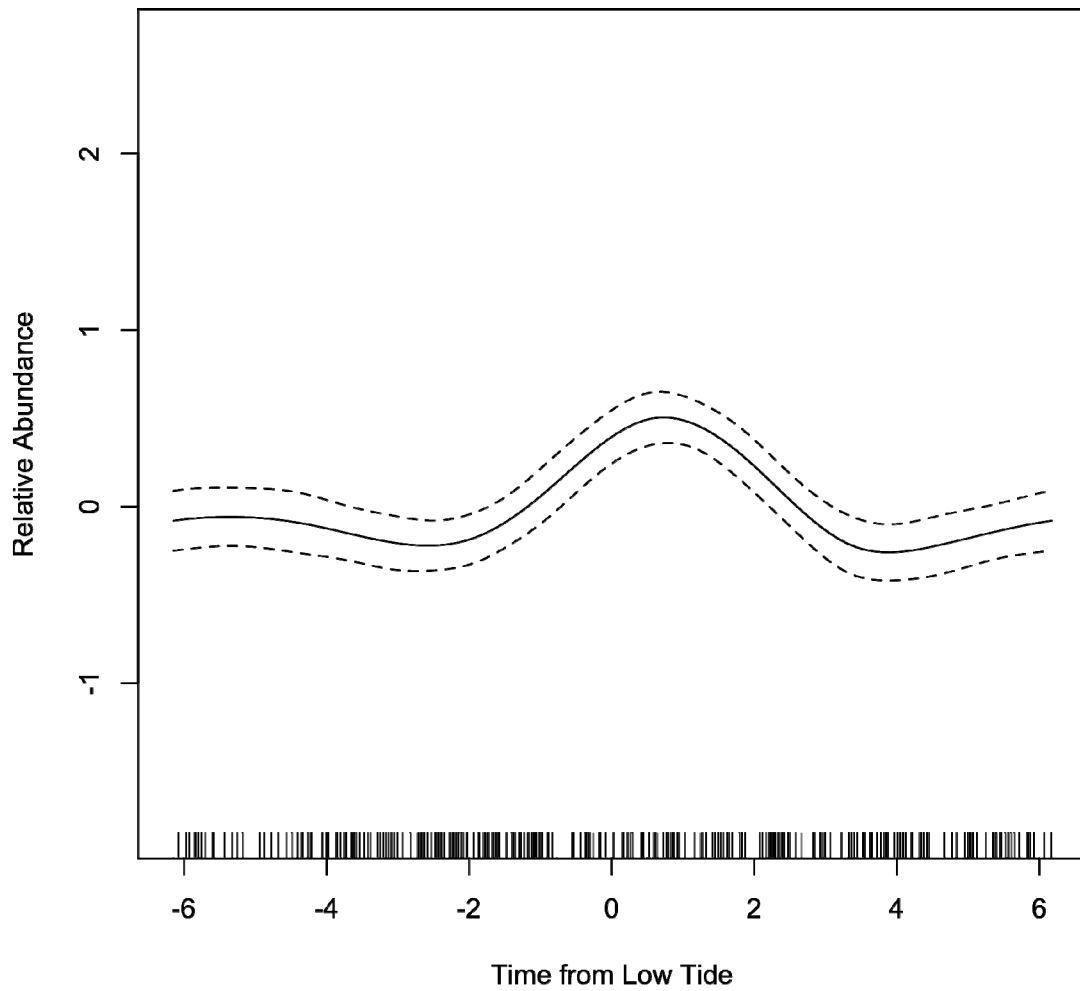


Figure 38: GAMM coefficient estimates (and standard errors) for kittiwakes observed by wind direction at Billia Croo.

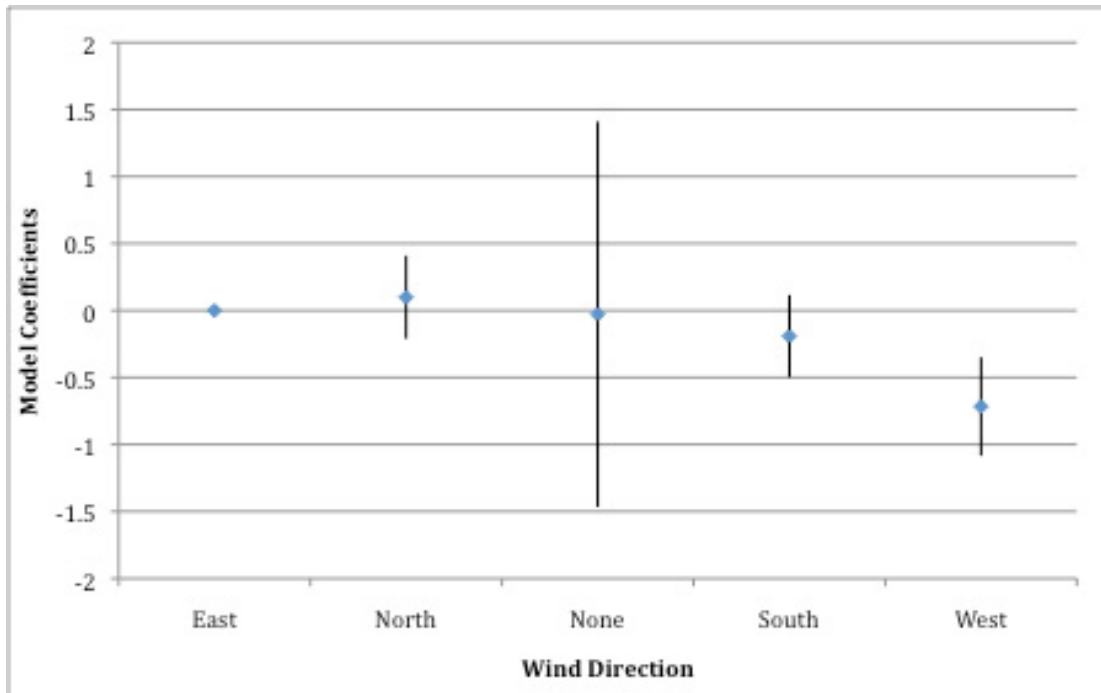


Figure 39: GAMM coefficient estimates (and standard errors) for kittiwakes observed by glare extent at Billia Croo.

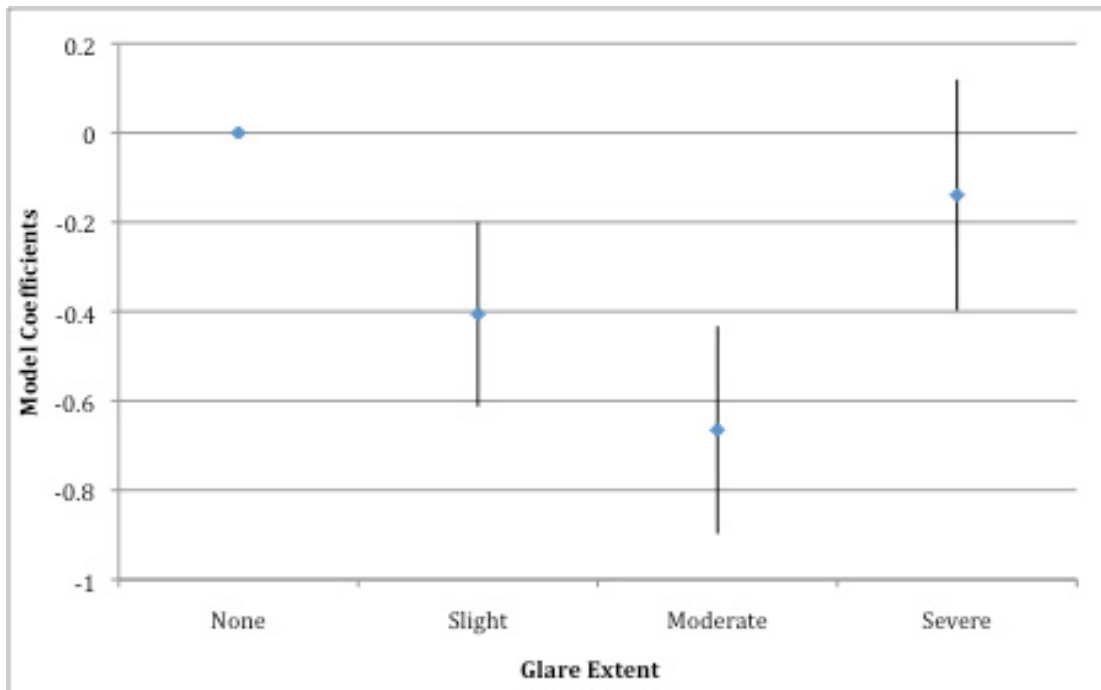
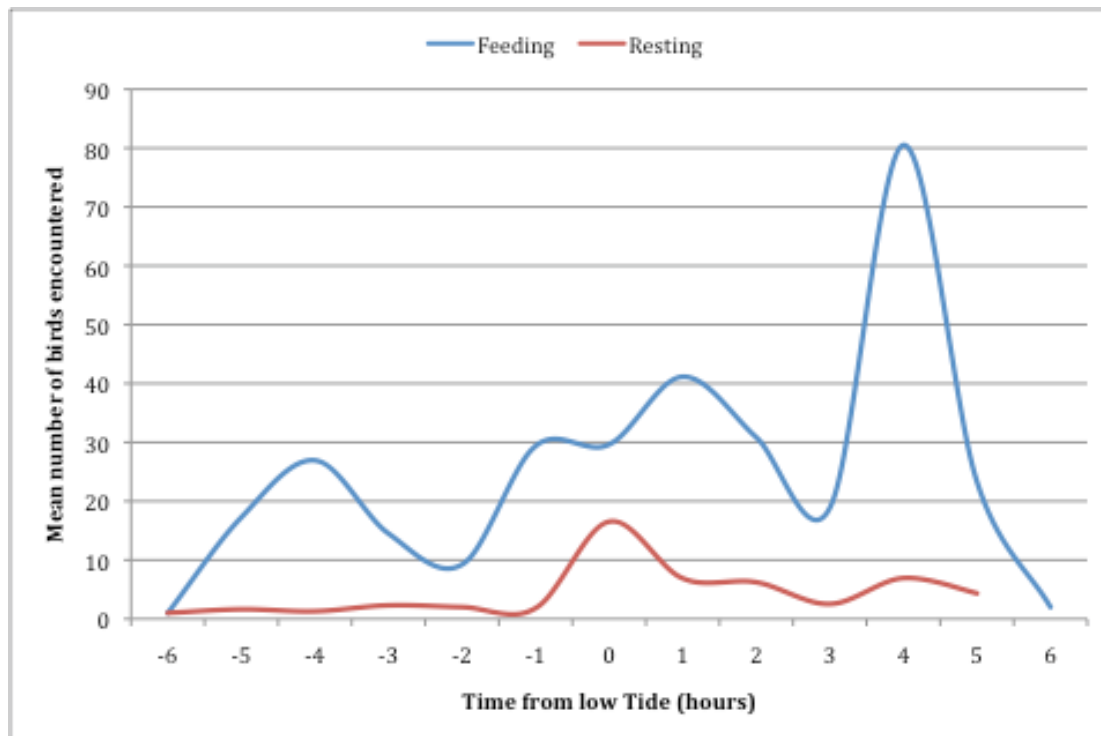


Figure 40: Mean number of feeding and resting kittiwakes observed per hour, throughout the day at Billia Croo.



Arctic Tern

Table 16: The significance of the parametric and smooth terms in the chosen model for Arctic tern use of Billia Croo.

Model: gamm(NUMBER~s(JULIANDAY,bs="cs")+s(TIMEHOUR)+WINDIR2+oGLAREEXTENT +Observer, correlation=corAR1(form=~1|DAYLAPSE), family=negative.binomial(theta=1), gamma=1.4,data=atern1)

Significance of parametric terms:

| | df | F | p-value | Signif. |
|----------------|----|--------|----------|---------|
| Wind Direction | 3 | 7.498 | 0.000172 | *** |
| Glare Extent | 3 | 4.497 | 0.005709 | ** |
| Observer | 1 | 22.179 | 1.01E-05 | *** |

Approximate significance of smooth terms:

| | edf | Ref.df | F | p-value | Signif. |
|----------------|-------|--------|-------|----------|---------|
| s(Julian Day) | 1.866 | 1.866 | 29.53 | 5.88E-10 | *** |
| s(Time of Day) | 5.103 | 5.103 | 6.768 | 2.25E-05 | *** |

Table 17: Parameter estimates, standard errors, probability values for the GAMM investigating Arctic tern counts as a function of Julian day, time of day, wind direction, glare extent and observer.

| | Estimate | Std. error | Wald | Pr (> W) | Signif. |
|-----------------------|-----------|------------|--------|-----------|---------|
| (Intercept) | 1.262311 | 0.800656 | 1.577 | 0.118785 | |
| Wind Direction: North | -0.002141 | 0.844206 | -0.003 | 0.997983 | |
| Wind Direction: South | 0.81901 | 0.809466 | 1.012 | 0.31465 | |
| Wind Direction: West | -0.806692 | 0.875962 | -0.921 | 0.359825 | |
| Glare: Slight | -1.385732 | 0.382923 | -3.619 | 0.000514 | *** |
| Glare: Moderate | -0.274654 | 0.375514 | -0.731 | 0.466639 | |
| Glare: Severe | -0.146863 | 0.361627 | -0.406 | 0.685727 | |
| Observer: SW | 1.460506 | 0.310121 | 4.709 | 1.01E-05 | *** |

R-sq.(adj) = -0.133 Scale est. = 0.9389 n = 96

Figure 41: The estimated seasonal pattern of relative number of Arctic tern observed. The solid line is the smoothing curve for Julian day and dotted lines are 95% confidence bands.

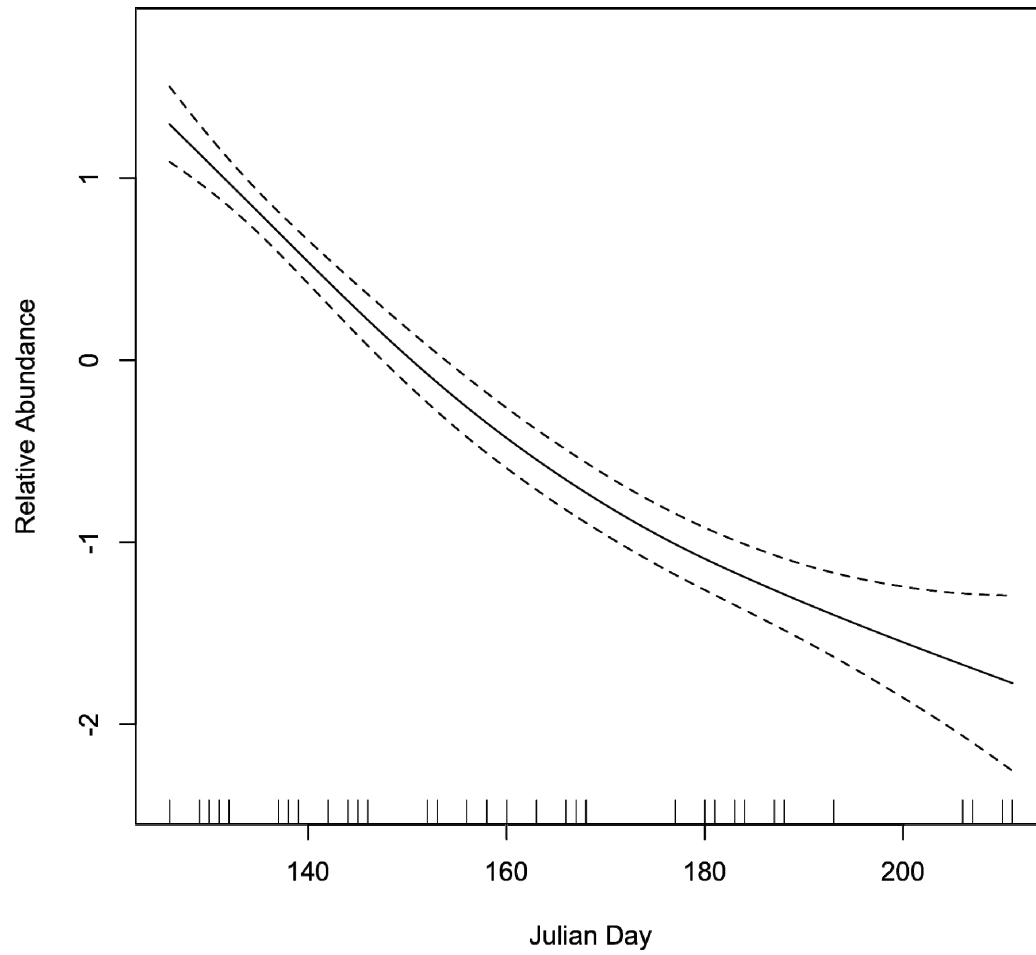


Figure 42: The estimated diurnal pattern of relative number of Arctic tern observed. The solid line is the smoothing curve for time of day (hours) and dotted lines are 95% confidence bands.

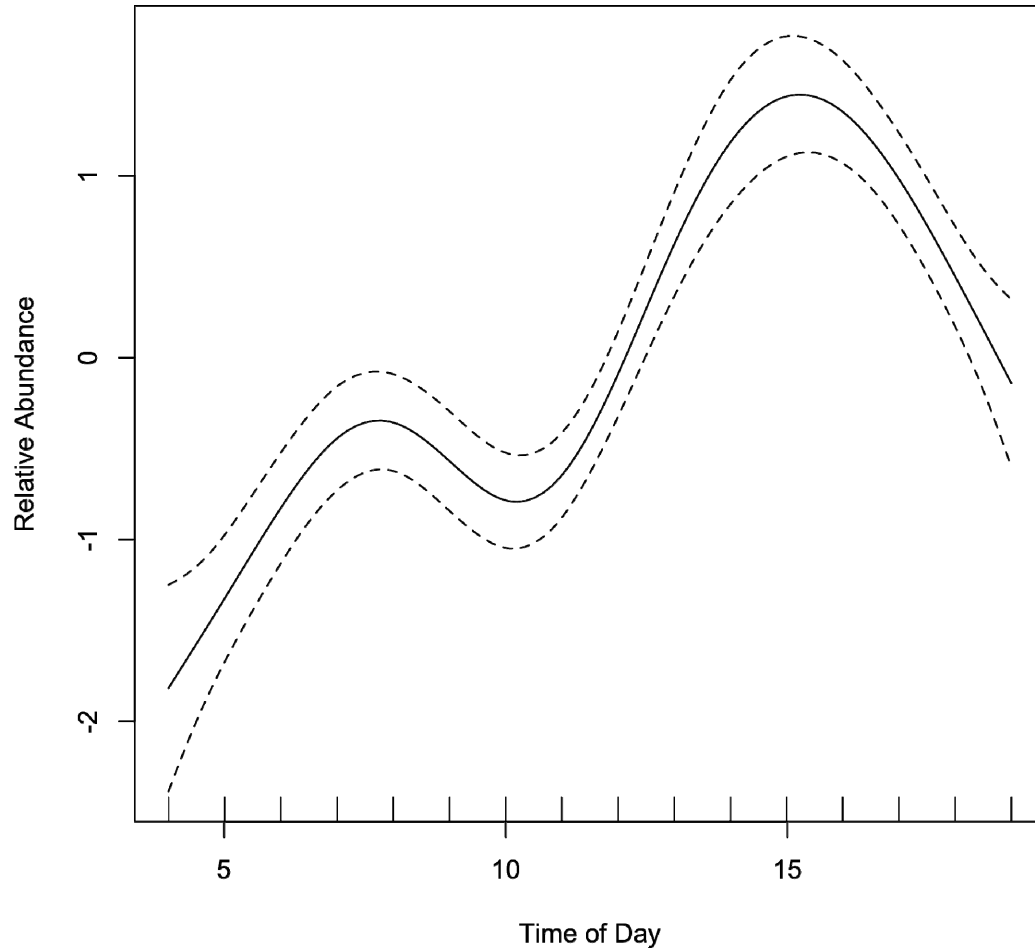


Figure 43: GAMM coefficient estimates (and standard errors) for Arctic tern observed by wind direction at Billia Croo.

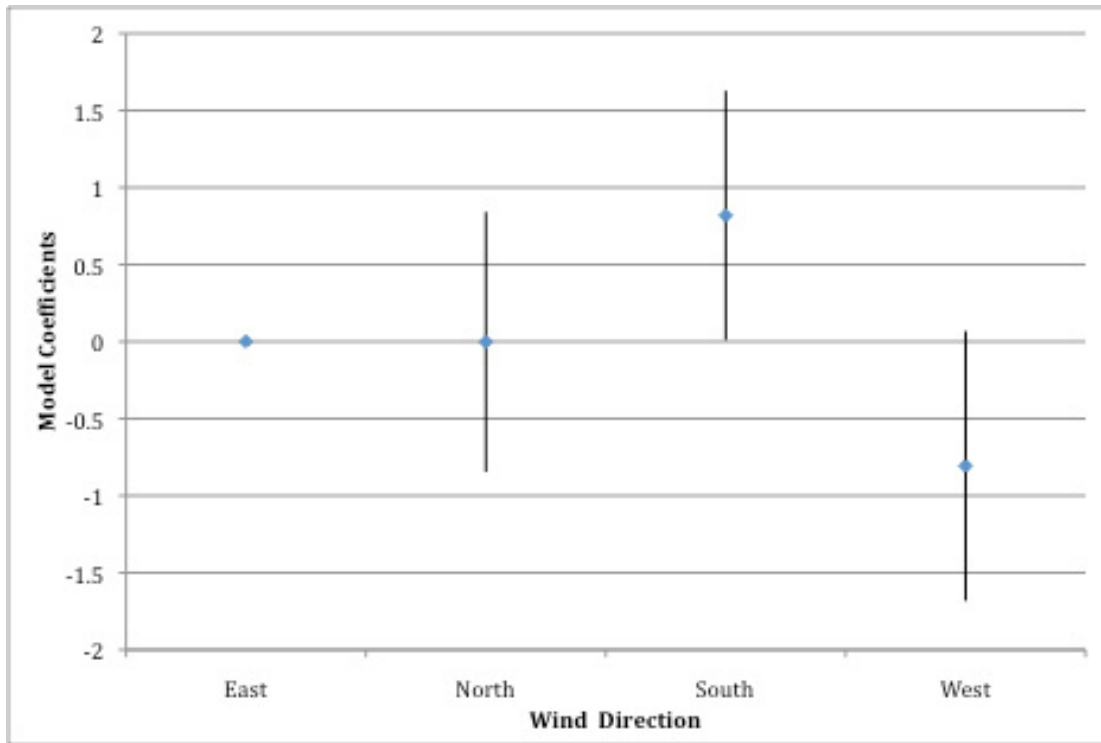
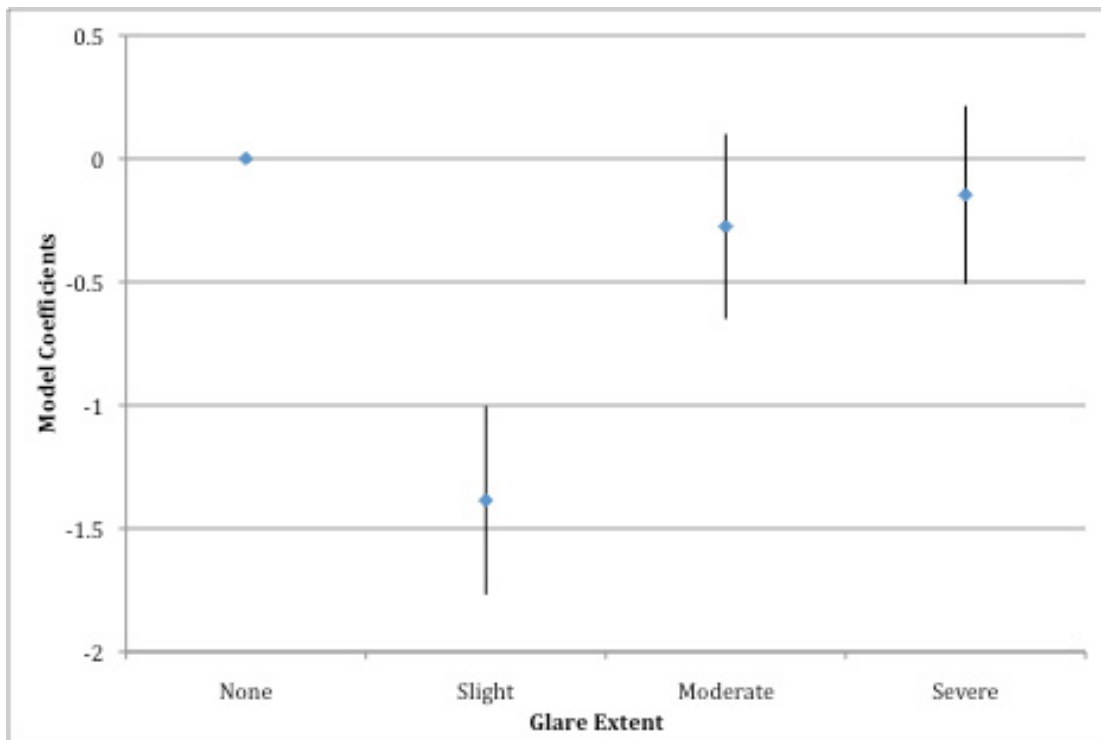


Figure 44: GAMM coefficient estimates (and standard errors) for Arctic tern observed by glare extent at Billia Croo.



Guillemot

Table 18: The significance of the parametric and smooth terms in the chosen model for guillemot use of Billia Croo.

Model: `gamm(NUMBER~s(JULIANDAY,bs="cc")+oGLAREEXTENT, correlation=corAR1(form=~1|DAYLAPSE),family=negative.binomial(theta=1),gamma=1.4,data=guill5k1)`

Significance of parametric terms:

| | df | F | p-value | Signif. |
|--------------|----|-------|---------|---------|
| Glare Extent | 3 | 2.545 | 0.0543 | . |

Approximate significance of smooth terms:

| | edf | Ref.df | F | p-value | Signif. |
|---------------|-------|--------|-------|----------|---------|
| s(Julian Day) | 4.614 | 4.614 | 7.553 | 1.10E-06 | *** |

Table 19: Parameter estimates, standard errors, probability values for the GAMM investigating guillemot counts as a function of Julian day and glare extent.

| | Estimate | Std. error | Wald | Pr (> W) | Signif. |
|-----------------|----------|------------|--------|-----------|---------|
| (Intercept) | 0.7728 | 0.0739 | 10.457 | <2e-16 | *** |
| Glare: Slight | -0.0544 | 0.1184 | -0.459 | 0.6459 | |
| Glare: Moderate | -0.1908 | 0.1474 | -1.294 | 0.1957 | |
| Glare: Severe | -0.3893 | 0.1667 | -2.335 | 0.0196 | * |

R-sq.(adj) = 0.00748 Scale est. = 5.9826 n = 4472

Figure 45: The estimated seasonal pattern of relative number of guillemots observed. The solid line is the smoothing curve for Julian day and dotted lines are 95% confidence bands.

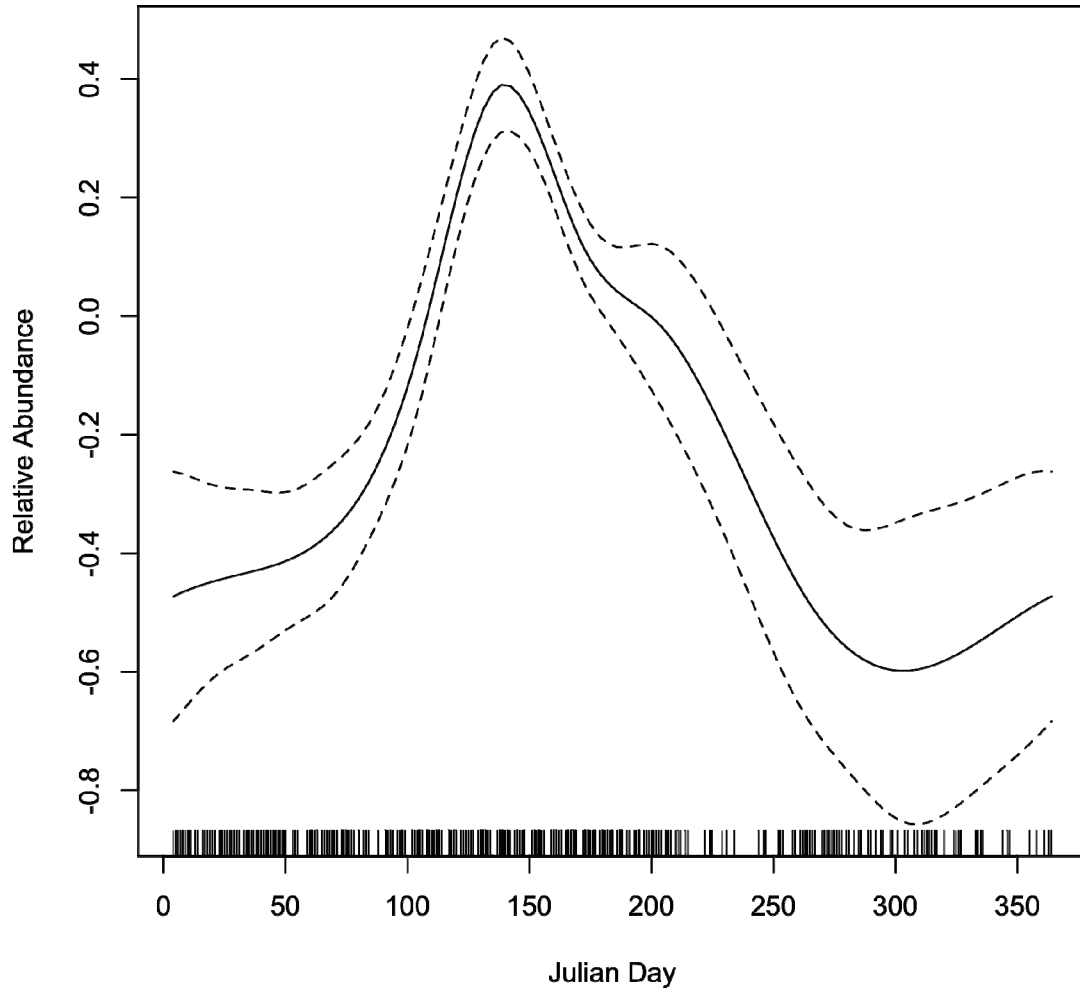


Figure 46: GAMM coefficient estimates (and standard errors) for guillemots observed by glare extent at Billia Croo.

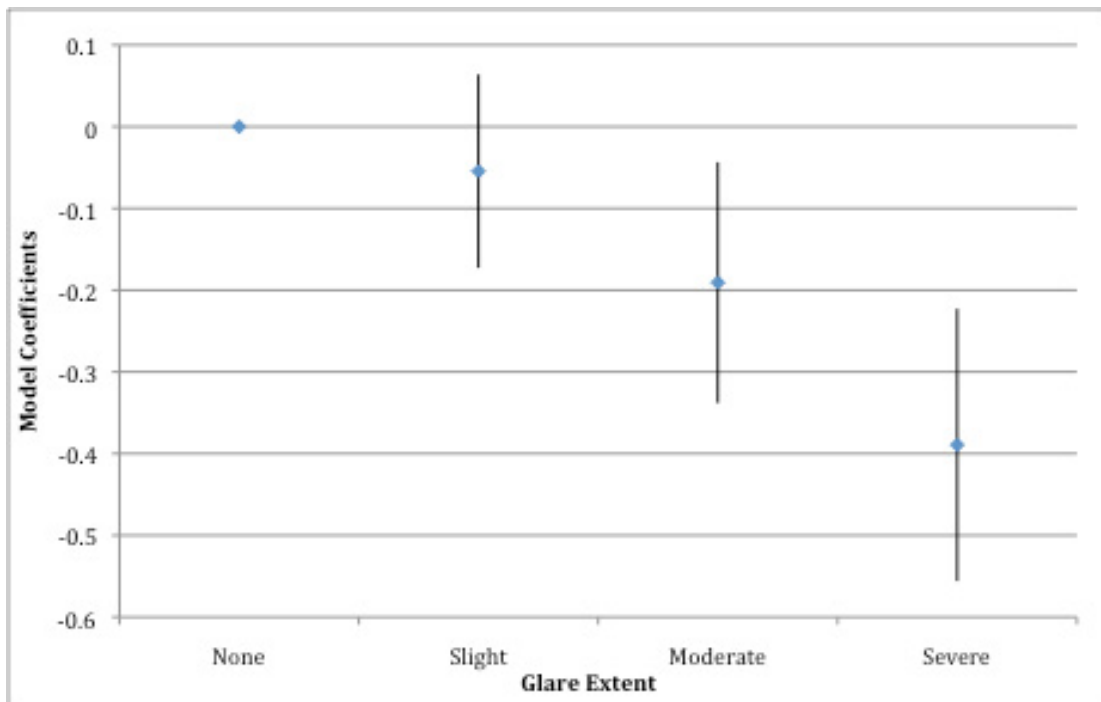


Figure 47: Mean number of feeding and resting guillemots observed per hour, throughout the day at Billia Croo.

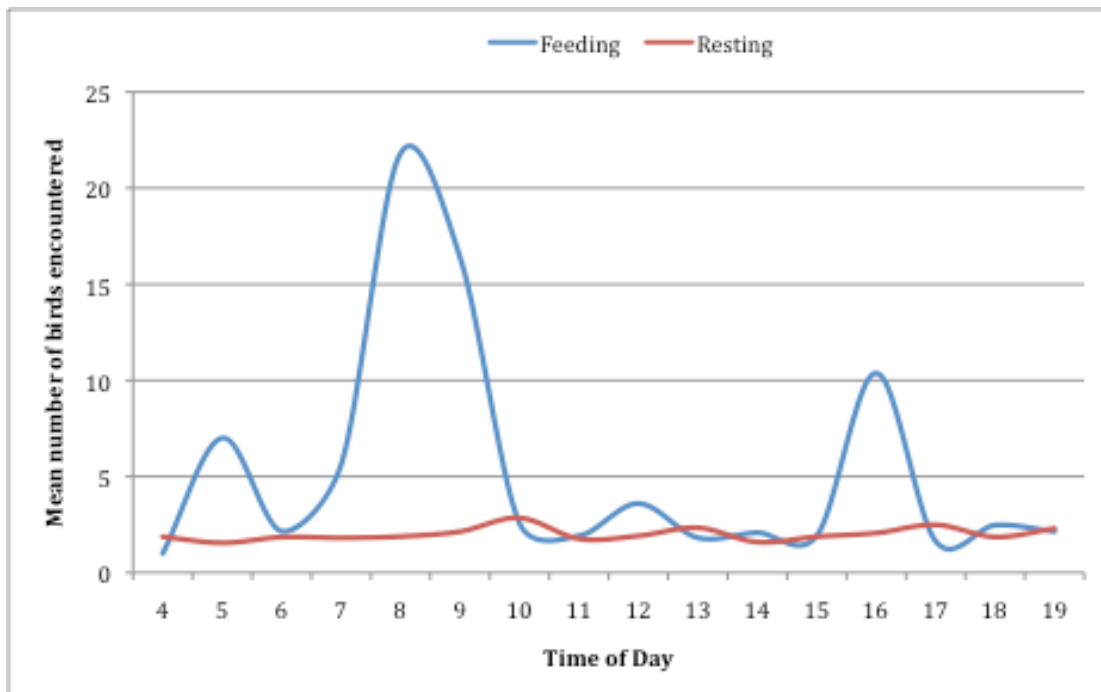
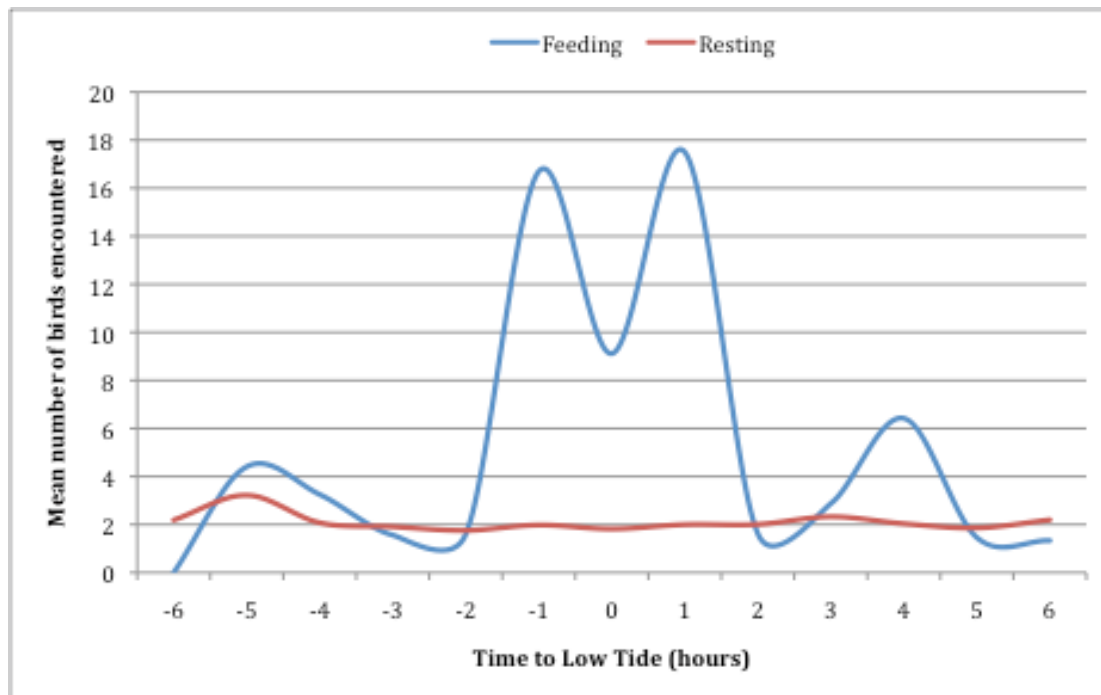


Figure 48: Mean number of feeding and resting guillemots observed per hour, by time from low tide at Billia Croo.



Razorbill

Table 20: The significance of the parametric and smooth terms in the chosen model for razorbill use of Billia Croo.

Model: `gamm(NUMBER~s(Long,Lat)+s(JULIANDAY,bs="cc"), correlation=corAR1 (form=~1|DAYLAPSE), family=negative.binomial(theta=5.55), gamma=1.4, data=razor1)`

Approximate significance of smooth terms:

| | edf | Ref.df | F | p-value | Signif. |
|---------------|-------|--------|-------|---------|---------|
| s(Long,Lat) | 2 | 2 | 7.249 | 0.00094 | *** |
| s(Julian Day) | 2.344 | 2.344 | 4.176 | 0.01235 | * |

Table 21: Parameter estimates, standard errors, probability values for the GAMM investigating razorbill counts as a function of latitude and longitude and Julian day.

| | Estimate | Std. Error | t | value | Pr(> t) | Signif. |
|-------------|----------|------------|---|-------|----------|---------|
| (Intercept) | 0.64343 | 0.07895 | | 8.15 | 6.14E-14 | *** |

R-sq.(adj) = 0.104 Scale est. = 1.2898 n = 184

Figure 49: The estimated spatial pattern of relative number of razorbills observed. The solid line is the smoothing curve for 0, red dotted lines are -1 standard error from the smoothing curve and the green dotted lines are +1 standard error from the smoothing curve.

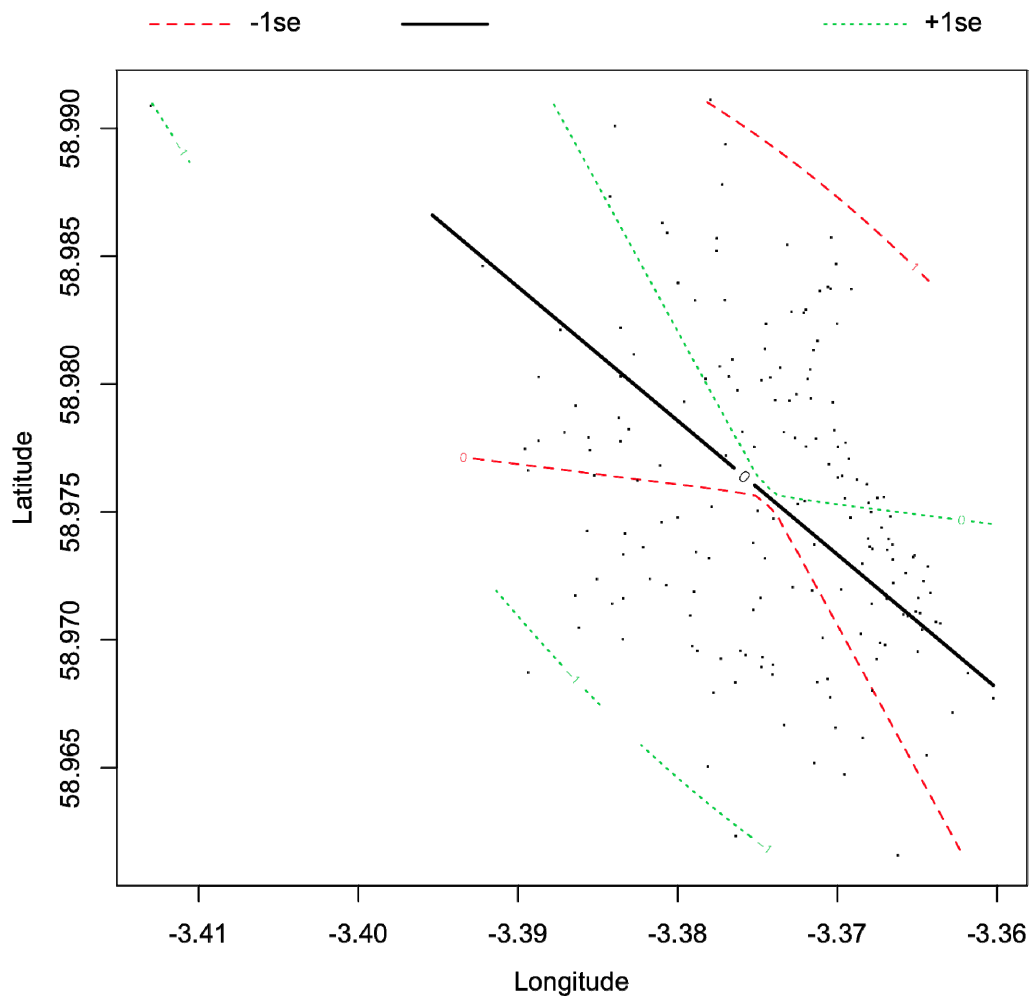


Figure 50: The estimated seasonal pattern of relative number of razorbills observed. The solid line is the smoothing curve for Julian day and dotted lines are 95% confidence bands.

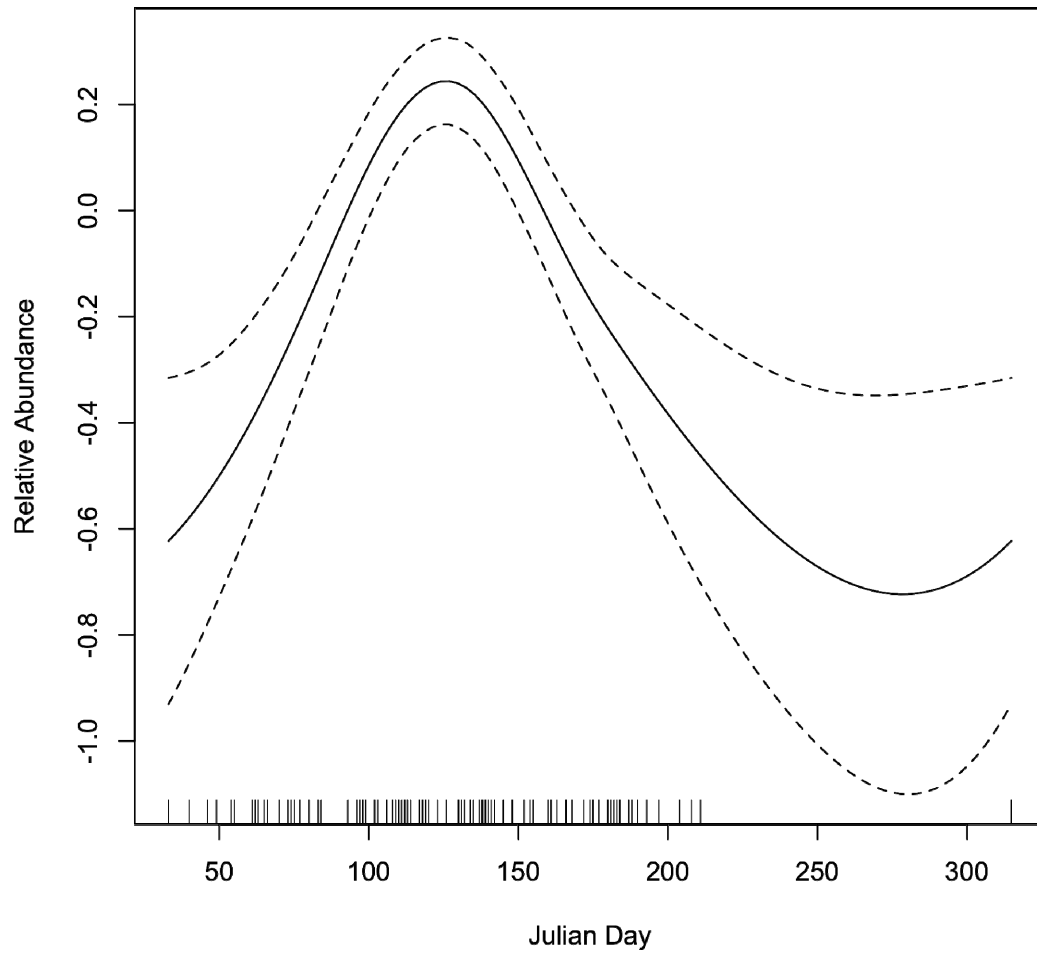


Figure 51: Mean number of feeding and resting razorbills observed per hour, throughout the day at Billia Croo.

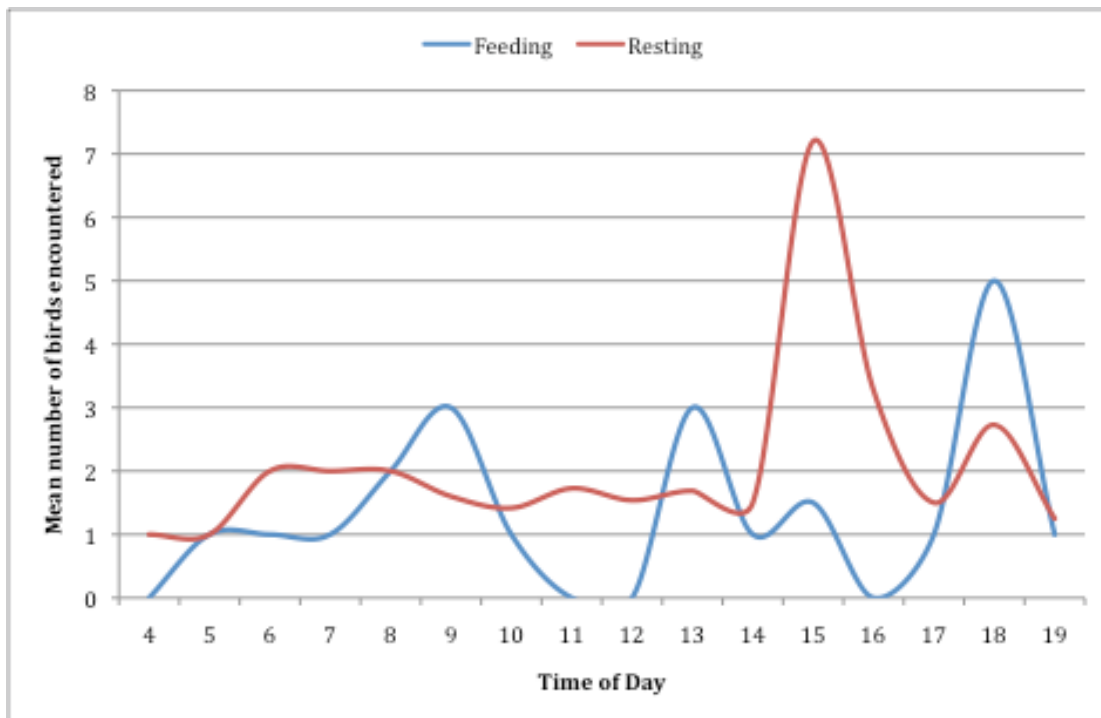
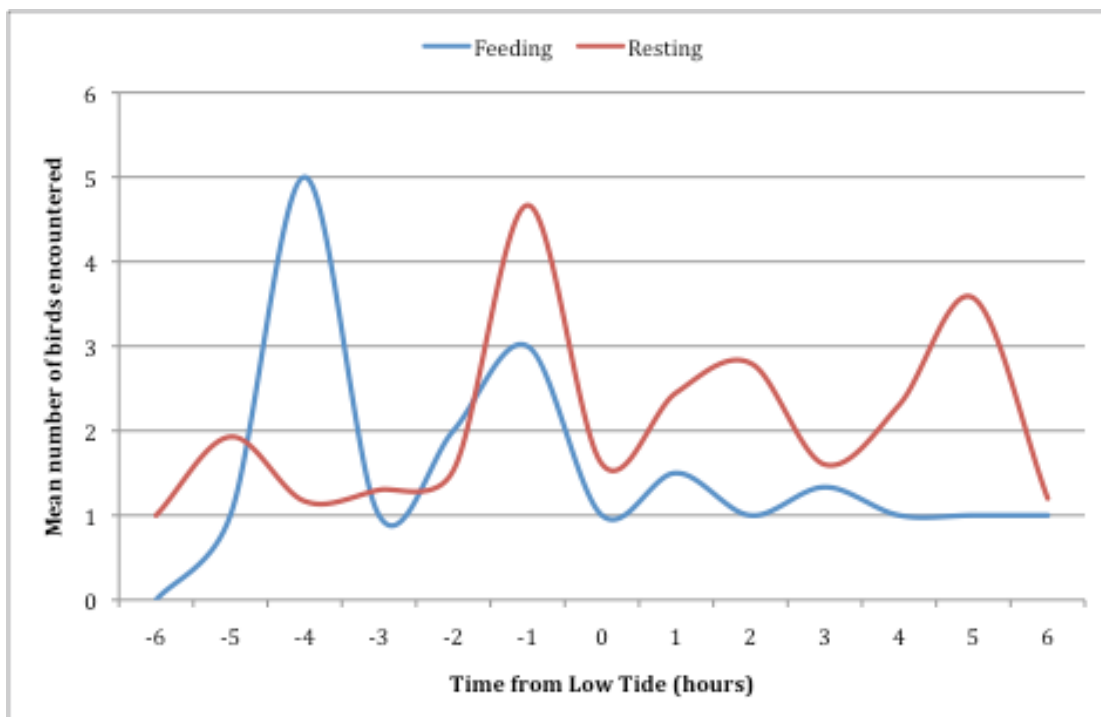


Figure 52: Mean number of feeding and resting razorbills observed per hour, by time from low tide at Billia Croo.



Black Guillemot

Table 22: The significance of the parametric and smooth terms in the chosen model for black guillemot use of Billia Croo.

Model: `gamm(NUMBER~s(Long,Lat)+s(JULIANDAY,bs="cc")+s(TIMEHOUR,bs="cs")+WIND.STRENGTH, correlation=corAR1(form=~1|DAYLAPSE), family=negative.binomial(theta=1), gamma=9.99,data=tystie1)`

Significance of parametric terms:

| | df | F | p-value | Signif. |
|---------------|----|------|---------|---------|
| Wind Strength | 1 | 3.68 | 0.0552 | . |

Approximate significance of smooth terms:

| | edf | Ref.df | F | p-value | Signif. |
|---------------|--------|--------|--------|----------|---------|
| s(Long,Lat) | 16.849 | 16.849 | 3.048 | 2.82E-05 | *** |
| s(Julian Day) | 5.14 | 5.14 | 13.555 | 2.59E-13 | *** |
| s(Timehour) | 4.926 | 4.926 | 15.137 | 1.99E-14 | *** |

Table 23: Parameter estimates, standard errors, probability values for the GAMM investigating black guillemot counts as a function of latitude and longitude, Julian day, time of day and glare extent.

| | Estimate | Std. error | Wald | Pr (> W) | Signif. |
|---------------|----------|------------|--------|-----------|---------|
| (Intercept) | 0.40158 | 0.03598 | 11.162 | <2e-16 | *** |
| Wind Strength | -0.02171 | 0.01132 | -1.918 | 0.0552 | . |

R-sq.(adj) = 0.11 Scale est. = 0.25557 n = 1922

Figure 53: The estimated spatial pattern of relative number of black guillemot observed. The solid line is the smoothing curve for 0, red dotted lines are -1 standard error from the smoothing curve and the green dotted lines are +1 standard error from the smoothing curve.

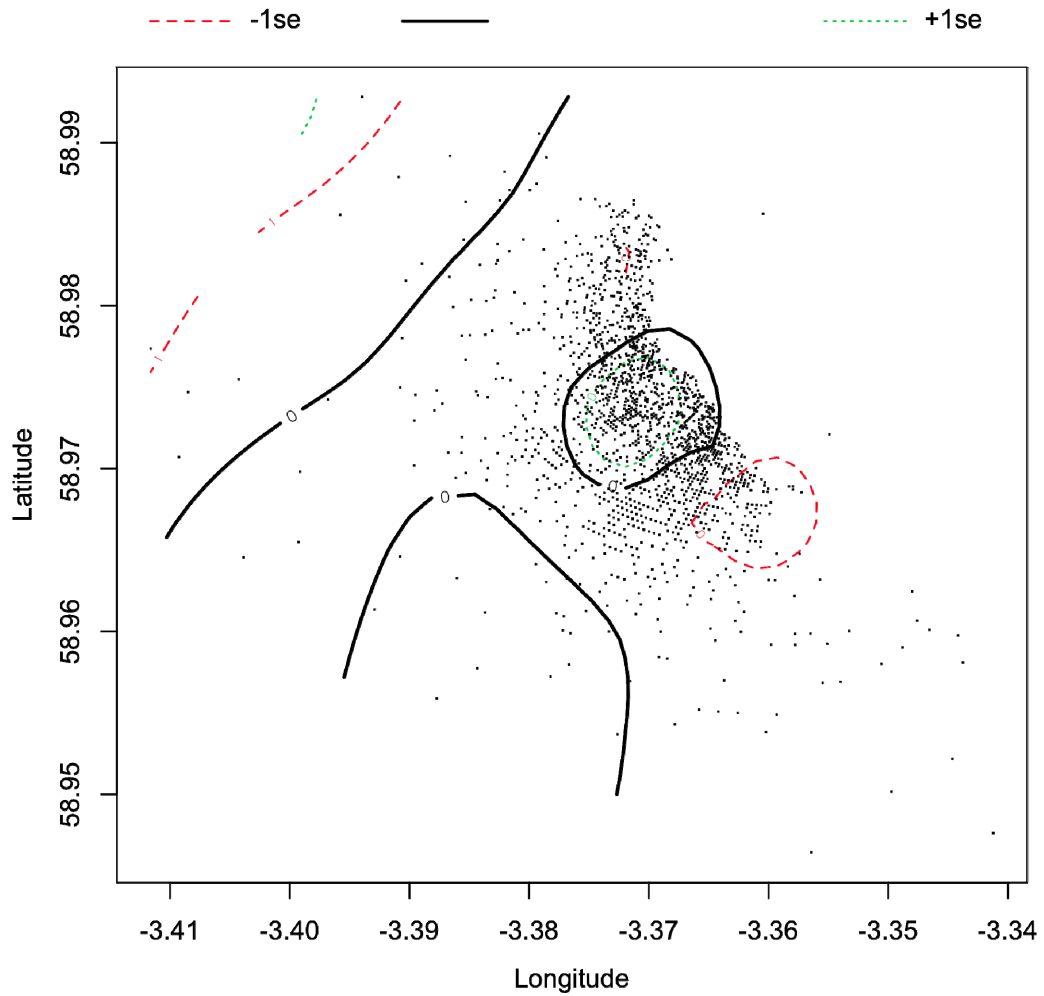


Figure 54: The estimated seasonal pattern of relative number of black guillemot observed. The solid line is the smoothing curve for Julian day and dotted lines are 95% confidence bands.

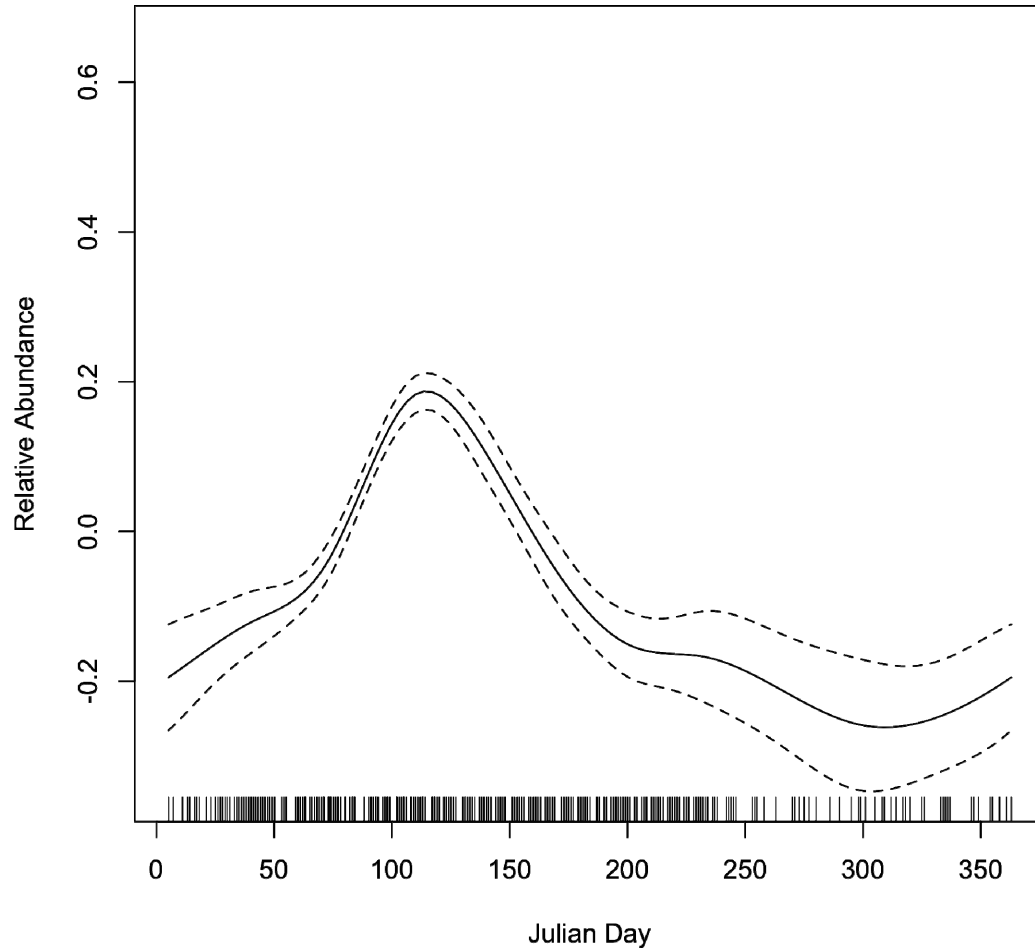


Figure 55: The estimated diurnal pattern of relative number of black guillemot observed. The solid line is the smoothing curve for time of day (hours) and dotted lines are 95% confidence bands.

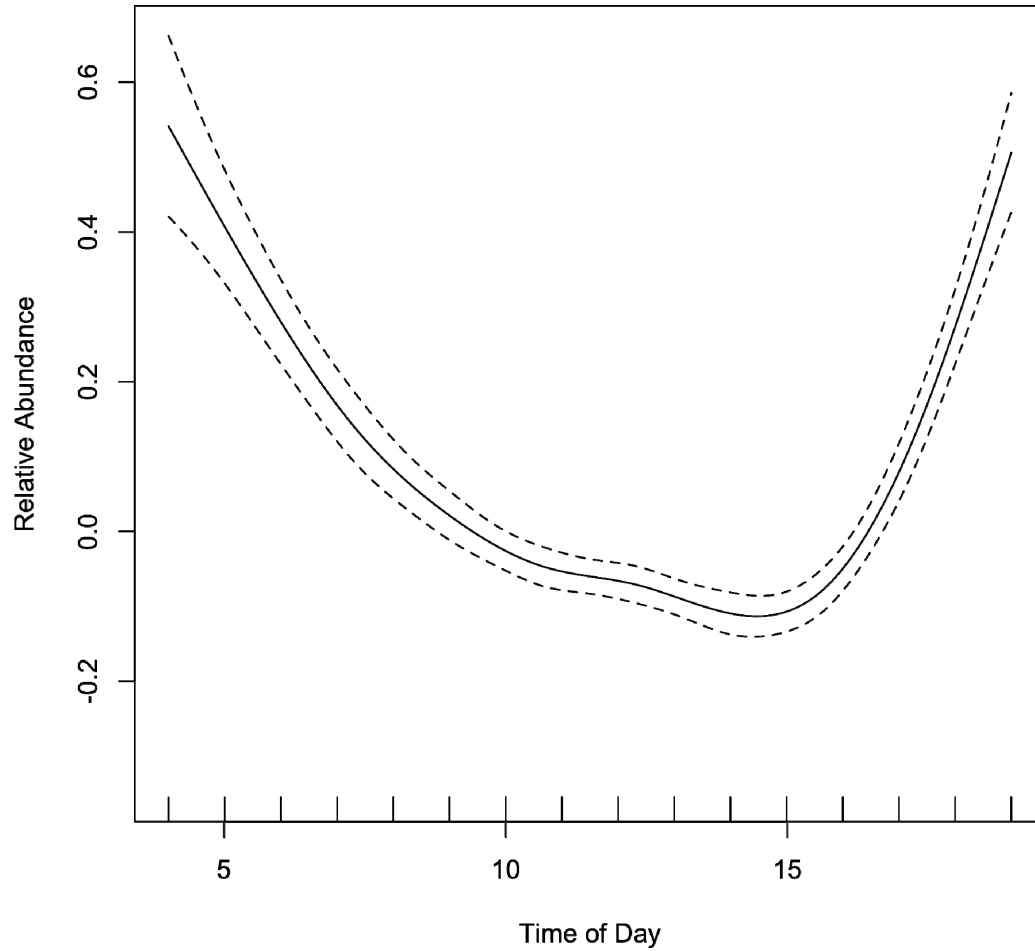


Figure 56: Mean number of black guillemots observed per hour during different wind strengths, using the Beaufort Scale, at Billia Croo.

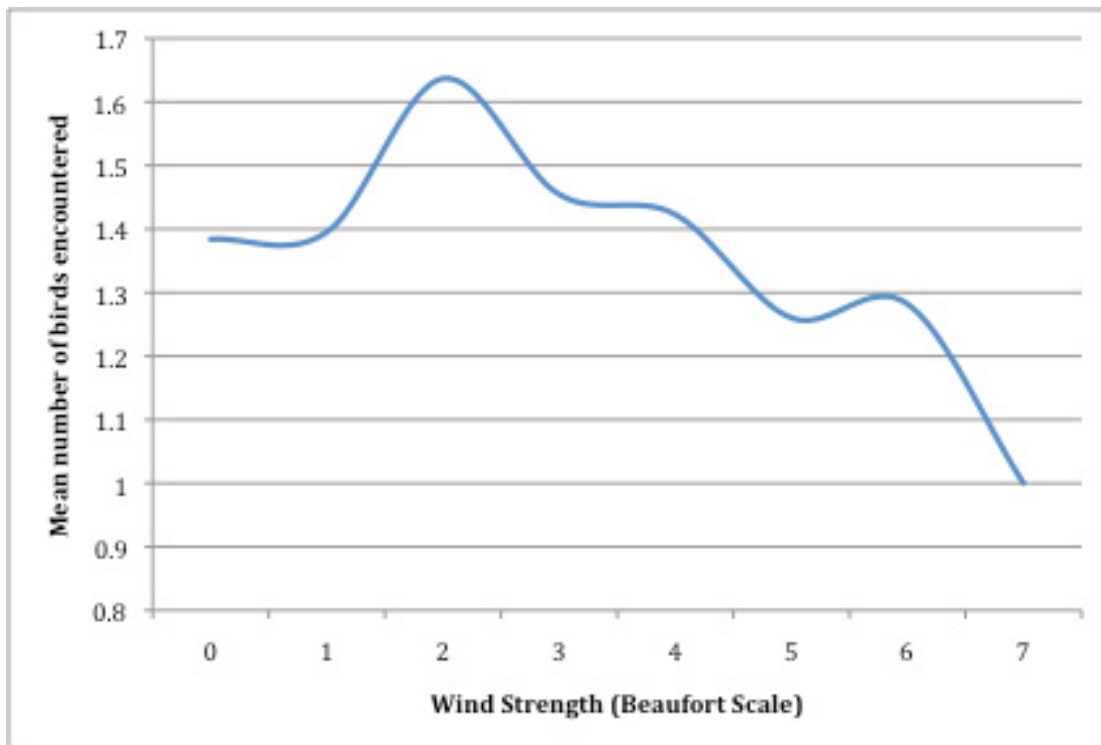


Figure 57: Mean number of feeding and resting black guillemot observed per hour, throughout the day at Billia Croo.

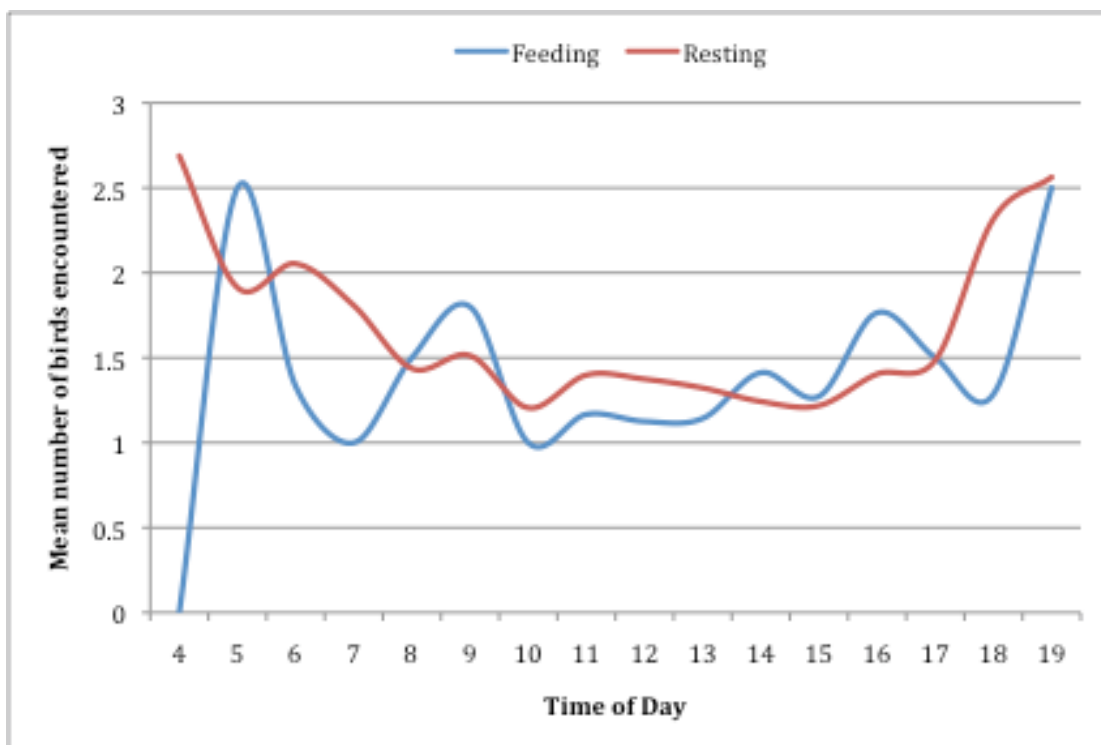
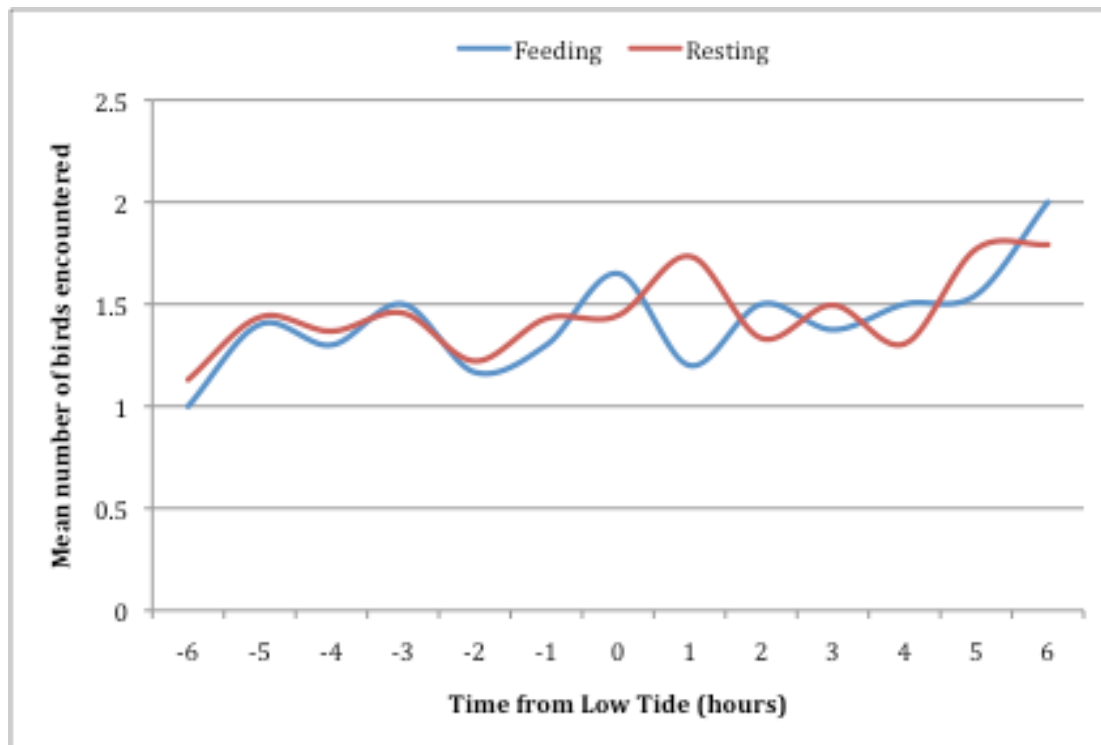


Figure 58: Mean number of feeding and resting black guillemot observed per hour, by time from low tide at Billia Croo.



Atlantic Puffin

Table 24: The significance of the parametric and smooth terms in the chosen model for puffin use of Billia Croo.

Model: `gamm(NUMBER~s(Long,Lat)+s(JULIANDAY,bs="cc")+s(TIMEHOUR,bs="cs")+s(TimetolowHR2,bs="cc")+oGLAREEXTENT+Observer, correlation=corAR1(form=~1|DAYLAPSE), family=negative.binomial(theta=9.99), gamma=1.4, data=puffin1)`

Significance of parametric terms:

| | df | F | p-value | Signif. |
|--------------|----|-------|---------|---------|
| Glare Extent | 3 | 2.748 | 0.0414 | * |

Approximate significance of smooth terms:

| | edf | Ref.df | F | p-value | Signif. |
|------------------|-------|--------|-------|---------|---------|
| s(Long,Lat) | 4.241 | 4.241 | 2.172 | 0.0673 | . |
| s(Julian Day) | 2.03 | 2.03 | 3.758 | 0.0235 | * |
| s(Timehour) | 1.622 | 1.622 | 4.639 | 0.0156 | * |
| S(TimetoLowTide) | 1.259 | 1.259 | 1.887 | 0.1673 | |

Table 25: Parameter estimates, standard errors, probability values for the GAMM investigating puffin counts as a function of latitude and longitude, Julian day, time of day, time to low tide, glare extent and observer.

| | Estimate | Std. error | Wald | Pr (> W) | Signif. |
|-----------------|----------|------------|--------|-----------|---------|
| (Intercept) | 0.47285 | 0.0849 | 5.569 | 4.45E-08 | *** |
| Glare: Slight | 0.12458 | 0.12174 | 1.023 | 0.30673 | |
| Glare: Moderate | 0.38075 | 0.14265 | 2.669 | 0.00789 | ** |
| Glare: Severe | 0.19346 | 0.15378 | 1.258 | 0.20904 | |
| Observer: SW | -0.21008 | 0.09127 | -2.302 | 0.02182 | * |

R-sq.(adj) = 0.0697 Scale est. = 0.78303 n = 455

Figure 59: The estimated spatial pattern of relative number of puffin observed. The solid line is the smoothing curve for 0, red dotted lines are -1 standard error from the smoothing curve and the green dotted lines are +1 standard error from the smoothing curve.

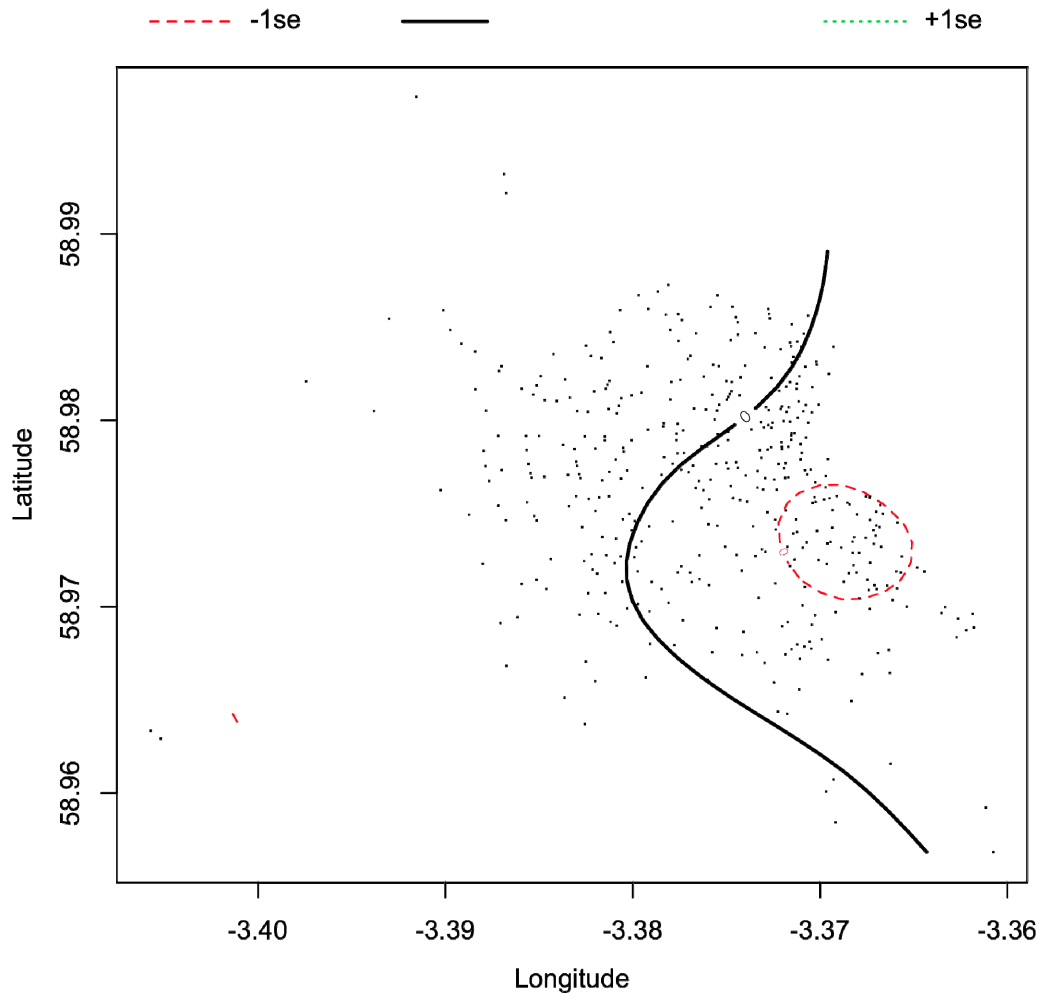


Figure 60: The estimated seasonal pattern of relative number of puffin observed. The solid line is the smoothing curve for Julian day and dotted lines are 95% confidence bands.

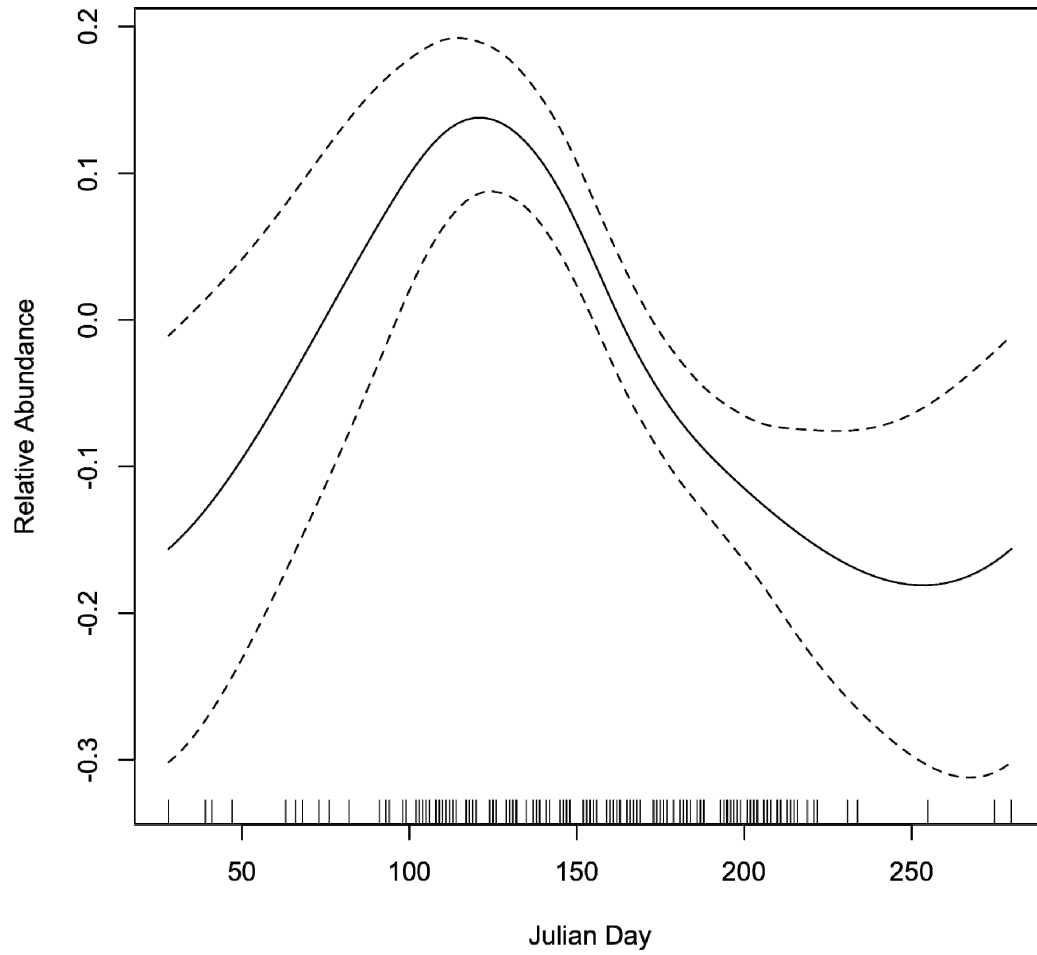


Figure 61: The estimated diurnal pattern of relative number of puffin observed. The solid line is the smoothing curve for time of day (hours) and dotted lines are 95% confidence bands.

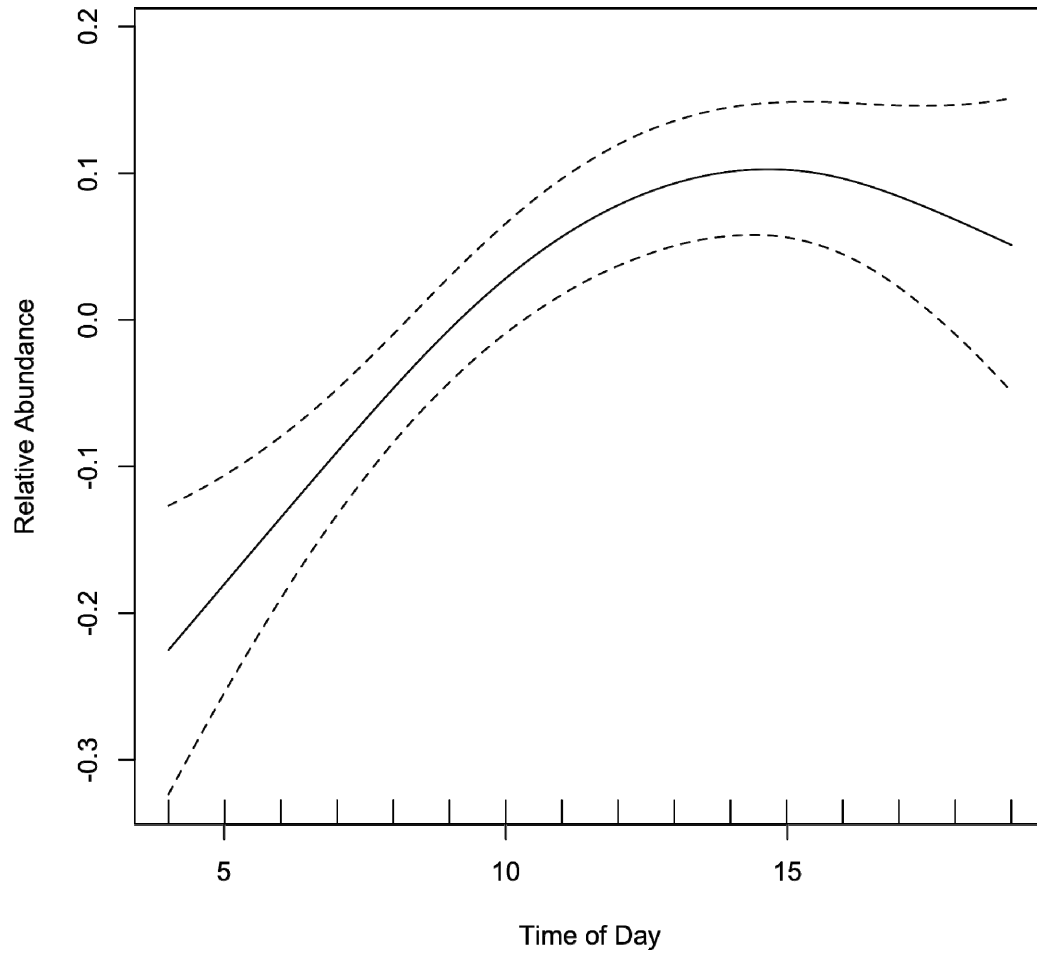


Figure 62: The estimated pattern of change in relative number of puffin observed across the semi-diurnal tidal cycle. The solid line is the smoothing curve for time from low tide (hours) and dotted lines are 95% confidence bands.

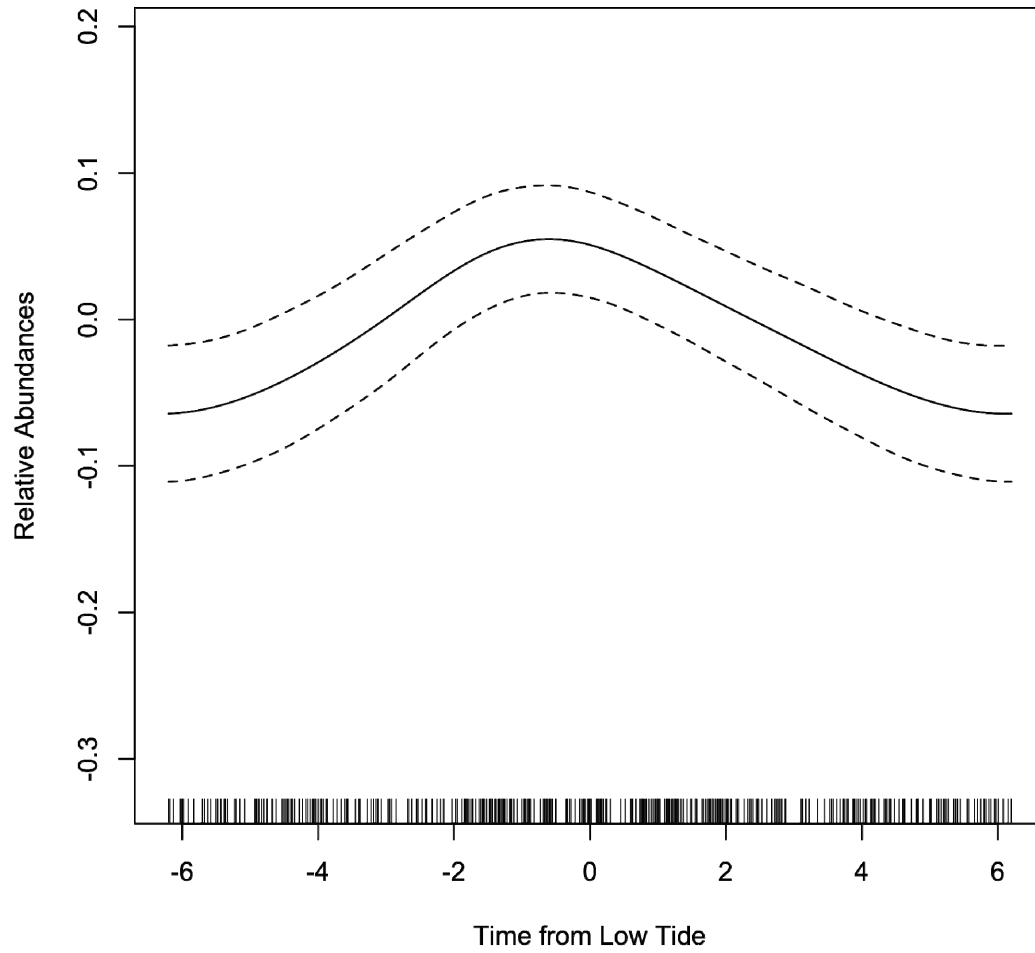


Figure 63: GAMM coefficient estimates (and standard errors) for puffin observed by glare extent at Billia Croo.

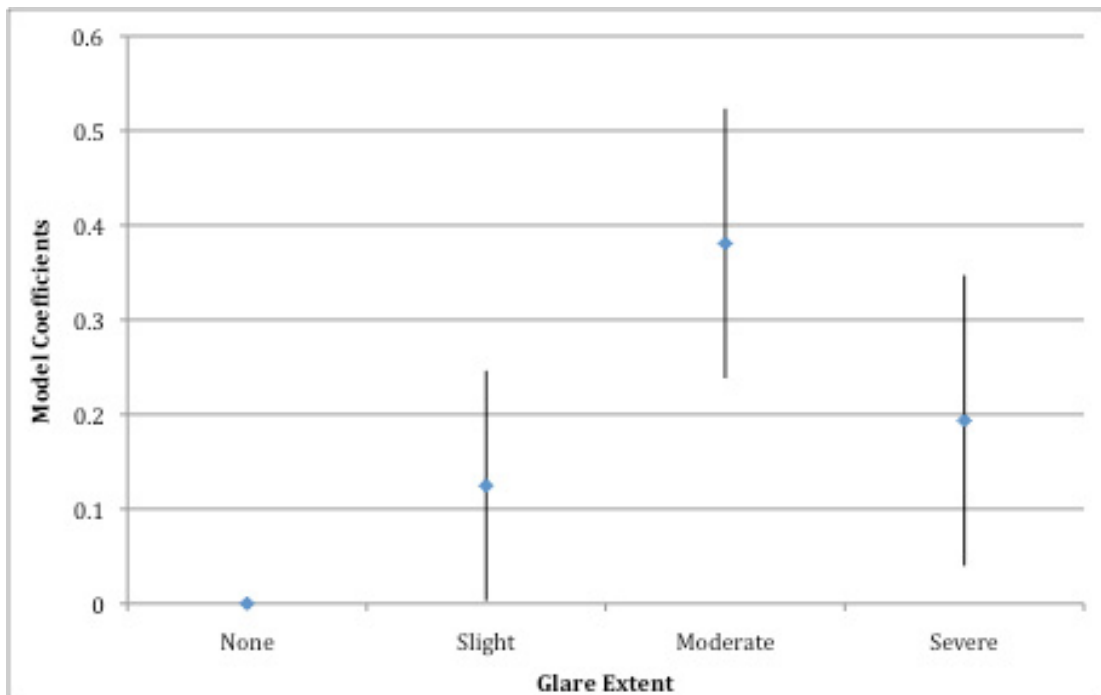


Figure 64: Mean number of feeding and resting puffin observed per hour, throughout the day at Billia Croo.

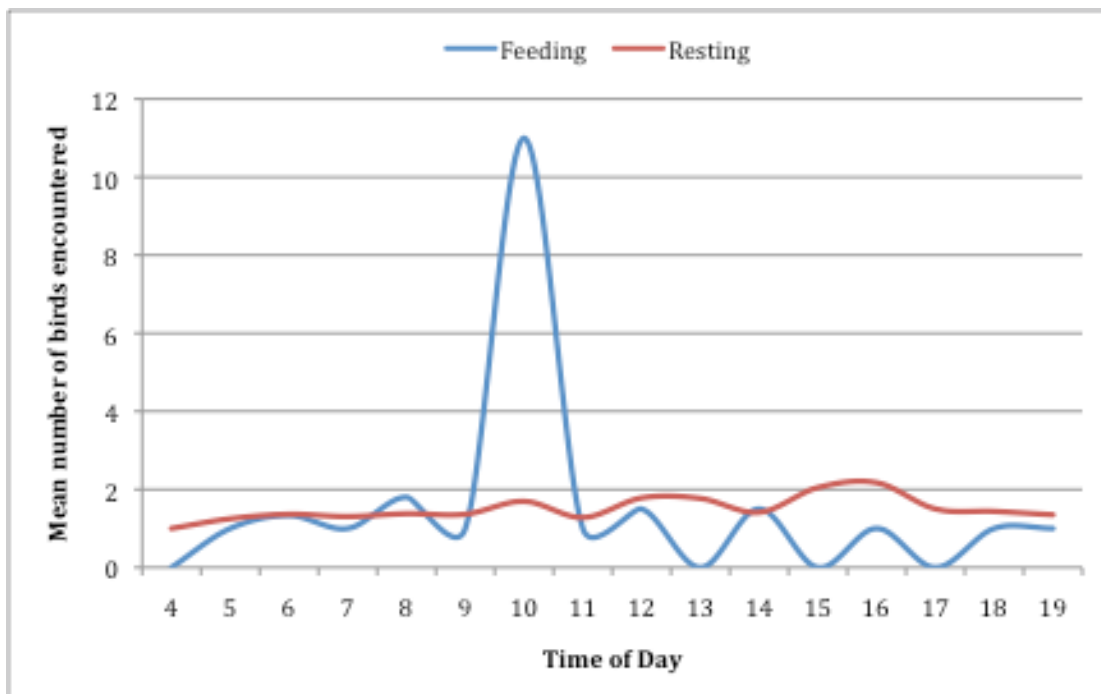
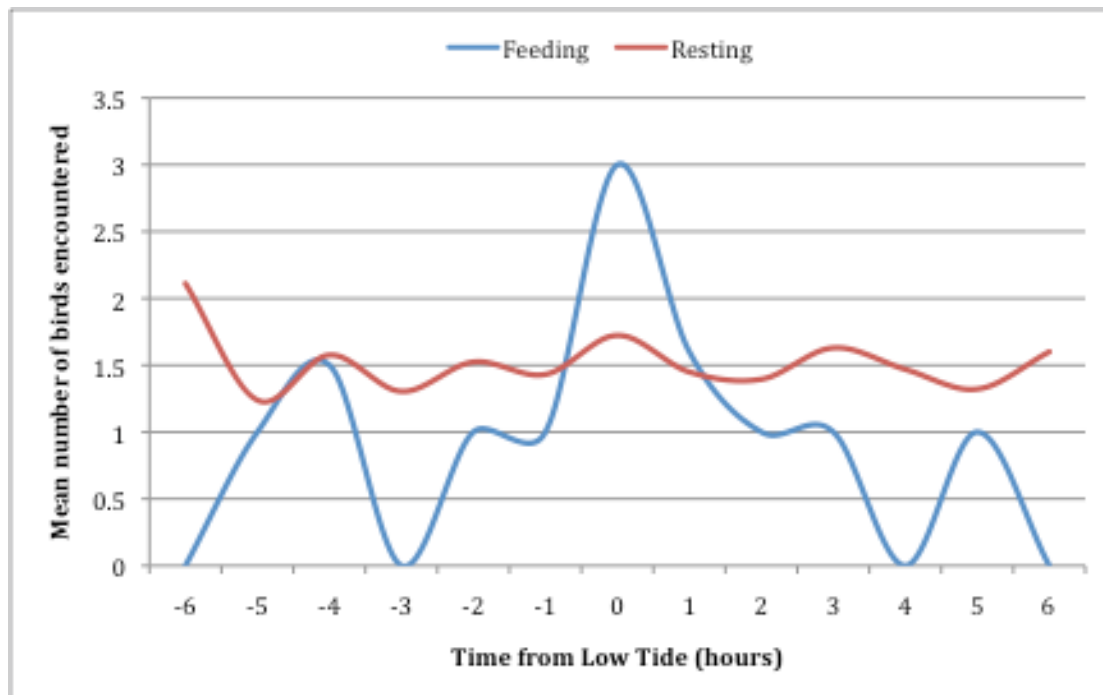


Figure 65: Mean number of feeding and resting puffin observed per hour, by time from low tide at Billia Croo.



All Seals

Table 26: The significance of the parametric and smooth terms in the chosen model for seal use of Billia Croo.

Model: `gamm(NUMBER~s(Long,Lat)+s(JULIANDAY, bs="cc")+WINDIR2+WINDSTRENGTH, correlation=corAR1(form=~1|DAYLAPSE), family=negative.binomial (theta=9.99), gamma=1.4,data=seal1)`

Significance of parametric terms:

| | df | F | p-value | Signif. |
|----------------|----|--------|----------|---------|
| Wind Direction | 3 | 11.943 | 1.68E-07 | *** |
| Wind Strength | 1 | 6.589 | 0.0106 | * |

Approximate significance of smooth terms:

| | edf | Ref.df | F | p-value | Signif. |
|---------------|-------|--------|-------|---------|---------|
| s(Long,Lat) | 18.89 | 18.89 | 7.413 | <2e-16 | *** |
| s(Julian Day) | 2.359 | 2.359 | 3.432 | 0.0262 | *** |

Table 27: Parameter estimates, standard errors, probability values for the GAMM investigating seal counts as a function of latitude and longitude, Julian day, wind direction and strength.

| | Estimate | Std. error | Wald | Pr (> W) | Signif. |
|-----------------------|-----------|------------|--------|-----------|---------|
| (Intercept) | 0.323061 | 0.062546 | 5.165 | 3.81E-07 | *** |
| Wind Direction: North | -0.37567 | 0.063584 | -5.908 | 7.46E-09 | *** |
| Wind Direction: South | -0.343621 | 0.063549 | -5.407 | 1.11E-07 | *** |
| Wind Direction: West | -0.368388 | 0.070067 | -5.258 | 2.39E-07 | *** |
| Wind Strength | 0.024495 | 0.009543 | 2.567 | 0.0106 | * |

R-sq.(adj) = 0.653 Scale est. = 0.080914 n = 422

Figure 66: The estimated spatial pattern of relative number of all seals observed. The solid line is the smoothing curve for 0, red dotted lines are -1 standard error from the smoothing curve and the green dotted lines are +1 standard error from the smoothing curve.

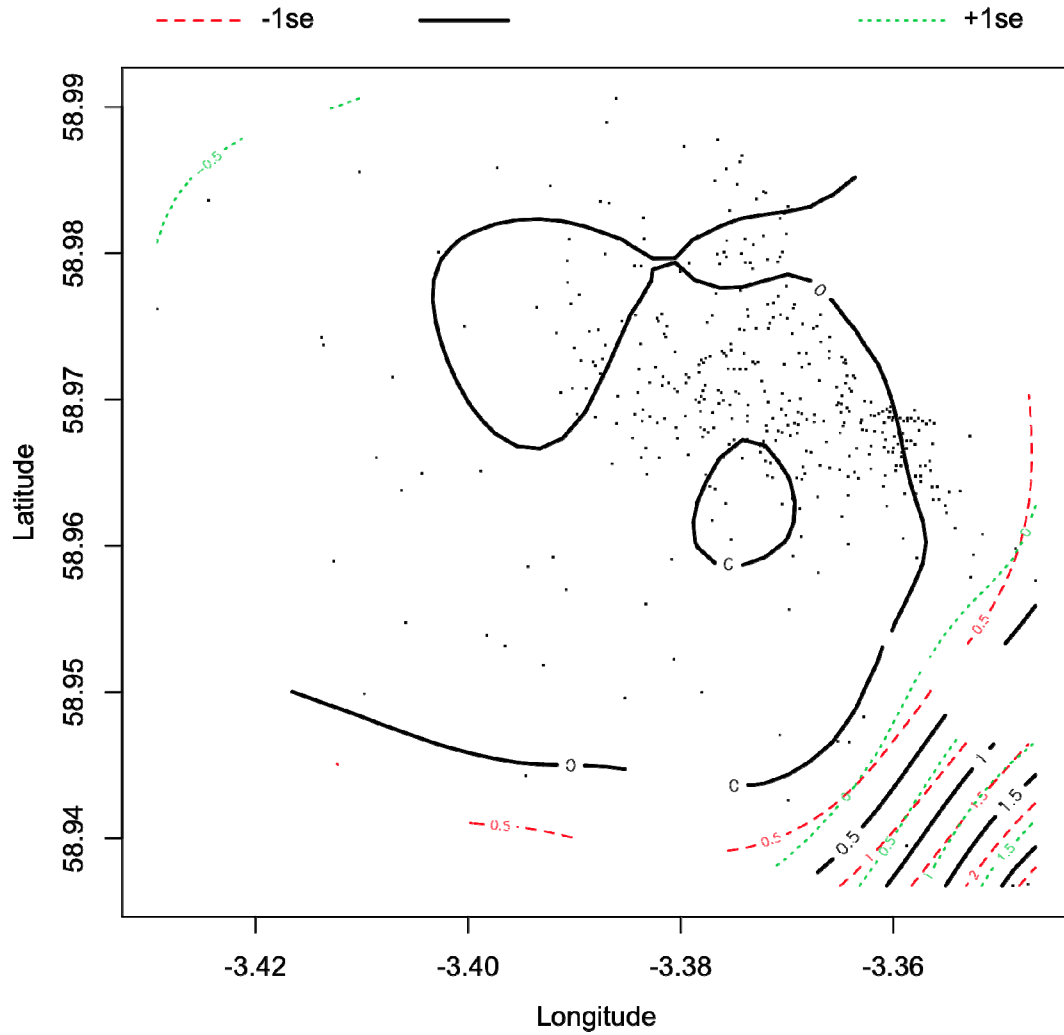


Figure 67: The estimated seasonal pattern of relative number of seals observed. The solid line is the smoothing curve for Julian day and dotted lines are 95% confidence bands.

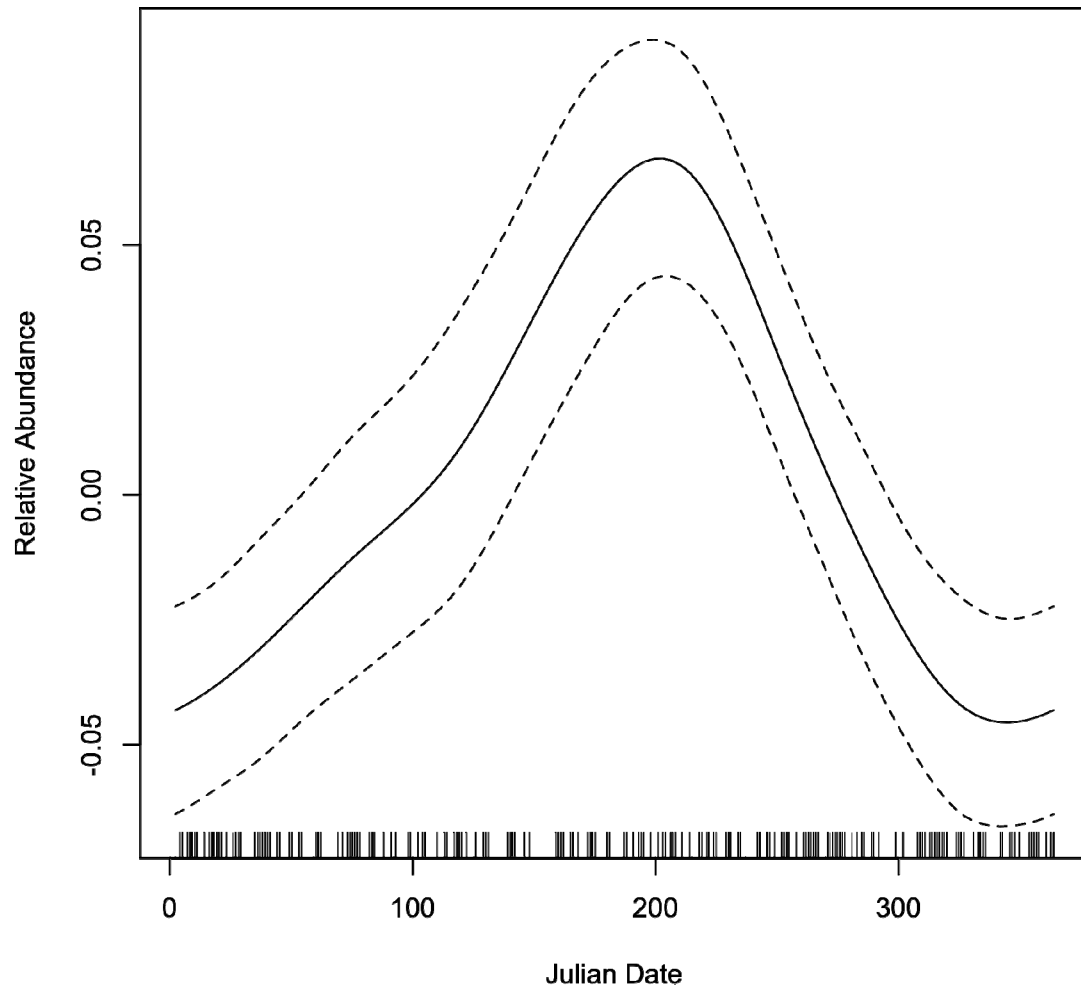


Figure 68: GAMM coefficient estimates (and standard errors) for all seals observed by wind direction at Billia Croo.

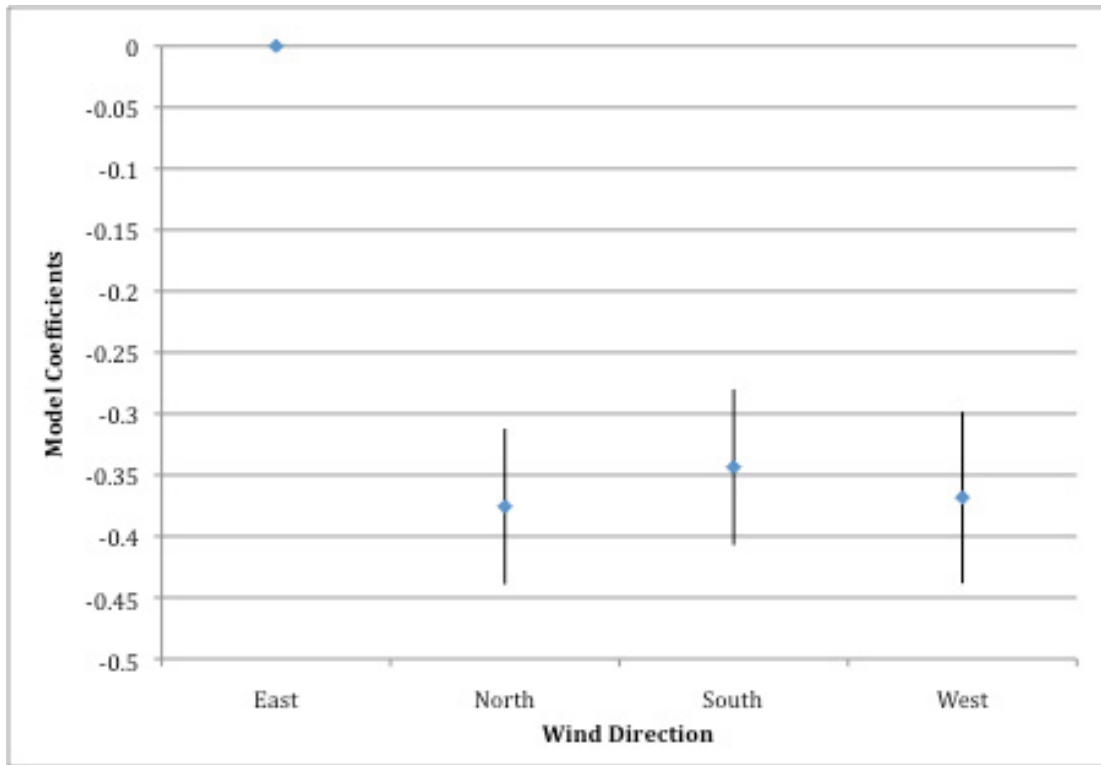


Figure 69: Mean number of seals encountered, by wind strength at Billia Croo.

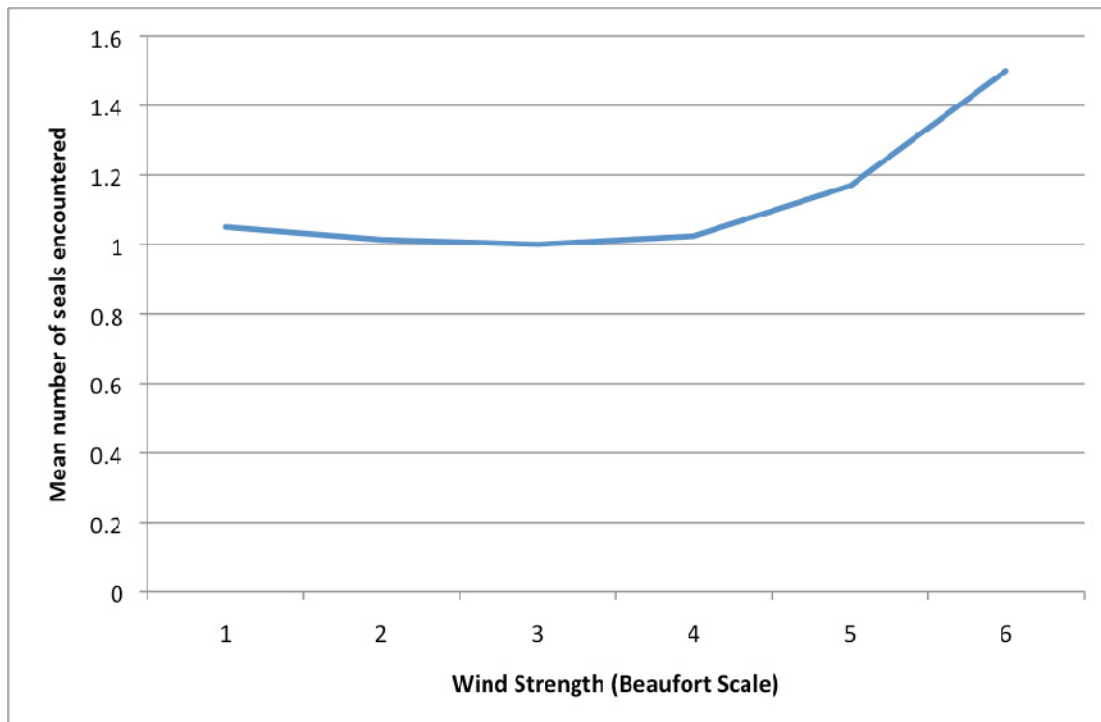


Figure 70: The proportion of all seal observations by season and species at Billia Croo.

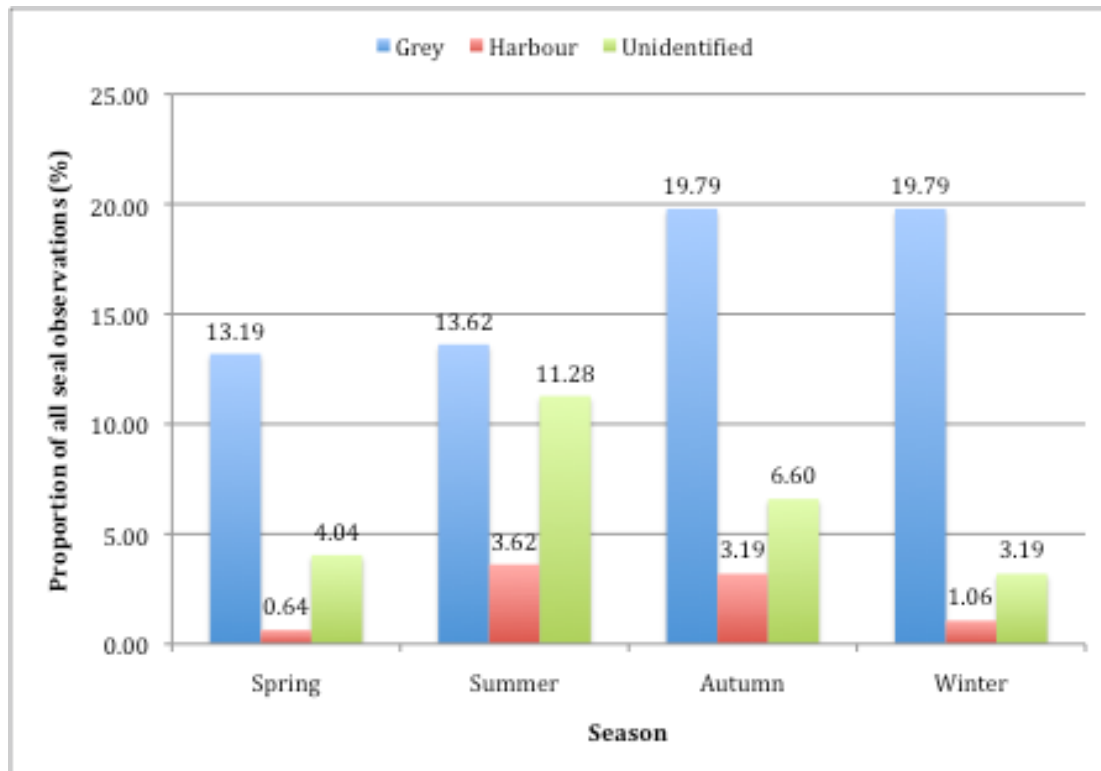
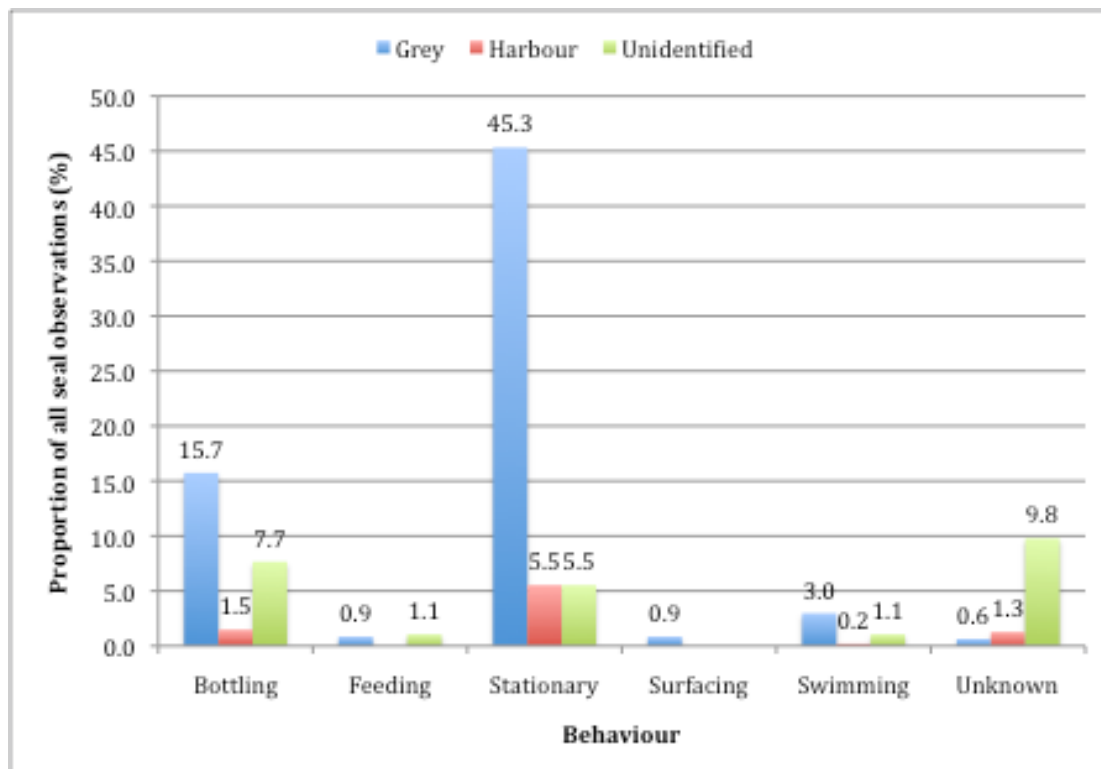


Figure 71: The proportion of all seal observations by behaviour and species at Billia Croo.



Harbour Porpoise

Table 28: The significance of the parametric and smooth terms in the chosen model for harbour porpoise use of Billia Croo.

Model: gamm(NUMBER~s(Long,Lat)+s(JULIANDAY, bs="cc")+oGLAREEXTENT, correlation=corAR1(form=~1|DAYLAPSE),family=negative.binomial(theta=9.99), gamma=1.4, data=hporp1)

Significance of parametric terms:

| | df | F | p-value | Signif. |
|--------------|----|-------|---------|---------|
| Glare Extent | 3 | 2.859 | 0.0383 | * |

Approximate significance of smooth terms:

| | edf | Ref.df | F | p-value | Signif. |
|---------------|-------|--------|-------|---------|---------|
| s(Long,Lat) | 2 | 2 | 3.975 | 0.02037 | * |
| s(Julian Day) | 2.424 | 2.424 | 4.95 | 0.00485 | ** |

Table 29: Parameter estimates, standard errors, probability values for the GAMM investigating harbour porpoise counts as a function of latitude and longitude, Julian day and glare extent.

| | Estimate | Std. error | Wald | Pr (> W) | Signif. |
|-----------------|----------|------------|--------|-----------|---------|
| (Intercept) | 0.68926 | 0.0624 | 11.046 | < 2e-16 | *** |
| Glare: Slight | 0.12206 | 0.09499 | 1.285 | 0.20037 | |
| Glare: Moderate | -0.05145 | 0.12737 | -0.404 | 0.68671 | |
| Glare: Severe | -0.40531 | 0.15052 | -2.693 | 0.00772 | ** |

R-sq.(adj) = 0.0903 Scale est. = 0.40302 n = 198

Figure 72: The estimated spatial pattern of relative number of harbour porpoise observed. The solid line is the smoothing curve for 0, red dotted lines are -1 standard error from the smoothing curve and the green dotted lines are +1 standard error from the smoothing curve.

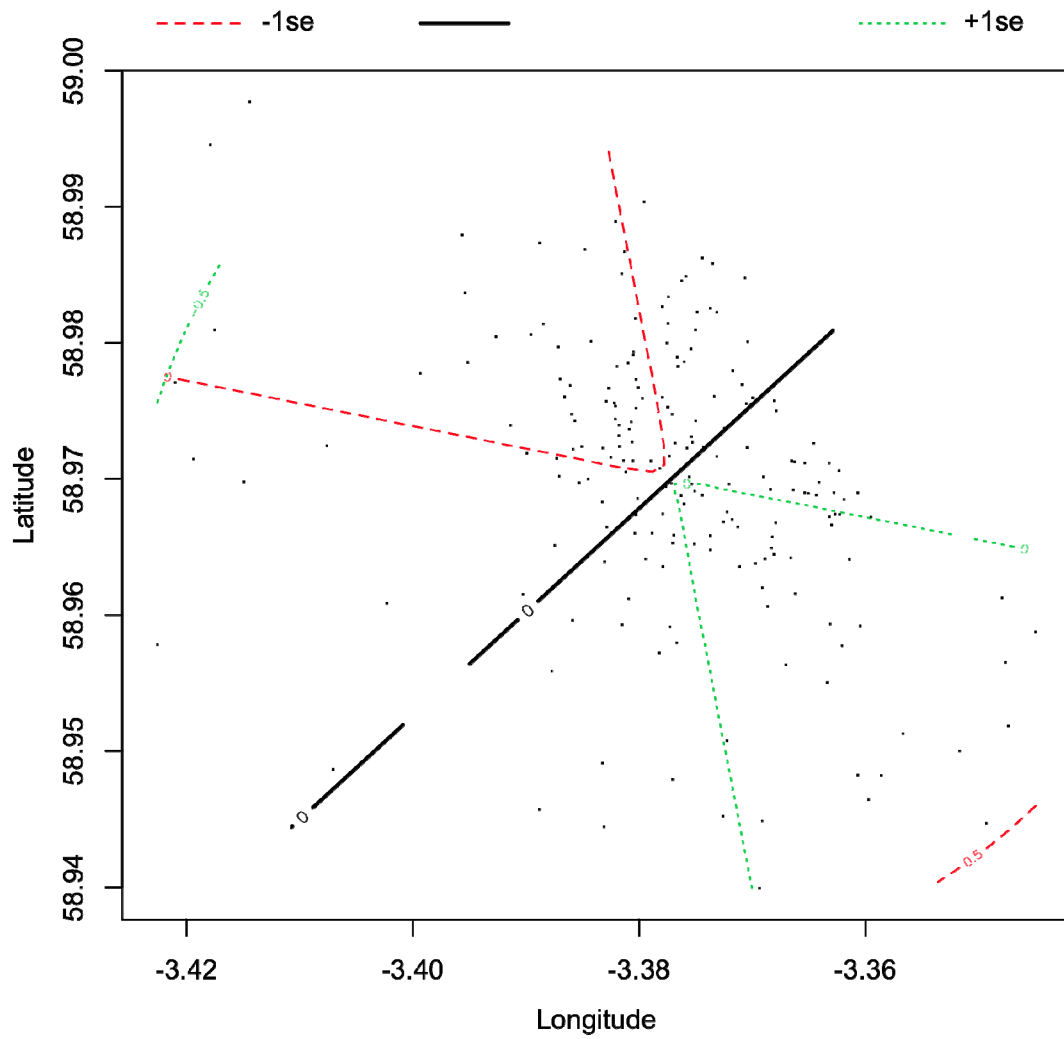


Figure 73: The estimated seasonal pattern of relative number of harbour porpoise observed. The solid line is the smoothing curve for Julian day and dotted lines are 95% confidence bands.

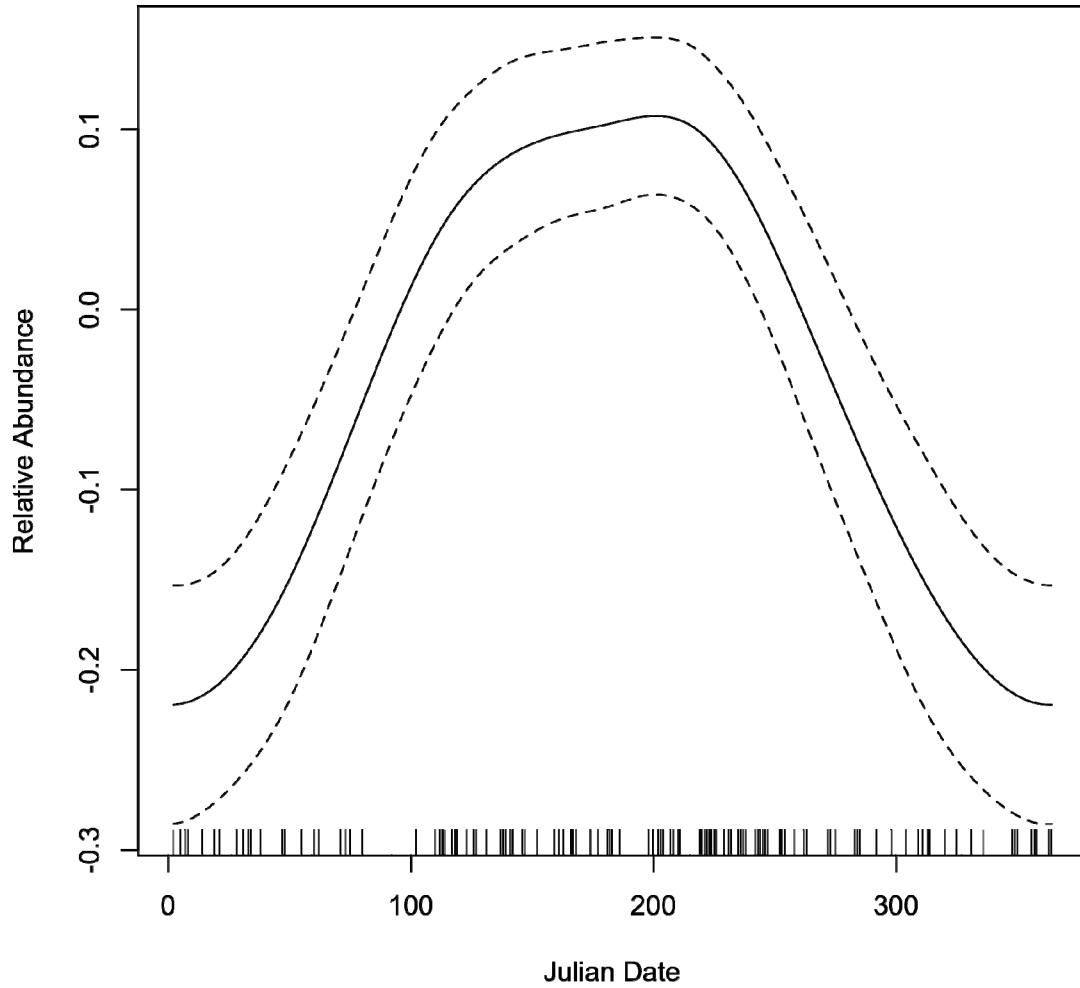


Figure 74: GAMM coefficient estimates (and standard errors) for harbour porpoise observed by glare extent at Billia Croo.

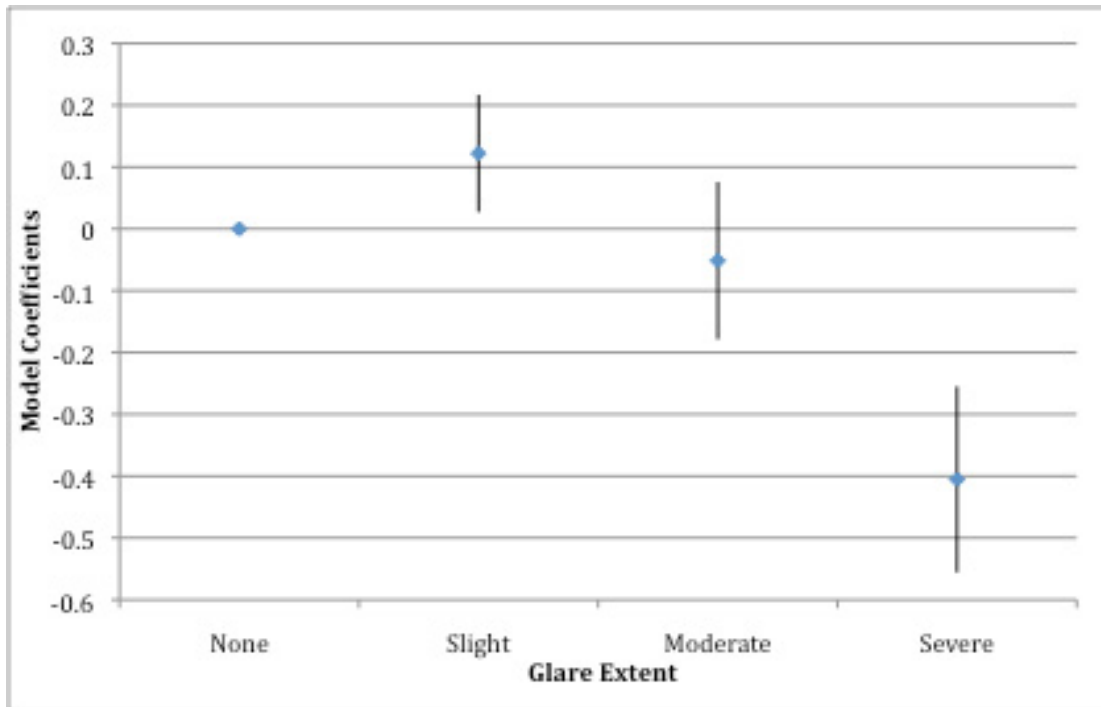
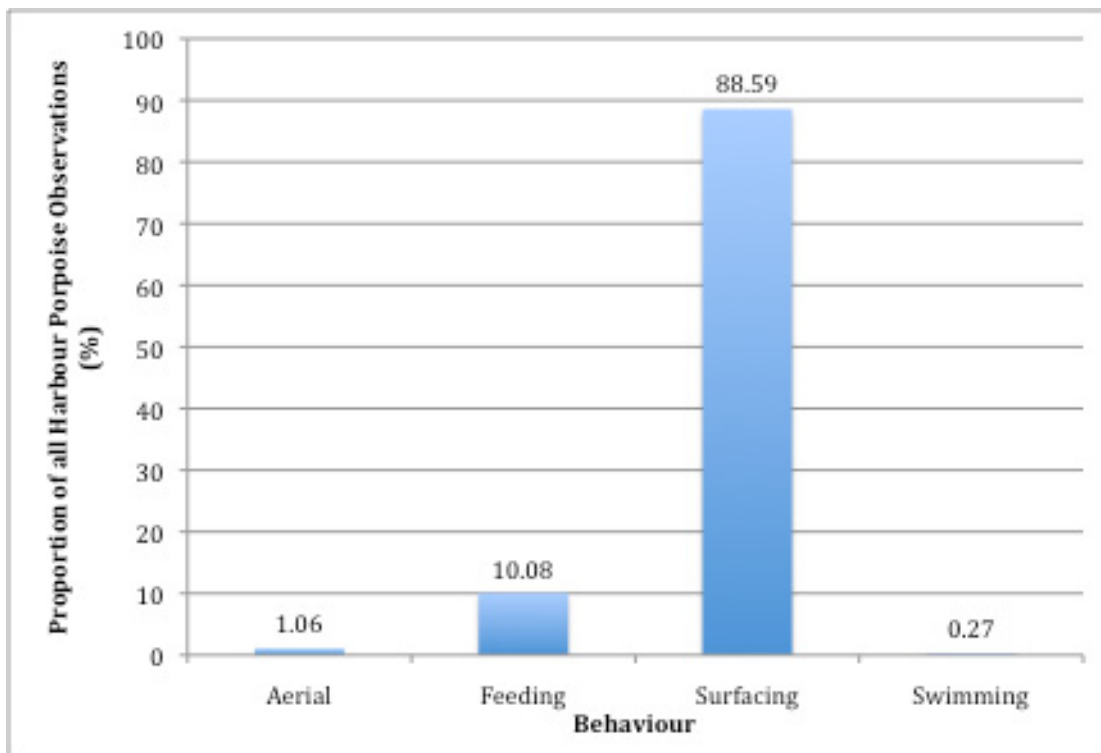


Figure 75: The proportion of all harbour porpoise observations by behaviour at Billia Croo.



ANNEX 2: DISTRIBUTION MAPS WITHIN 5KM OF BLACK CRAIG

Common Eider

Figure 76: Map showing the seasonal distribution of common eider observations at Billia Croo

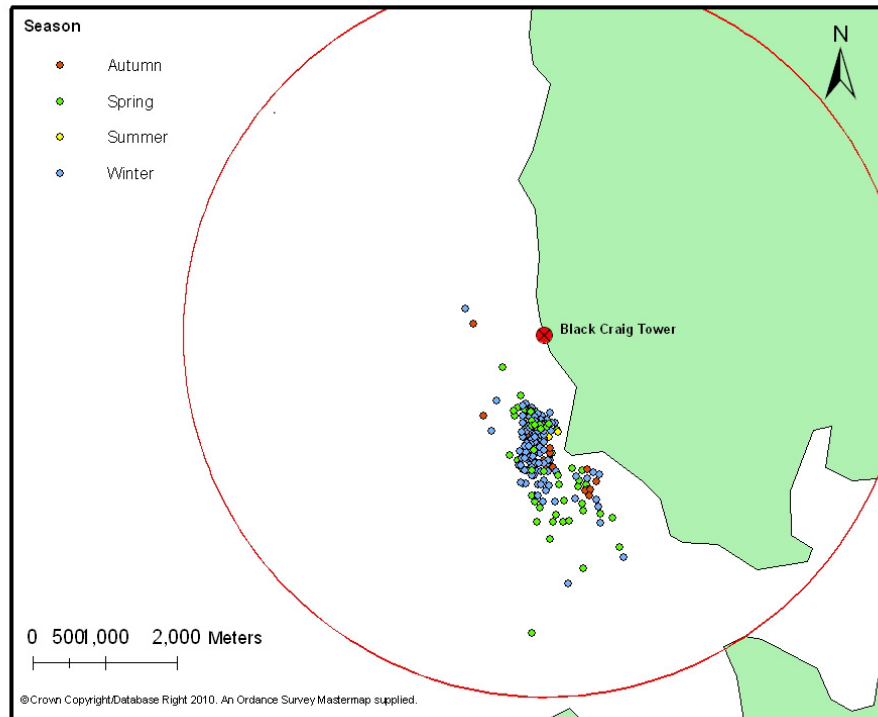
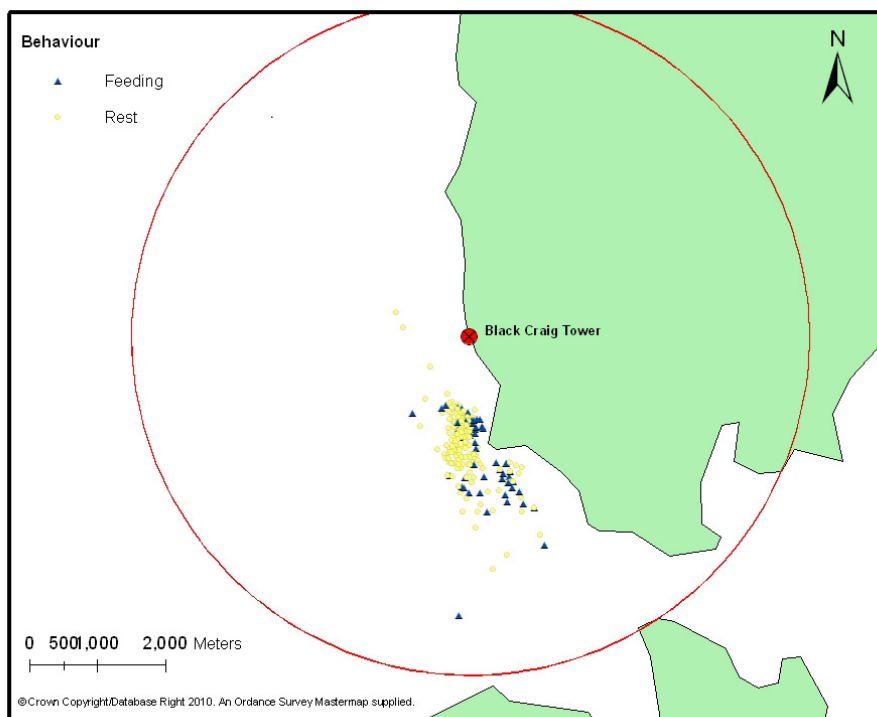
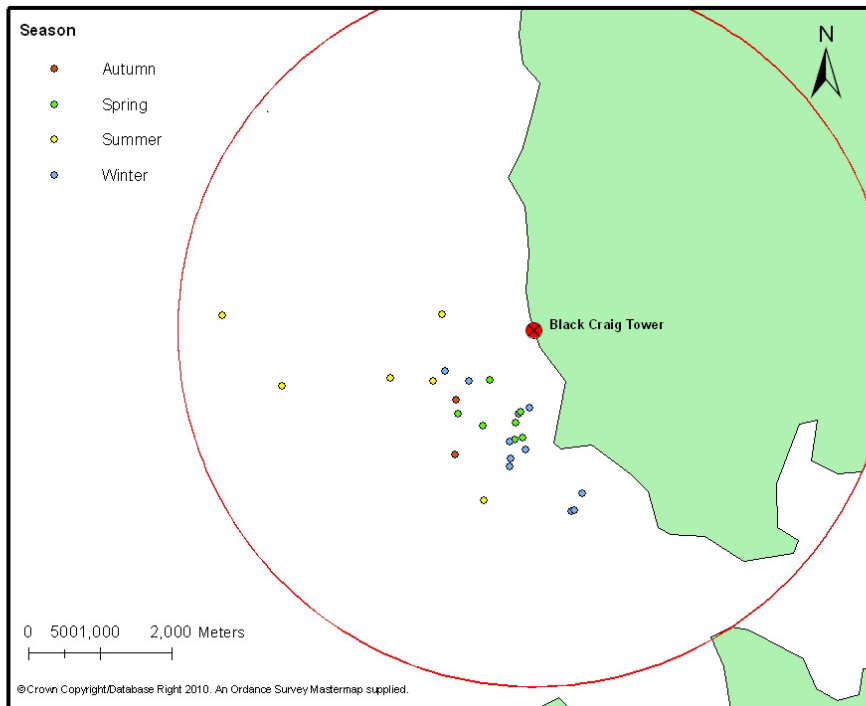


Figure 77: Map showing the distribution of observed feeding and resting common eider at Billia Croo



Red-throated Diver

Figure 78: Map showing the seasonal distribution of red-throated diver observations at Billia Croo



Northern Fulmar

Figure 79: Map showing the seasonal distribution of fulmar observations at Billia Croo

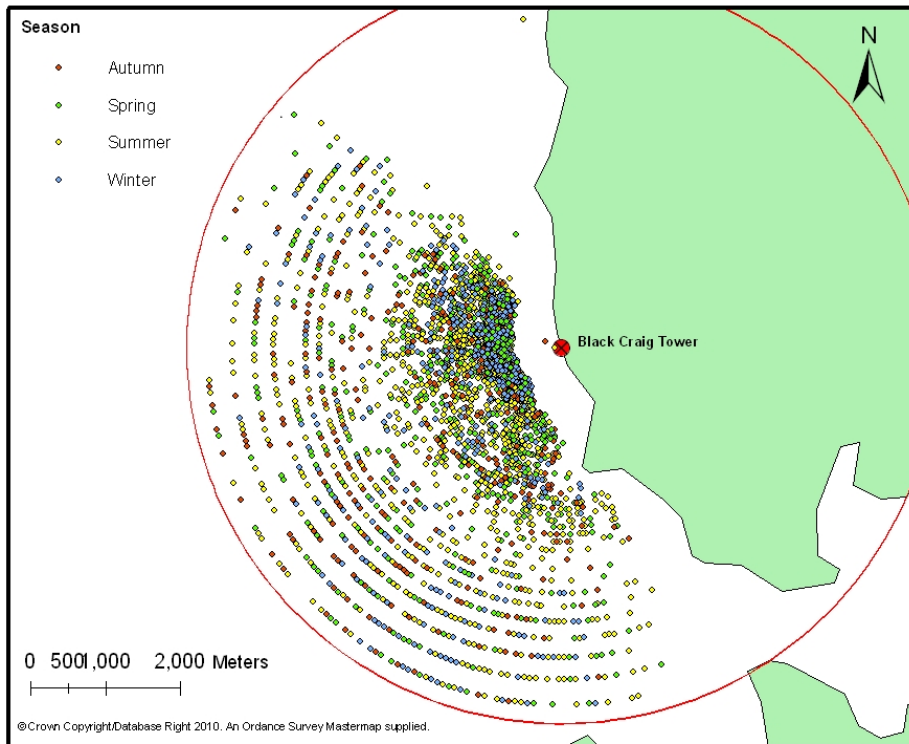
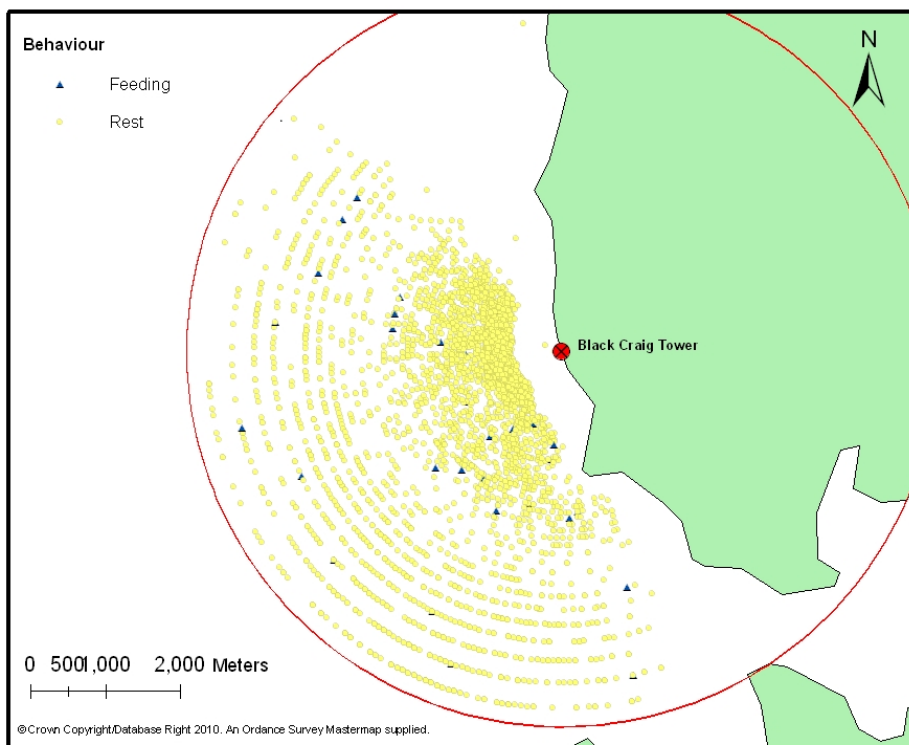


Figure 80: Map showing the distribution of observed feeding and resting fulmar at Billia Croo



Northern Gannet

Figure 81: Map showing the seasonal distribution of northern gannet observations at Billia Croo

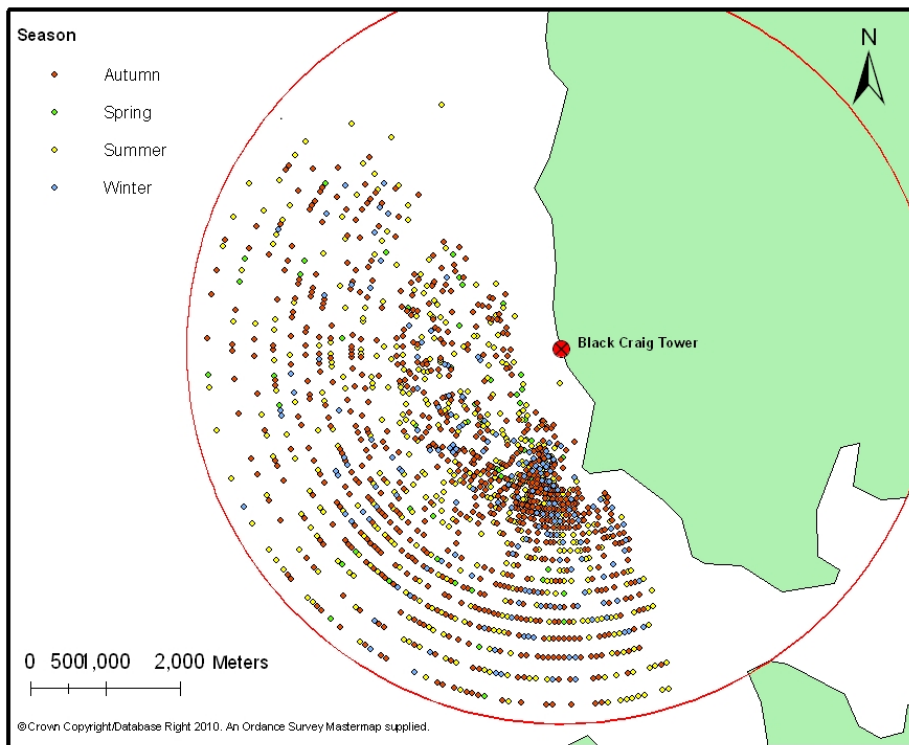
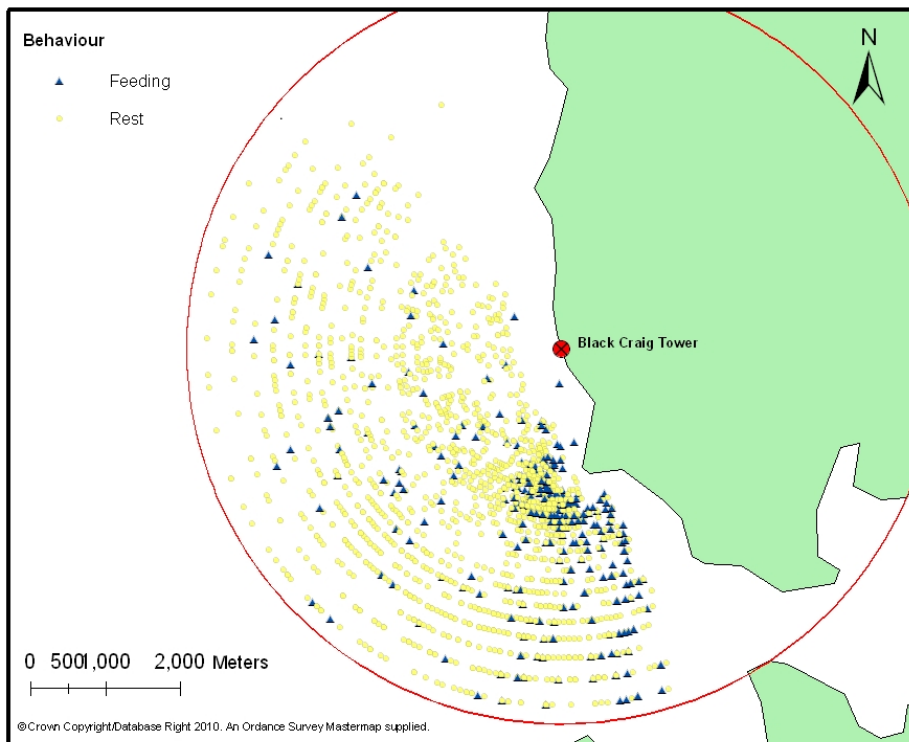


Figure 82: Map showing the distribution of observed feeding and resting northern gannet at Billia Croo



European Shag

Figure 83: Map showing the seasonal distribution of European shag observations at Billia Croo

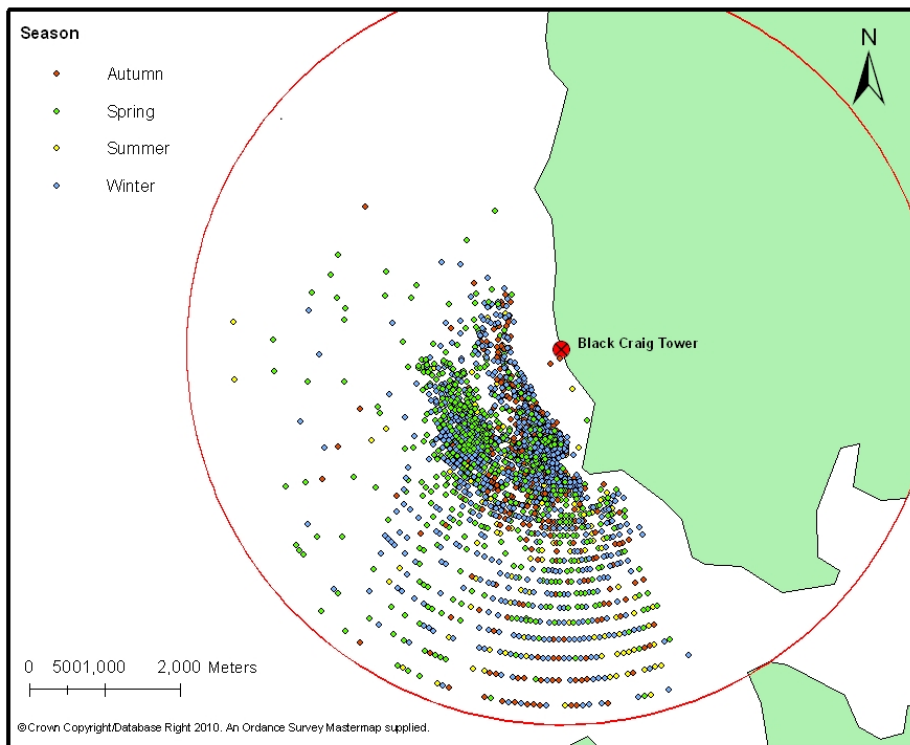
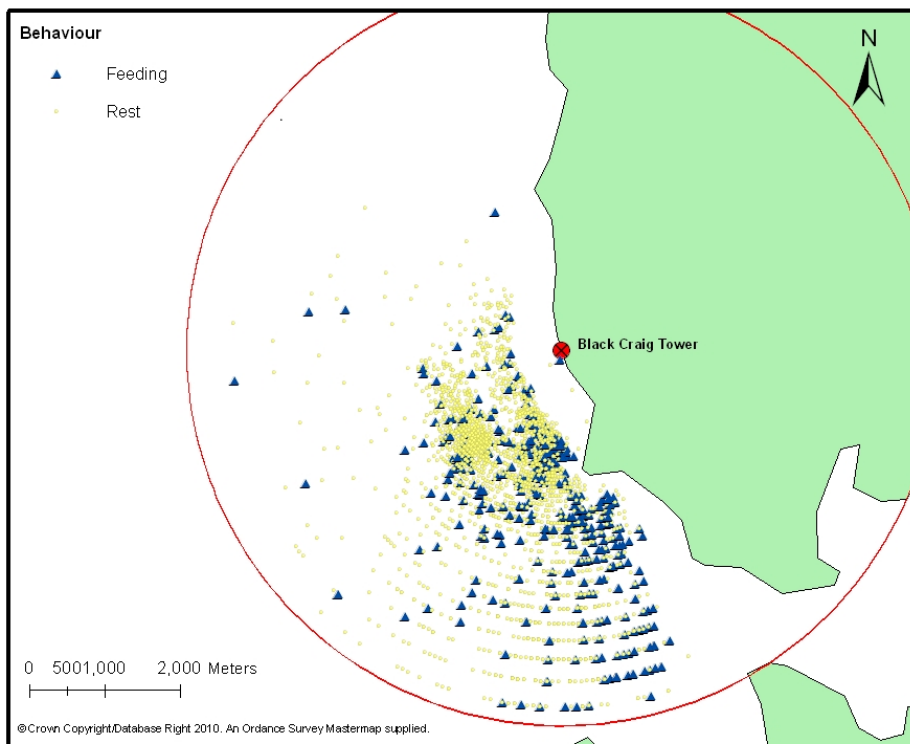


Figure 84: Map showing the distribution of observed feeding and resting European shag at Billia Croo



Skuas

Figure 85: Map showing the seasonal distribution of great skua observations at Billia Croo

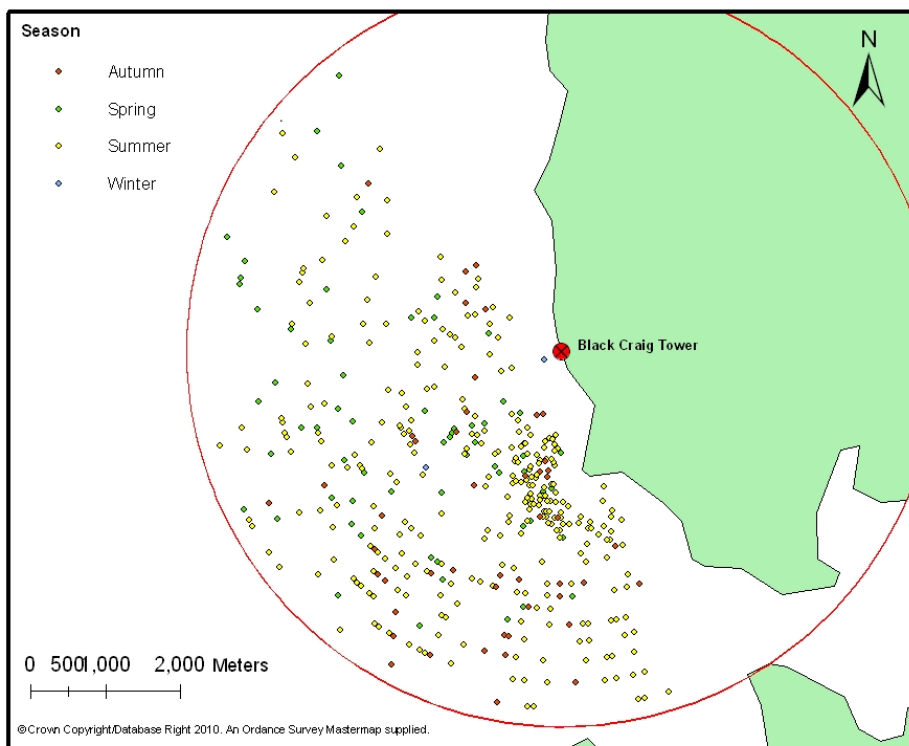


Figure 86: Map showing the distribution of observed feeding and resting great skua at Billia Croo

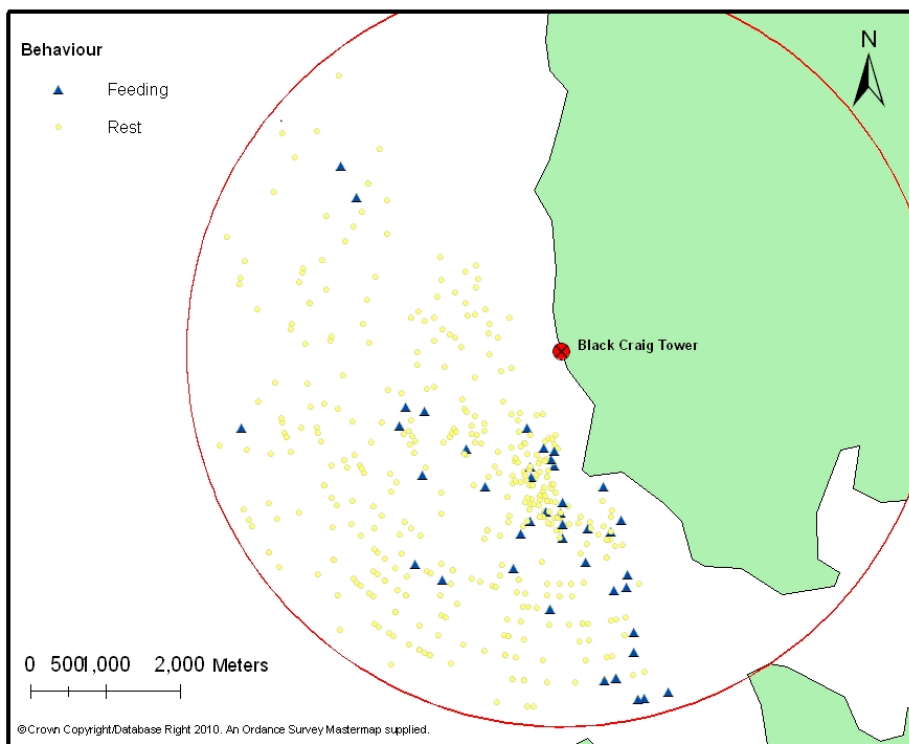
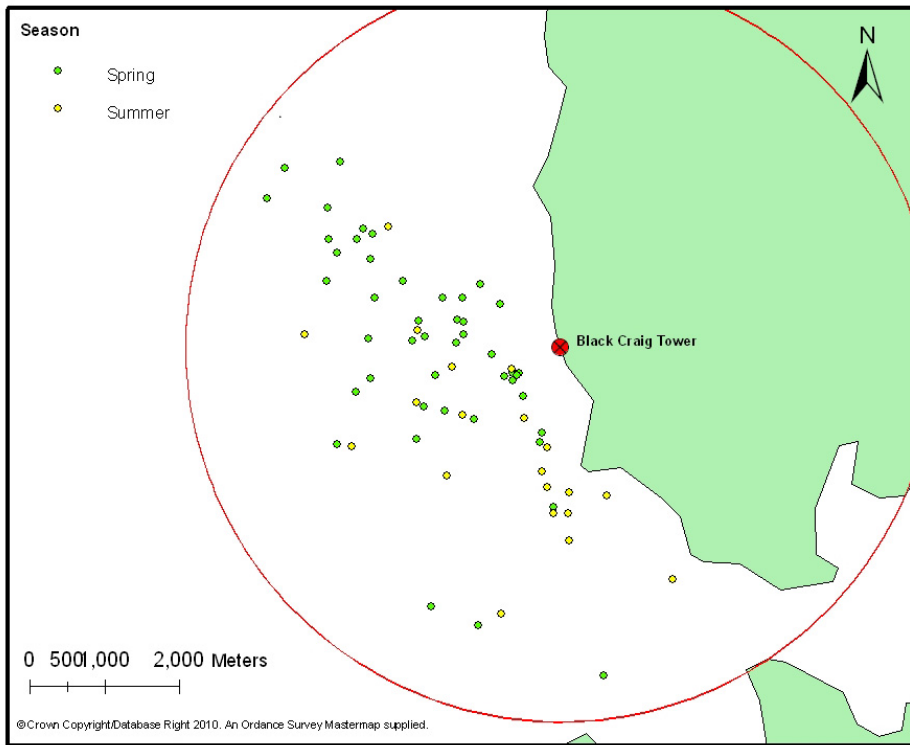


Figure 87: Map showing the seasonal distribution of Arctic skua observations at Billia Croo



Gulls

Figure 88: Map showing the seasonal distribution of *Larus spp.* observations at Billia Croo

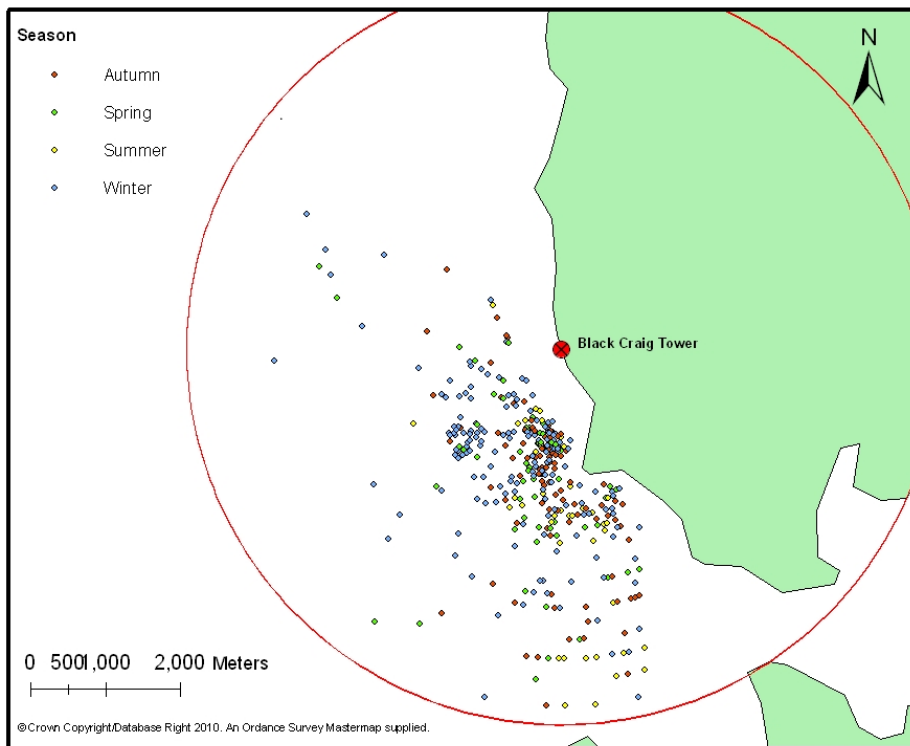
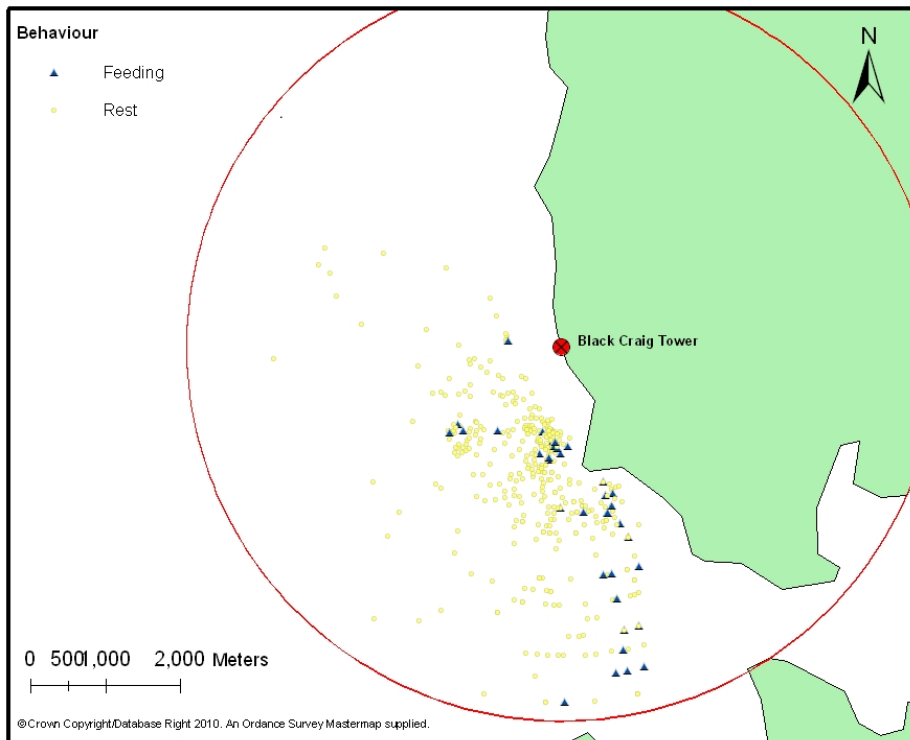
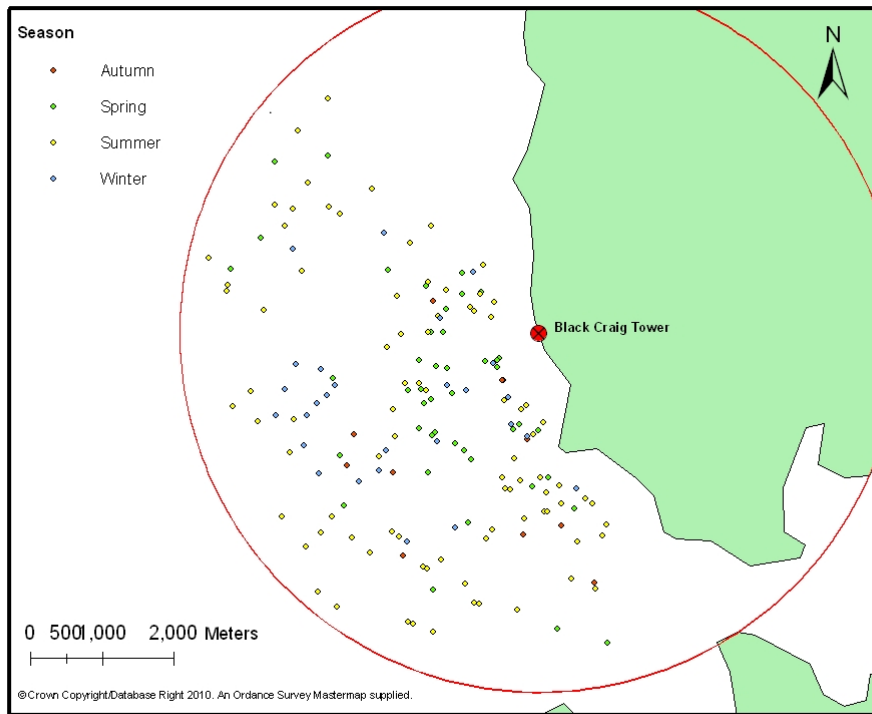


Figure 89: Map showing the distribution of observed feeding and resting *Larus spp.* at Billia Croo



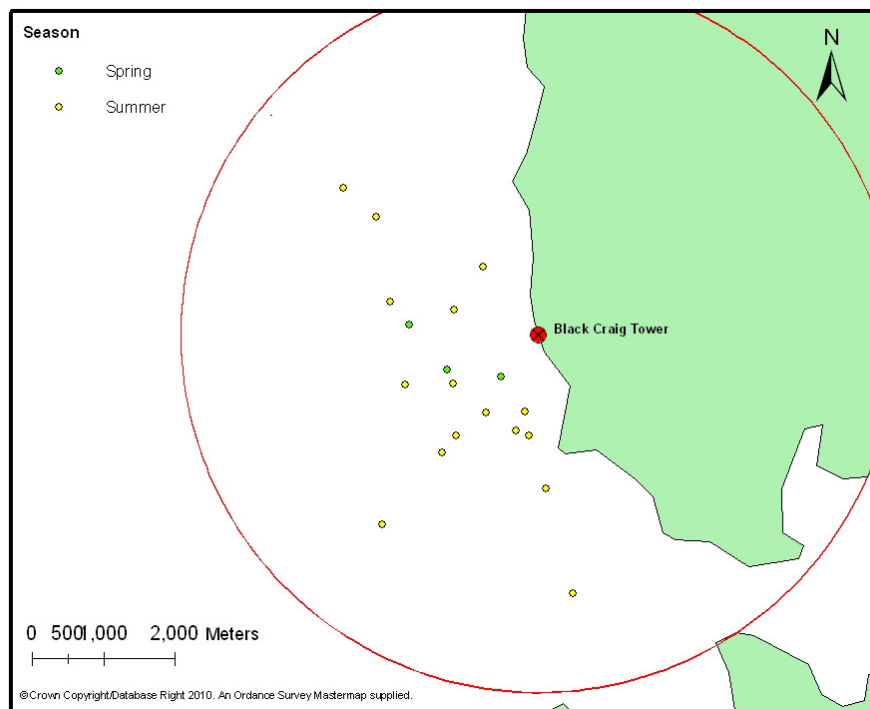
Black-legged Kittiwake

Figure 90: Map showing the seasonal distribution of black-legged kittiwake observations at Billia Croo



Arctic Tern

Figure 91: Map showing the seasonal distribution of Arctic tern observations at Billia Croo



Auks

Figure 92: Map showing the seasonal distribution of common guillemot observations at Billia Croo

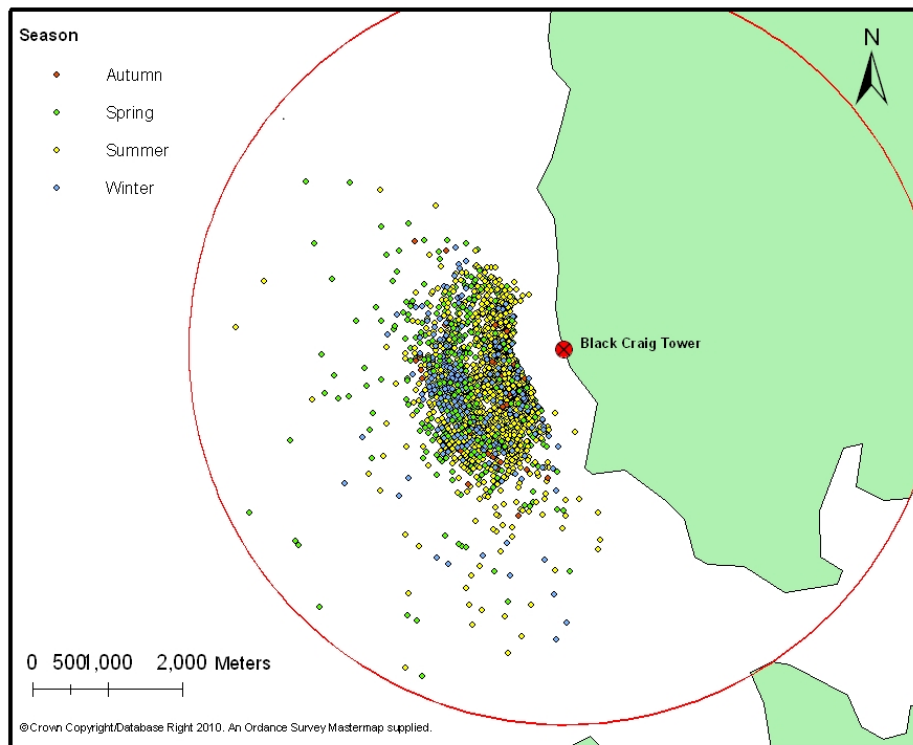


Figure 93: Map showing the distribution of observed feeding and resting common guillemot at Billia Croo

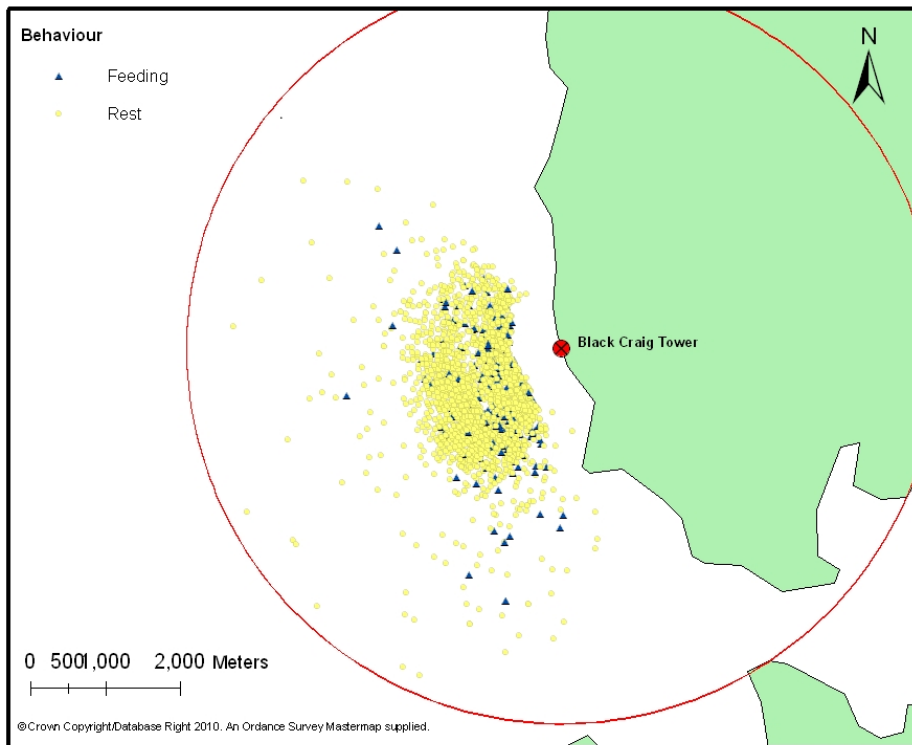


Figure 94: Map showing the seasonal distribution of razorbill observations at Billia Croo

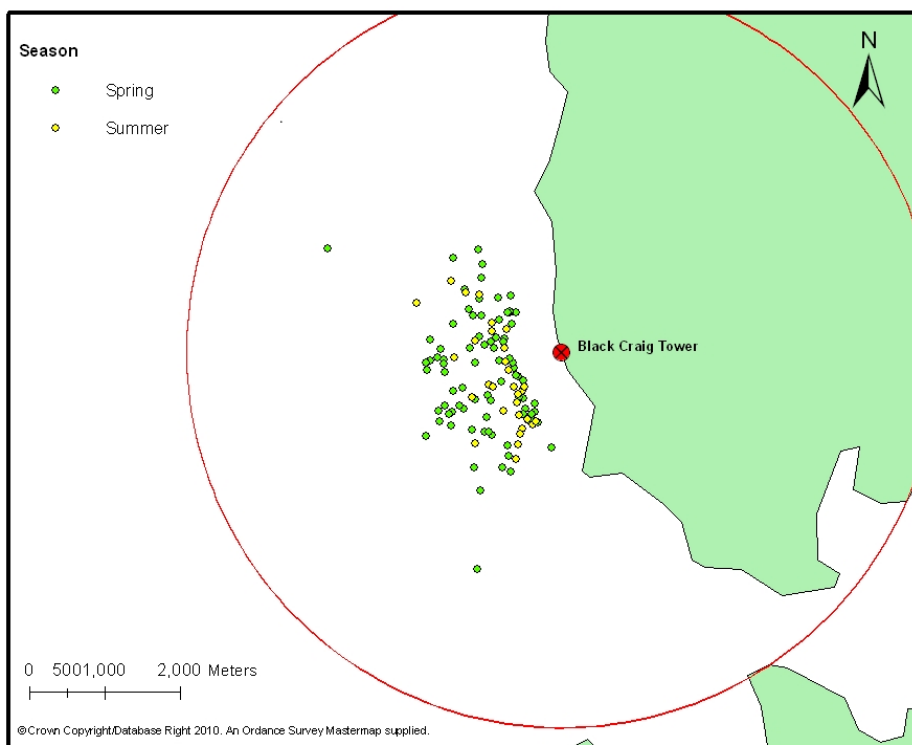


Figure 95: Map showing the distribution of observed feeding and resting razorbill at Billia Croo

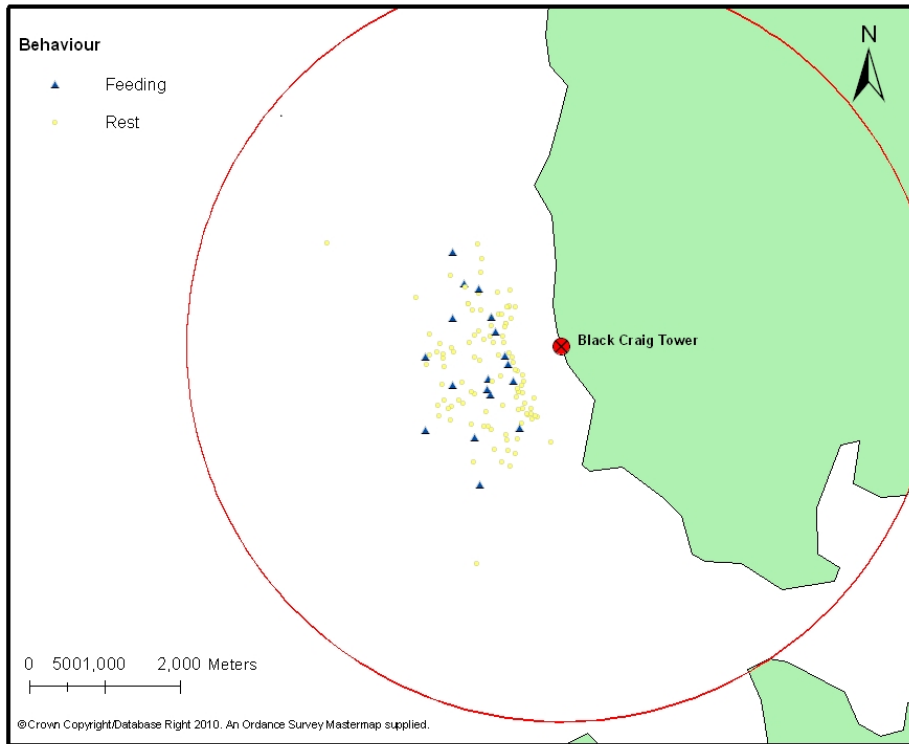


Figure 96: Map showing the seasonal distribution of black guillemot observations at Billia Croo

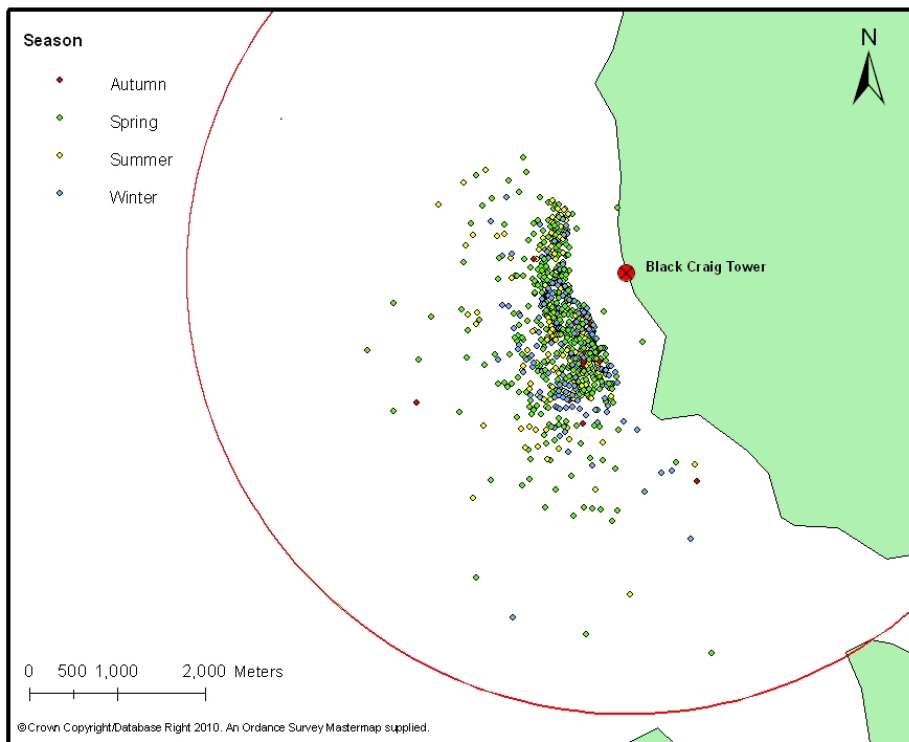


Figure 97: Map showing the distribution of observed feeding and resting black guillemot at Billia Croo

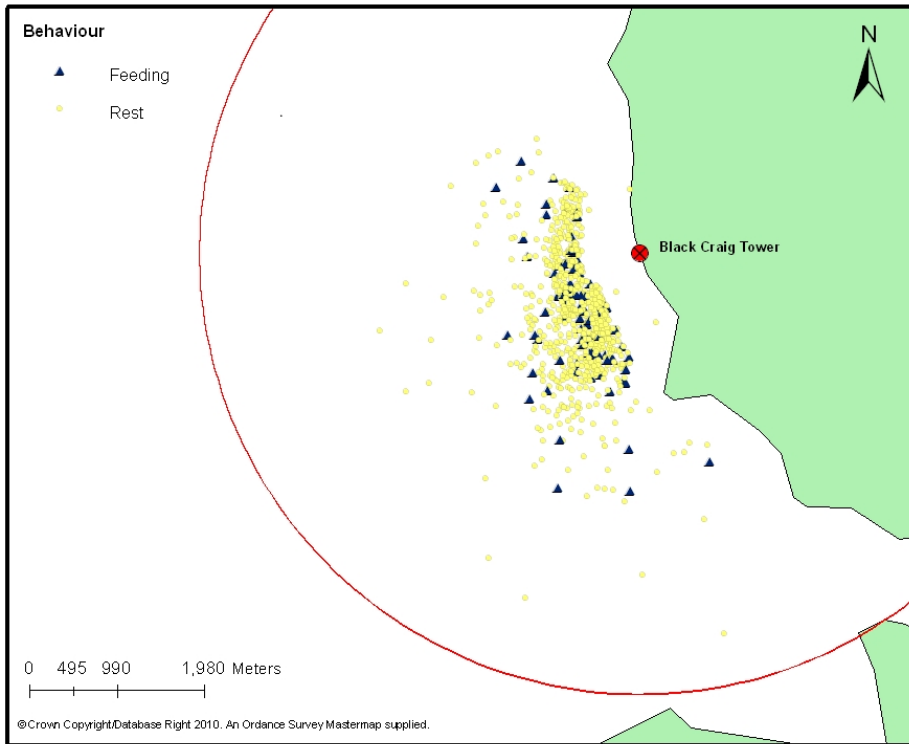


Figure 98: Map showing the seasonal distribution of Atlantic puffin observations at Billia Croo

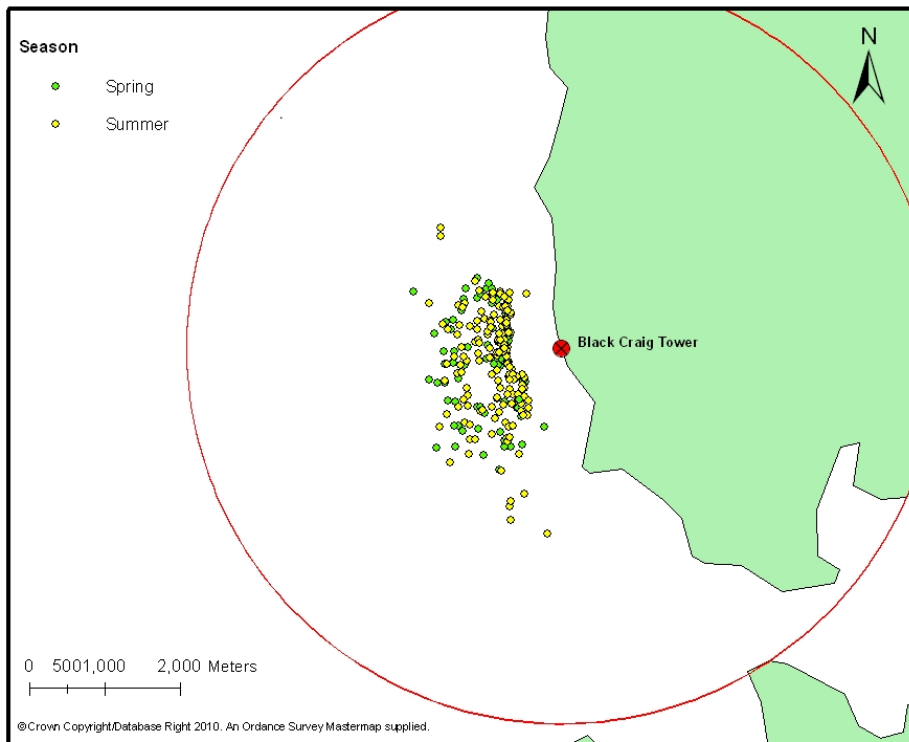
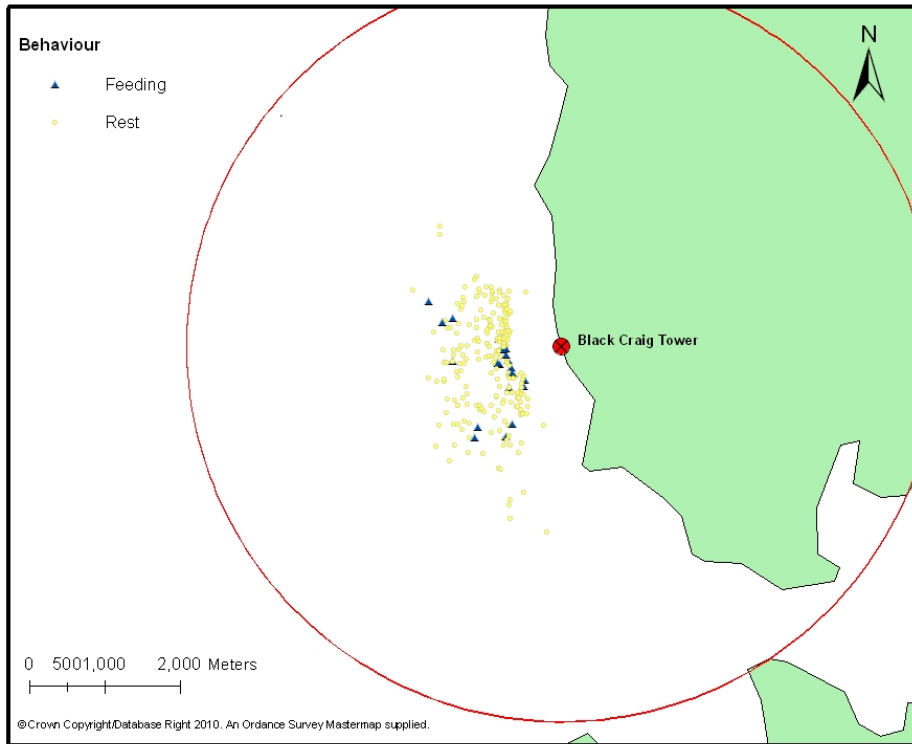


Figure 99: Map showing the distribution of observed feeding and resting Atlantic puffin at Billia Croo



ANNEX 3: AN EXAMPLE OF THE R SCRIPT USED

```
#Making factors ordinal
shag5K1$oGLAREEXTENT<-
ordered(shag5K1$GLARE.EXTENT,levels=c("None","Slight","Moderate","Severe"))
levels(shag5K1$oGLAREEXTENT)
shag5K1$oSEASON<-
ordered(shag5K1$SEASON,levels=c("Spring","Summer","Autumn","Winter"))
levels(shag5K1$oSEASON)
shag5K1$oTIDE<-
ordered(shag5K1$TIDE2,levels=c("High.Slack","Ebb","Low.Slack","Flood"))
levels(shag5K1$oTIDE)

#The chosen GAMM for Shags
shag5Knb5<-
gamm(NUMBER~s(Long,Lat)+s(JULIANDAY,bs="cc")+s(TimetolowHR2,bs="cc")+oGLARE
EXTENT+Observer,
correlation=corAR1(form=~1|DAYLAPSE),family=negative.binomial(theta=1),gamm
a=1.4,data=shag5K1)
summary(shag5Knb5$gam, cor=corAR1(form=~1|DAYLAPSE))
anova(shag5Knb5$gam)
gam.check(shag5Knb5$gam)
summary(shag5Knb5$lme)

plot(shag5Knb5$gam, select = c(1), xlab="Longitude", ylab="Latitude")
plot(shag5Knb5$gam, select = c(2), xlab="Julian Day", ylab="Relative
Abundance")
plot(shag5Knb5$gam, select = c(3), xlab="Time from Low Tide (hour)",
ylab="Relative Abundance")

op <- par(mfrow = c(2, 2))
plot(shag5Knb5$gam, select = c(1), xlab="Julian Day", ylab="Model
Coefficients",ylim=c(-0.4,0.4))
plot(shag5Knb5$gam, select = c(2),xlab="Time of Day (Hour)", ylab="Model
Coefficients")
E <- resid(shag5Knb6$lme, type = "normalized")
F <- fitted(shag5Knb6$lme)
plot(x = F, y = E, xlab = "Fitted values", ylab = "Residuals")
par(op)

#calculating theta
shag5Ktheta <-
gam(NUMBER~s(Long,Lat)+s(JULIANDAY,bs="cc")+s(TimetolowHR2,bs="cc"),family=
negbin(c(1,10)),data=shag5K1,method="REML")
plot(shag5Ktheta,pages=1)
print(shag5Ktheta)

shag5Ktheta1 <-
gam(NUMBER~s(Long,Lat)+s(JULIANDAY,bs="cc")+s(TimetolowHR2,bs="cc")+s(Timet
olowHR2,bs="cc"),family=negbin(c(1,10)),optimizer="perf",data=shag5K1)
plot(shag5Ktheta1,pages=1)
print(shag5Ktheta1)

shag5Ktheta$family$getTheta()
shag5Ktheta1$family$getTheta()
```

www.snh.gov.uk

© Scottish Natural Heritage 2013
ISBN: 978-1-85397-978-1

Policy and Advice Directorate, Great Glen House,
Leachkin Road, Inverness IV3 8NW
T: 01463 725000

You can download a copy of this publication from the SNH website.



Scottish Natural Heritage
Dualchas Nàdair na h-Alba

All of nature for all of Scotland
Nàdar air fad airson Alba air fad